BSCM

Biomedical Sciences and Clinical Medicine

Volume 64 | Number 2 | April - June 2025 | ISSN 2774-1079 (Online)

BSCM
Biomedical Sciences and Clinical Medicine

Volume 64 No.2 Apr.-Jun. 2025
https://he01.tci-thaijo.org/index.php/CMMJ-MedCMJ/index

CONTENTS

Original Articles

Review Article

Case Report

Biomedical Sciences and Clinical Medicine 2025;64(2):90-99.
doi: 10.12982/BSCM.2025.16
https://he01.tci-thaijo.org/index.php/CMMJ-MedCMJ/index

Original Article

Open Access

Construction of Thai Monosyllabic Word Lists for Speech Recognition Test of Adults

Paphawee Mana[1], Kwanchanok Yimtae[1,2] and Panida Thanawirattananit[1,2]

[1]Department of Otorhinolaryngology, Faculty of Medicine, [2]Khon Kaen Ear, Hearing, and Balance Research Group, Khon Kaen University, Khon Kaen, Thailand

Correspondence:
Panida Thanawirattananit, MA, Department of Otorhinolaryngology, Faculty of Medicine, Khon Kaen University, 123 Mittraphap Rd., Nai-Muang, Muang District, Khon Kaen 40002, Thailand.
E-mail: panith@kku.ac.th

Received: June 18, 2024;
Revised: August 22, 2024;
Accepted: October 30, 2024

ABSTRACT

OBJECTIVE The objective of this study was to construct new Thai monosyllabic word lists that are phonetically balanced and to study the accuracy of speech recognition measuring tests for adults.

METHODS This study creation of four Thai monosyllabic word lists (KKU lists) of twenty-five words each in a CD recording based upon an accuracy evaluation. The 76 participants recruited were between 19 and 70 years of age and were recruited based on four groups of hearing level. Each group of 19 subjects consisted of people with normal hearing as well as people with moderate, moderately severe, and severe sensorineural hearing loss with symmetrical hearing. Only the dominant ear of each of the participants was chosen for testing. Audiometry in that ear was conducted using randomized nine-word lists from the four newly constructed Khon Kaen University lists (KKU lists) and five lists of RAMA SD lists-1 from the original Thai monosyllabic word lists (OTL) [OTL consisted of RAMA SD list-1 (there are 5 lists) and RAMA SD list-2 (there are 4 lists)]. The participant's accurately spoken words will be recorded as a number and percentage.

RESULTS No statistically significant differences were found in the speech recognition scores of any of the four KKU lists among the four participant groups ($p > 0.05$). Similar to Kasmer and Brown's study, the speech recognition scores (SRS) of the KKU lists and OTL lists declined as the degree of the severity of hearing loss increased. The score range (min-max) at each level of hearing loss for all nine-word lists was in the standard value range. However, the SRS of the KKU lists were found to be closer to the standard reference than the scores from the OTL list.

CONCLUSIONS The KKU lists can provide more accurate score results and more precise diagnoses of hearing loss and can also be applied in clinical examination and speech recognition testing.

KEYWORDS Thai monosyllabic word lists, phonetic balance, speech recognition scores

INTRODUCTION

Speech recognition scores are used for analysis when seeking to address patient socialization problems among sensorineural hearing loss patients including assessing the severity of communication problems, evaluating the effects of hearing rehabilitation and identifying the pathologies of the hearing loss. Both Speech Recognition Scores

(SRS) and Speech Discrimination Scores (SDS) are one part of speech audiometry evaluation using monosyllabic word lists. In 1930, Fletcher and Steinberg developed the first word list, the Western Electric 4A test (later called the 4C test) (1). That assessment uses an analog recording to obtain a stable voice volume based on evaluation of the perceived sound clarity. This helped examiners evaluate the severity of the hearing loss and to determine how it affected communication. In addition, Ronald C. Egan, who was later the President of Harvard University, developed another word list in 1948 which is known as the Phonetically Balanced 50 (PB-50) (2). Egan's objective was to appraise speech comprehension. The PB-50 consists of 20-word lists for speech recognition tests, each consisting of 50 words that are used in daily life. This experiment was later considered to be a prototype for evolving new word lists. The correlation between the speech recognition score and the degree of hearing loss indicates that the score will be lower when the degree of hearing loss is greater (3, 4). Additionally, inaccuracies in SRS can occur when a live voice rather than a recording is used for testing. Using voice recordings in speech recognition tests can ameliorate this inaccuracy issue (5). In addition, to obtain more accurate scores, the language used in the examination should be the examinees' mother tongue with which they are familiar and that they use in their daily lives (6, 7).

Consonants, vowels, and tones are joined together as speech sounds. Previous studies have shown that consonant sounds can affect speech frequency changes (8). Speech recognition problems in sensorineural hearing loss patients can be described by the fact that an initial consonant of words may be identified in the frequency range in which those patients are hard of hearing (9, 10). Tone is another a variable that enables words to have different meanings. Thai is one of the languages in the world that has five tones (11). Vowel sounds can improve pronunciation skill and final consonant sounds may act as an enhancer of cognitive competency in the Thai language (12, 13). The Computerized Speech Laboratory (CSL) system is a tool that can be utilized in the analysis of sound waves. It can be used to assess human voices, which are composed of component waves that have different complex shapes and levels of frequency (14). In regard to recording speech, the quality of the speaker's voice recording will affect the test results and can be assessed through listening. The method known as GIRBAS (grade, roughness, breathiness, asthenia, strain scale) has been widely used and is accepted as a standard test in clinical settings (15). An evaluation score of zero, which indicates good sound quality, is used to select sounds in a recording. In evaluating recordings, female and male voices have been found to be not significantly different with regard to the speech classification values, but the speech of women's voices has more variability between words than the speech of men's voices (16, 17).

In Thailand, the original Thai monosyllabic word lists (OTL) that are currently used were created more than 40 years ago. It has been found that some of the words on these lists are not commonly used today. Additionally, there are duplicate words in some word lists as well as issues of phonetic imbalance. For that reason, new Thai monosyllabic word lists have been developed to provide more accurate score results and more precise diagnoses of hearing loss. The objectives of the current study are: 1) to construct new Thai monosyllabic word lists that are phonetically balanced and 2) to determine the accuracy of the new Thai monosyllabic word lists for speech recognition testing in adults (KKU lists).

METHODS

This study was approved by the Khon Kaen University Ethical Committee for Human Research (HE651273) and was registered in the Thai Clinical Trials (TCTR20220810005). Before participating in this trial, full written informed consent was obtained from all participants. This study was conducted in two steps as shown in the study flow (Figure 1).

Word list construction and recording

A total of 283 familiar words were selected from the Thai National Corpus (National Thai Language Data Archive Under the Royal Patronage of Her Royal Highness Princess Maha Chakri Sirindhorn), and were arranged in order from highest to lowest frequency found in daily use. The study selected 283 words from a list of 400 most familiar words. The principles criteria for selection were as follows: 1) the words were

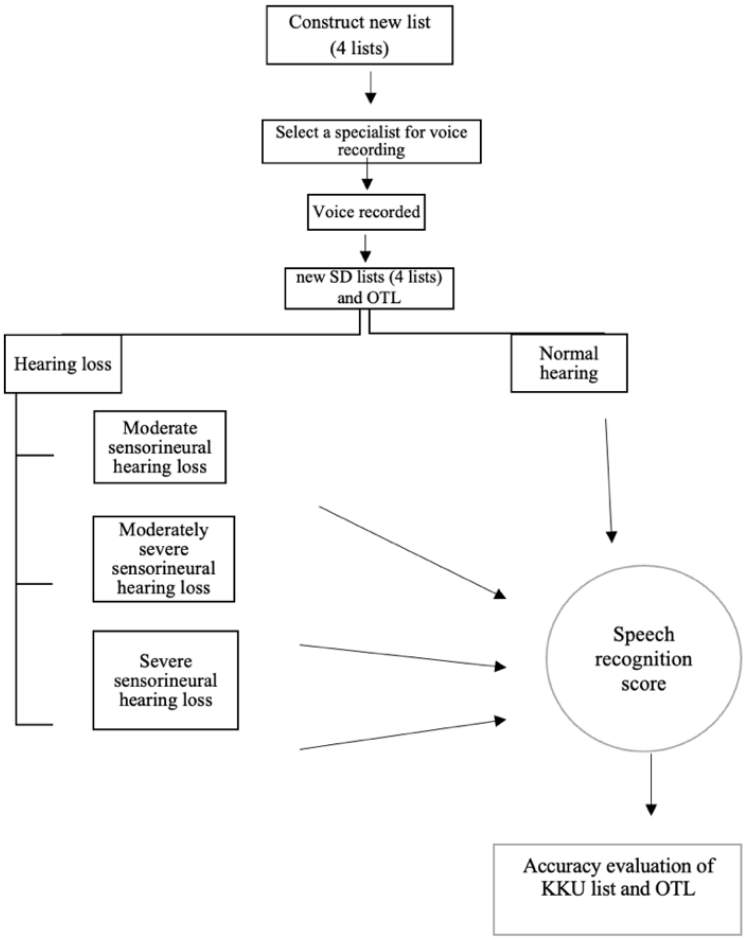

Figure 1. The flow of the study

meaningful, 2) they were not diphthongs, 3) they were polite words, and 4) there were no /r/ sounds. The words were sorted according to the frequency of the initial consonant sounds. In addition, 109 words that have high-tone consonants (> 2,000 Hz), 79 words that have mid-tone consonants (500-2,000 Hz), and 95 words with low-tone consonants (< 500 Hz) were selected. A higher number of high-tone initial consonants was selected due to their effects on changes to the perception of sounds in the Thai language. All words were analyzed for mean frequency using the CSL. Following the CSL analysis, the words were arranged into three groups based on mean frequency: low-tone (< 175 Hz), mid-tone (175-220 Hz), and high-tone (> 220 Hz). Distribution of selected words in each list was based on both the initial consonant sounds and the mean frequency of the words (Table 1). The four lists of 25 words each are called a KKU list (Table 2). Arrangement of the words within the word lists and the ordering of the word lists was done using a random distribution method.

A voice model was chosen from among three candidates, all of whom were Thai male vocal professionals. To be considered, the mother tongue of candidates had to be Thai, and they had to show good voice quality as measured by the GIRBAS Scale (grade, instability, roughness, breathiness, asthenia, and strain) that were established with a GIRBAS grade of 0. The four KKU lists and the five OTL (RAMA SD-1) lists were recorded in a standard double-walled room using a condenser microphone and a 6.5 cm diameter windshield positioned approximately 20 cm from the speaker's mouth at an angle of 0 degrees to the speaker. The microphone was linked to a sound level meter to control the loudness at 63 dB SPL during sound recording. From time to time, the speaker was given a break. While recording, two audiologists evaluated each word for its natural sound. The audio was recorded in an MPEG-1 Audio Layer 3 (.mp3) audio file format. Before being examined, the sound had to be calibrated using a pure tone

Table 1. The number of words according to the distribution of the initial consonants and the average speech frequency of the words in each set of the KKU lists

	KKU list 1	KKU list 2	KKU list 3	KKU list 4
Low-tone consonant and low-tone mean frequency words	2	2	2	2
Low-tone consonant and mid-tone mean frequency words	3	3	3	3
Low-tone consonant and high-tone mean frequency words	3	3	3	3
Mid-tone consonant and low-tone mean frequency words	3	3	3	3
Mid-tone consonant and mid-tone mean frequency words	3	3	3	3
Mid-tone consonant and high-tone mean frequency words	3	3	3	3
High-tone consonant and low-tone mean frequency words	2	2	2	2
High-tone consonant and mid-tone mean frequency words	3	3	3	3
High-tone consonant and high-tone mean frequency words	3	3	3	3

KKU list, Khon Kaen University lists

Table 2. KKU lists

KKU list 1		KKU list 2		KKU list 3		KKU list 4	
	IPA		IPA		IPA		IPA
เก่า (old)	ŋîap	โลก (world)	lôːk	ผ่าน (pass)	pʰàːn	ใหญ่ (big)	jàì
เงียบ (silent)	kàw	อ่อน (soft)	ʔɔ̀ːn	แดง (red)	dɛːŋ	เกาะ (island)	kɔ̀ː
เลือก (select)	lɯ̂ak	วัน (day)	wan	คิด (think)	kʰít	ยอก (peak)	jɔ̂ːt
หนึ่ง (one)	nɯ̀ŋ	ญาติ (relative)	jâːt	นิ่ง (still)	nîŋ	ไทย (Thai)	tʰaj
ยิ้ม (smile)	jím	พิมพ์ (print)	pʰim	ข่าว (news)	kʰàːw	ตั้ง (set up)	tâŋ
ตา (eye)	tāː	เปิด (open)	pɤ̀ːt	ผิว (skin)	pʰǐw	ลม (wind)	lom
พื้น (floor)	pʰɯ́ːn	หน่วย (unit)	nùaj	ท่าน (you)	tʰâːn	ชุด (suit)	tɕʰút
เที่ยว (trip)	tʰîaw	วิ่ง (run)	wíŋ	เล็ก (small)	lék	ขาย (sell)	kʰaːj
ขาด (lack)	kʰàːt	ข้าม (cross)	kʰâːm	ไฟ (fire)	faj	แก้ว (glass)	kɛ́ːw
สอบ (test)	sɔ̌ːp	ต่ำ (low)	tàm	ตัด (cut)	tàt	เลิก (quit)	lêːk
เพื่อน (friend)	pʰɯ̂ːn	พ่อ (father)	phɔ̂ː	บอก (tell)	bɔ̀ːk	เพิ่ม (add)	pʰɤ̂m
ลืม (forget)	lɯ́m	พื้น (practice)	fɯ́k	เชื่อ (believe)	tɕʰɯ̂ːa	สี่ (four)	sìː
จุด (point)	tɕùt	พูด (speak)	phúːt	พืช (plant)	pʰɯ̂ːtɕʰ	บาท (bath)	baːt
ใช่ (correct)	tɕʰâj	ส่ง (send)	sòŋ	มือ (hand)	mɯː	ชื่อ (name)	tɕʰɯ̂ː
คุย (talk)	kʰuːi	คู่ (couple)	kʰûː	เกิด (born)	kɤ̂ːt	ห้าม (forbid)	hâːm
แพทย์ (doctor)	pʰɛːtˆ	หลัง (back)	lǔŋ	สอง (two)	sɔ̌ːŋ	จ่าย (pay)	tɕàːj
แบ่ง (divide)	bɛ̀ːŋ	กอง (pile)	kɔ̄ːŋ	นอก (outside)	nɔ̀ːk	ออก (exit)	ʔɔ̀ːk
ป่า (forest)	pàː	สาว (young lady)	saːw	ใต้ (under)	tâj	ยาก (difficult)	jaːk
ข้าว (rice)	kʰâːw	แทน (replace)	tɛːn	ถูก (correct)	tʰùːk	เพชร (diamond)	pʰɛ̌ː.tɕʰɤː
ห้อง (room)	hɔ̂ːŋ	ยาย (grandmother)	jaːj	หนุ่ม (young man)	nùm	ถาม (ask)	tʰǎːm
ตอบ (answer)	tɔ̂ːp	ต้น (tree)	tôn	ป้า (aunt)	pâː	น้ำ (water)	nám
หัว (head)	hǔa	ห่าง (far)	hàːŋ	แยก (separate)	jɛ̀ːk	เส้น (line)	sên
แสน (hundred thousand)	sɛ̌ːn	ชอบ (like)	tɕʰɔ̂ːp	โต๊ะ (table)	tóʔ	ปิด (close)	pìt
นก (bird)	nók	ขาว (white)	kʰǎːw	ใส่ (put)	sài	แต่ง (decorate)	tɛ̀ŋ
ง่าย (easy)	ŋâːj	ใหม่ (new)	mài	กว้าง (wide)	kwâːŋ	ดิน (soil)	din

* The International Phonetic Alphabet (IPA); KKU list, Khon Kaen University lists

at the frequency of 1 kHz, with the volume unit meter (VU meter) set at 0 and the loudness set to 60 dB.

Accuracy testing of the word lists

The participants

A total of 76 native Thai-speaking patients from the Ear, Nose, and Throat Outpatient Department at Khon Kaen University's Srinagarind Hospital, with an age range of 19-70 years, participated in the study between June 2021 and February 2022. There were four sample groups: 19 participants with normal hearing (≤ 25 dB HL), 19 with moderate Sensorineural hearing loss (SNHL) (41-55 dB HL), 19 with moderately severe SNHL (56-70 dB HL), and 19 with severe SNHL (71-90 dB HL) (18, 19). Configuration of hearing loss had not been specified and was considered to be symmetrical, i.e., the same in both ears. All participants had undergone normal otolaryngology examina-

tions and all were born in Thailand. Their native language was Thai, and they had normal speech production organs. Individuals who had severe dizziness, secretions from their ears, psychopathy, or mental problems, as well as those who communicated abnormally or who were uncooperative were excluded.

The testing procedures

Audiometry, consisting of both pure tone audiometry and speech audiometry, was performed with all participants. In cases where audiometric test results had been obtained more than 30 days prior, a re-test was performed. Only the dominant ear of each of the participants was chosen for testing using the nine word lists. Before testing, the participants received a brief set of instructions from the audiologist. The audiometer was calibrated at 1 KHz pure tone, with 60 dB set for the 0 VU meter. Testing was conducted using an AC40 clinical audiometer with an IP30 insert earphone transducer. The SRS were determined using the most comfortable level, and the word lists were randomly presented in a sequential order. The results were recorded by two audiologists at the time of testing.

Statistical analyses

To test the hypotheses of the study, the data was analyzed using descriptive analysis, with statistical significance set at 0.05.

The accuracy of the Thai monosyllabic word lists (KKU lists) and the standard OTL test were determined and are presented as percentages and averages.

The consistency of each of the word lists in the Thai monosyllabic speech test which tested the speech discrimination of adults (KKU lists) for all 4 word lists and the standard OTL word lists test for all 5 word lists was analyzed using the intraclass correlation coefficient.

RESULTS

The demographic characteristics of the participants are presented in Table 3. There were 41 males and 35 females with an average age of 46 years in the hearing level groups. The configuration that was discovered consists of 50 flat audiograms (70%), 17 gradually sloping audiograms (20%) and 9 sharply sloping audiograms (10%). The majority of the participants were age 51 to 60 years.

Table 3. Demographics of participants

Characteristics	n=76 n (%)
Genders	
Male	41 (54)
Female	35 (46)
Age (in years)	
19–30	20 (26)
31–40	7 (9)
41–50	8 (11)
51–60	28 (37)
61–70	13 (17)
Ear with better hearing	
Right ear	
Female	15 (20)
Male	25 (33)
Totals	40 (53)
Left ear	
Female	20 (26)
Male	16 (21)
Totals	36 (47)

The current study found no statistically significant differences ($p > 0.05$) in the SRS in the KKU lists or the OTL. In the normal hearing group, no significant differences in the SRS between the KKU lists and OTL were found in an analysis performed using the paired-sample t-test. In all three groups with hearing impairment, it was found that the SRS for the KKU lists and OTL were statistically significantly different ($p < 0.001$) (Table 4).

The relationships between the hearing levels and the SRS in each of the nine-word lists were examined descriptively using correlations. The Pearson's correlation coefficient produced a negative value among all groups of participants ($r = -0.879$; $p < 0.001$) (Figure 2). It was found that as the pure tone average (PTA) increased, the SRS decreased. In the hearing-impaired groups, the SRS in the KKU lists and the OTL were similar with the exception of the OTL (RAMA SD-1) where the SRS were higher than for the other word lists (the linear of RAMA SD-1 % word) (Figure 2). As a result, the authors re-analyzed the statistical relationships after eliminating the RAMA SD-1 scores and found a decrease in the average SRS of the OTL in all participant groups. Analysis using the paired-sample t-test found no significant differences between the OTL and the KKU lists, especially in the severe hearing loss group ($p = 0.083$) (Table 5).

Table 4. The means and standard deviations of the SRS of the KKU lists and OTL

		Mean±SD		Min		Max		Significant level
		Words counted	Word %	Words counted	Word %	Words counted	Word %	
Normal hearing	Totals	24.73±0.51	98.92±2.03	23	92	25	100	0.070
	OTL	24.68±0.53	98.74±2.12	23	92	25	100	
	KKU lists	24.79±0.47	99.16±1.88	23	92	25	100	
Moderate hearing loss	Totals	20.58±1.66	82.33±6.66	17	68	24	96	< 0.001
	OTL	20.94±1.67	83.75±6.70	17	68	24	96	
	KKU lists	20.14±1.55	80.57±6.21	17	68	23	92	
Moderately severe hearing loss	Totals	16.89±1.80	67.56±7.17	12	48	22	88	< 0.004
	OTL	17.18±1.83	68.72±7.31	12	48	22	88	
	KKU lists	16.53±1.72	66.11±6.77	12	48	20	80	
Severe hearing loss	Totals	10.15±3.42	40.58±13.68	4	16	19	76	< 0.083
	OTL	10.45±3.45	41.81±13.82	5	20	19	76	
	KKU lists	9.76±3.36	39.05±13.43	4	16	18	72	

The statistical significance level was $p < 0.05$;
KKU list, Khon Kaen University lists; OTL, original Thai monosyllabic word lists

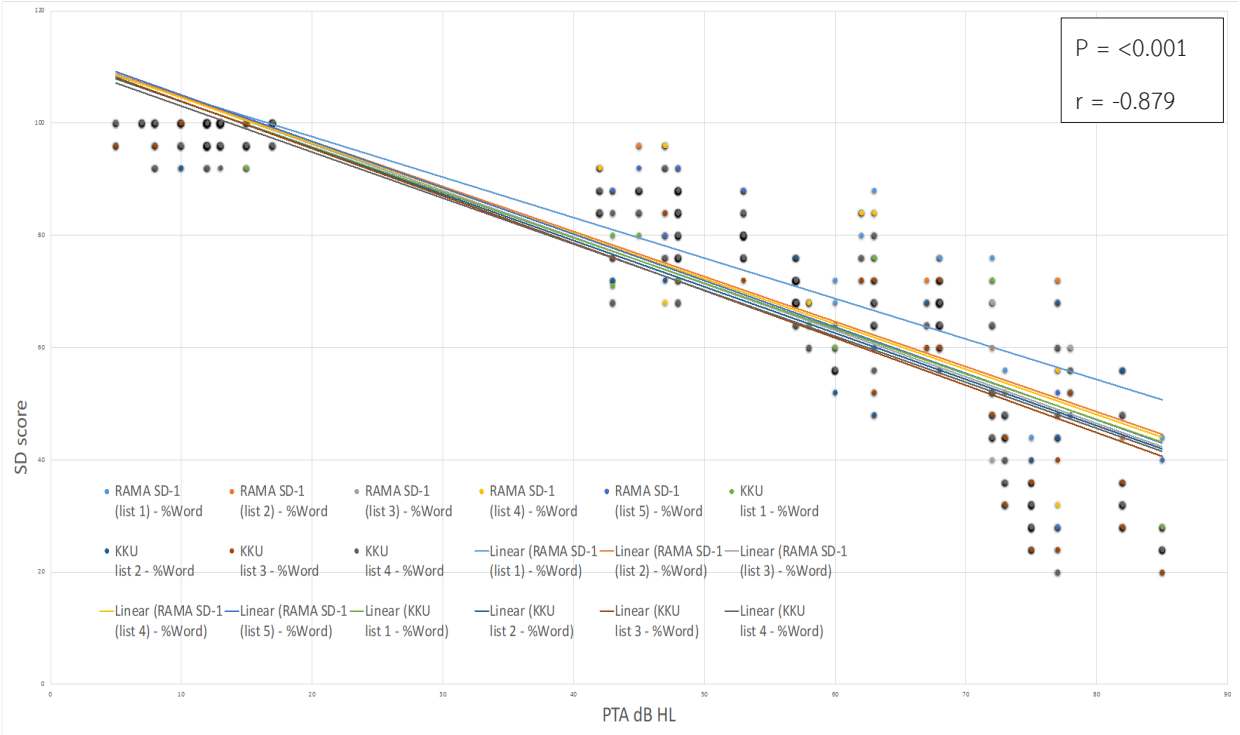

Figure 2. Pearson's correlation analysis of the PTA and the SRS of the OTL and the KKU lists for all the studied groups

Cronbach's alpha coefficient was used to measure the consistency within each word list in the KKU lists and the OTL as well as between the KKU lists and the OTL (Table 6).

DISCUSSION

Consonants, tones, and vowels come together creating the frequency changes of words that affect speech recognition (20). Moreover, tone is important in predicting words, particularly among individuals with sensorineural hearing loss who encounter difficulties with speech recognition. In 2018, Juthamanee demonstrated the confusion that can occur from Thai tonal differences (21). Low tones and rising tones can lead to a high degree of confusion. Particularly in cases of severe sensorineural hearing loss, ambivalence in speech recognition is found from low tones into

Table 5. The means and standard deviations of the SRS of the KKU lists and the OTL (without the SRS from RAMA SD-1 (list 1))

		Mean±SD		Min		Max		Significant level
		Words counted	Word %	Words counted	Word %	Words counted	Word %	
Normal hearing	Totals	24.73±0.51	98.92±2.03	23	92	25	100	0.131
	OTL	24.68±0.53	98.58±2.23	23	92	25	100	
	KKU lists	24.79±0.47	99.16±1.88	23	92	25	100	
Moderate hearing loss	Totals	20.58±1.66	82.33±6.66	17	68	24	96	< 0.001
	OTL	20.94±1.67	83.10±6.71	17	68	24	96	
	KKU lists	20.14±1.55	80.57±6.21	17	68	23	92	
Moderately severe hearing loss	Totals	16.89±1.80	67.56±7.17	12	48	22	88	< 0.001
	OTL	17.18±1.83	67.68±7.32	12	48	22	88	
	KKU lists	16.53±1.72	66.11±6.77	12	48	20	80	
Severe hearing loss	Totals	10.15±3.42	40.58±13.68	4	16	19	76	< 0.001
	OTL	10.45±3.45	40.47±13.32	5	20	19	76	
	KKU lists	9.76±3.36	39.05±13.43	4	16	18	72	

The statistical significance level was $p < 0.05$
KKU list, Khon Kaen University lists; OTL, original Thai monosyllabic word lists

Table 6. The internal consistency values of the PTL and the KKU lists

	OTL	KKU lists	Totals	Significant level
Normal hearing	0.714	0.738	0.807	0.000
Moderate hearing loss	0.953	0.946	0.974	
Moderately severe hearing loss	0.938	0.950	0.947	
Severe hearing loss	0.973	0.969	0.985	
Totals	0.995	0.996	0.998	

KKU list, Khon Kaen University lists; OTL, original Thai monosyllabic word lists

Table 7. The numbers of tones in each of the KKU lists

Tones	Words			
	KKU list 1	KKU list 2	KKU list 3	KKU list 4
Flat tone	3	5	3	5
Down tone	8	8	8	7
Falling tone	9	9	9	9
High tone	3	0	3	2
Rising tone	2	3	2	2

KKU list, Khon Kaen University lists; OTL, original Thai monosyllabic word lists

flat tones, from rising tones into low tones, and from rising tones into flat tones. Lertsukprasert illustrated that children who had experienced severe sensorineural hearing loss and who used hearing aids had low speech recognition scores, especially when hearing words with low tones and rising tones. For that reason, in word lists used in speech recognition tests there should be an awareness of the numbers of words with low tones and rising tones (22) in order to balance the difficulty of guessing words. In the current study, the four KKU lists classified the tones, especially the numbers of words with similar low tones and rising tones, in each word list. Moreover, the lists were phonetically balanced (Table 7). Each word list in the KKU lists was compose of 25 words. In situations involving complicated issues, choosing two word lists for more precising test results might be considered.

The score range (min-max) at each level of hearing loss for all nine-word lists was in the standard value range (Table 8). Thus, the KKU

Table 8. The standard value of speech recognition score compared with KKU lists and OTL.

Levels of hearing (18, 19)	Speech Recognition Scores				
	Standard values (23)	KKU lists		OTL	
	Min-Max	Min-Max	Mean	Min-Max	Mean
Normal (0-25 dB)	90-100%	92-100%	99.16%	92-100%	98.74%
Mild (26-40 dB)	75-89%	-	-	-	-
Moderate (41-55 dB)	60-74%	68-92%	80.57%	68-96%	83.75%
Moderately severe (56-70 dB)	50-59%	48-80%	66.11%	48-88%	68.72%
Severe (>70 dB)	<50%	16-72%	39.05%	20-76%	41.81%

KKU list, Khon Kaen University lists; OTL, original Thai monosyllabic word lists

lists can be used when performing clinical examinations and when determining speech recognition scores.

The averages of the speech recognition scores from the KKU lists and OTL were analyzed using the paired-sample t-test. The results indicate that there were no statistically significant differences among the participants in the normal hearing groups. This result is in accord with the findings of Kasmer, who suggested that people who have normal hearing (0-25 dB HL) have speech recognition scores between 90-100 (23).

The averages of the speech recognition scores between the KKU lists and the OTL among participants who had moderate, moderately severe, and severe sensorineural hearing loss, revealed statistically significant differences. Individuals with mild sensorineural hearing loss (26-40 dB HL) were excluded due to the overlap in the range of normal hearing and moderate sensorineural hearing loss in speech recognition scores (24, 25). Additionally, when the word lists from the KKU lists and the OTL were considered, the outcomes showed that the average scores from the RAMA SD-1 (list 1) differed from the other lists: SRS scores were higher than the other word lists which were found to be equal. However, using the paired-sample t-test to recalculate the scores after removing the RAMA SD-1 (list 1) found that the average scores from the OTL had declined for all hearing levels. Comparison between before the recalculations found the speech recognition scores from the OTL and the KKU lists for the severe sensorineural hearing loss groups had a statistically significant difference ($p < 0.001$), but after recalculation there was no statistically significant difference ($p = 0.083$). This change could be due to the fact that some participants had regularly received audiometry and had previously been tested with OTL, particularly with the RAMA SD-1 (list 1), the first word list used for testing and which is more frequently used than the others. It is very likely that these participants may have been more familiar with the OTL, even though they may have previously had audiometry testing using other word lists before entering the study. In other words, the lack of homogeneity in the OTL suggests that the RAMA SD-1 (list 1) may be easier than other lists and that it could also exhibit an uneven distribution of phonetic and phonemic balance (26, 27). However, when the Mean±SD of the KKU lists and the OTL were examined for the moderate and moderately severe groups, no differences of more than four percent were found between the groups. Regarding the clinical results, the results of SRS testing demonstrated that one correct word had shown a mean of four percent, which meant that there had been no significant differences in the clinical results.

The analyses of the speech recognition scores of the participants with normal hearing and those with severe sensorineural hearing loss showed that the SRS results with both the KKU lists and OTL were in accordance with the standard values (23). However, in the groups with moderate sensorineural hearing loss and moderately severe sensorineural hearing loss, the scores did not follow the standard values.

The differences between the KKU lists and the standard values could have occurred due to the fact that some participants had regularly used hearing aid devices prior to the testing. This may have led to higher scores than those of individuals who did not wear hearing aids despite having similar hearing levels. Another factor that can affect speech recognition scores is the duration

of hearing loss and of rehabilitation (28). Participants may have had different opportunities to gain access to hearing aid devices due to their financial status and to their understanding of the importance of hearing loss rehabilitation (29, 30). According to Downs, patients who have sensorineural hearing loss and who regularly wear hearing aid devices will have significantly better speech discrimination and will require reduced effort in understanding words compared to patients who have similar hearing abilities but who do not use hearing aid devices (31).

CONCLUSIONS

The Thai monosyllabic word lists for the speech recognition test in adults (KKU lists) show phonetic balance in each word list without effects related to the order of usage. The speech recognition scores for each word list of the KKU lists and the OTL, however, tend to decrease as the level of hearing increases. This demonstrates the consistency index value regarding the accuracy of each word list with the exception of the RAMA SD-1 (list 1). Hence, when selecting word lists to determine speech recognition scores, it is advisable to refrain from using the RAMA SD-1 (list 1) due to its limitations in terms of familiarity, phonetic balance, homogeneity of words within the list and elevated SRS. The average SRS from the KKU lists were determined to be closer to the standard value than to the OTL.

ACKNOWLEDGEMENTS

The authors would like to express their deepest gratitude to Prof. Dr. Kwanchanok Yimtae and to Assoc. Prof. Panida Thanawirattananit, for their guidance, support, and encouragement throughout the research process. Their expertise, invaluable feedback, and unwavering commitment have been instrumental in shaping this thesis.

FUNDING

This research was supported by the Faculty of Medicine of Khon Kaen University in Thailand which provided the resources and facilities necessary to conduct this research (Grant Number IN65250)

CONFLICT OF INTEREST

The authors have no conflicts of interest to report.

REFERENCES

1. Wilson R, McArdle R, Roberts H. A comparison of recognition performances in speech-spectrum noise by listeners with normal hearing on PB-50, CID W-22, NU-6, W-1 spondaic words, and monosyllabic digits spoken by the same speaker. J Am Acad Audiol. 2008; 19:496-506.
2. EGAN JP. Articulation testing methods. Laryngoscope. 1948;58:955-91.
3. Marshall L, Bacon S. Prediction of speech discrimination scores from audiometric data. Ear Hear. 1981;2: 148-55.
4. Karino S, Usami S, Kumakawa K, Takahashi H, Tono T, Naito Y, et al. Discrimination of Japanese monosyllables in patients with high-frequency hearing loss. Auris Nasus Larynx. 2016;43:269-80.
5. Mendel L, Owen S. A study of recorded versus live voice word recognition. Int J Audiol. 2011;50:688-93.
6. Haslam V. Psychometrically equivalent monosyllabic words for word recognition testing in Mongolian [dissertation]. Provo, Utah: Brigham Young University; 2009.
7. Hanson C. Development of speech recognition threshold and word recognition materials for native Vietnamese Speakers [dissertation]. Provo, Utah: Brigham Young University; 2014.
8. Miller G, Nicely P. An analysis of perceptual confusions among some English consonants. J Acoust Soc Am. 1955;27:338-52.
9. Bess F, Townsend T. Word discrimination for listeners with flat sensorineural hearing losses. J Speech Hear Disord. 1977;42:232-7.
10. deAndrade A, Iorio M, Gil D. Speech recognition in individuals with sensorineural hearing loss. Braz J Otorhinolaryngol. 2016;82:334-40.
11. Major R, Crystal D. A dictionary of linguistics and phonetics. Mod Lang J. 1992;76:426.
12. Arista M, Panjaitan S, Lubis Y. The role of vowel sound in english pronounciation. Cemara Education and Science. 2024;2:11-6.
13. Wilairatana P, Mizutani K, Kuntonbutr C, Tsutomu K, Ngamjarussrichai P. The effect of final consonants in the cognitive process of thai language. Information Engineering Express. 2019 May 31;5:37-6.
14. Munthuli A, Sirimujalin P, Tantibundhit C, Onsuwan C, Klangpornkun N, Kosawat K. Constructing time phonetically balanced word recognition test in speech audiometry through large written corpora. In 2014 17th Oriental Chapter of the International Committee for the Co-ordination and Standardization of Speech Databases and Assessment Techniques (COCOSDA) 2014 Sep 10 (pp. 1-5). IEEE.
15. Nemr K, Simoes-Zenari M, Cordeiro GF, Tsuji D, Ogawa A, Ubrig M, et al. GRBAS and Cape-V scales: high reliability and consensus when applied at different times. J Voice. 2012;26:812.e17-22. PubMed PMID: 23026732
16. Cambron N, Wilson R, Shanks J. Spondaic word detection and recognition functions for female and male speakers. Ear Hear. 1991;12:64-70.

17. Ji F, Xi X, Chen AT, Ying J, Wang Q, Yang S. Development of a Mandarin monosyllable test material with homogenous items (I): homogeneity selection. Acta Otolaryngol. 2011;131:962-9.
18. The Royal College of Otolaryngologists-Head and Neck Surgeons of Thailand (RCOT) [Internet]. 2021 [cited 2024 Aug 17]. Available from: https://www.rcot.org/2021/ForDoctor/Knowledge-and-CPG/Sections/Doctor-Audible-and-Hearing
19. Olusanya B, Davis A, Hoffman H. Hearing loss grades and the International classification of functioning, disability and health. Bull World Health Organ. 2019; 97:725-28.
20. Houston D, Bergeson T. Hearing versus Listening: Attention To Speech And Its Role In Language Acquisition In Deaf Infants With Cochlear Implants. Lingua. 2014;139:10-25.
21. Onsuwan C. Perception of Thai lexical tones in native- and foreign-language babble noise. Journal of Liberal Arts. 2018;18:134–63.
22. Lertsukprasert K, Suvanich R, Wattanawongsawang W, Kasemkosin N. Tonal perception ability of thai children with cochlear implants and hearing aids. Commun Disord Deaf Stud Hearing Aids. 2018; 6:1000186
23. Kasmer S, Brown DK. Audiology Science to practice. Third edit. San Diego, CA: Plural Publishing Inc; 2010.
24. Sweeney A, Carlson M, Ehtesham M, Thompson R, Haynes D. Surgical approaches for vestibular schwannoma. Curr Otorhinolaryngol Rep. 2014;2:256-64.
25. Wang A, Chinn S, Than K, Arts H, Telian S, El-Kashlan H, et al. Durability of hearing preservation after microsurgical treatment of vestibular schwannoma using the middle cranial fossa approach. J Neurosurg. 2013;119:131-8.
26. Heckendorf A, Wiley T, Wilson R. Performance norms for the VA compact disc versions of CID W-22 (Hirsh) and PB-50 (Rush Hughes) word lists. J Am Acad Audiol. 1997;8:163-72.
27. Poonyaban S, Aungsakulchai P, Tantibundhit C, Onsuwan C, Tiravanitchakul R, Kosawat K, et al. Phonetically balanced and psychometrically equivalent monosyllabic word lists for word recognition testing in Thai. In Proceedings of Meetings on Acoustics 2015 Nov 2 (Vol. 25, No. 1). AIP Publishing.
28. Simpson A, Matthews L, Cassarly C, Dubno J. Time from hearing aid candidacy to hearing aid adoption: a longitudinal cohort study. Ear Hear. 2019;40:468-76.
29. Michels T, Duffy M, Rogers D. Hearing loss in adults: Differential diagnosis and treatment. Am Fam Physician 2019;100:98-108.
30. Goel A, Bruce H, Williams N, Alexiades G. Long-term effects of hearing aids on hearing ability in patients with sensorineural hearing loss. J Am Acad Audiol. 2021;32:374-78.
31. Downs D. Effects of hearing and use on speech discrimination and listening effort. J Speech Hear Disord. 1982;47:189-93.

Biomedical Sciences and Clinical Medicine 2025;64(2):100-106.
doi: 10.12982/BSCM.2025.13
https://he01.tci-thaijo.org/index.php/CMMJ-MedCMJ/index

BSCM
Biomedical Sciences and Clinical Medicine

Original Article

Open Access

Incidence of and Risk Factors for Extrauterine Growth Restriction in Preterm Infants with Gestational Age Less Than 32 Weeks or Birth Weight Less Than 1,500 Grams

Nawinda Rueang-amnat and Mallika Pomrop

Department of Pediatrics, Faculty of Medicine, Chiang Mai University, Chiang Mai, Thailand

Correspondence:
Mallika Pomrop, MD,
Department of Pediatrics,
Faculty of Medicine, Chiang Mai University, 110 Intawarorot Rd, Amphur Muang, Chiang Mai 50200, Thailand.
E-mail: mallika.p@cmu.ac.th

Received: June 14, 2024;
Revised: November 16, 2024;
Accepted: December 2, 2024

ABSTRACT

OBJECTIVE To determine the incidence and risk factors for extrauterine growth restriction (EUGR) in preterm infants with gestational age (GA) less than 32 weeks or birth weight (BW) less than 1,500 grams.

METHODS A retrospective cohort study reviewed preterm infants admitted at Chiang Mai University Hospital between January 1, 2017, and December 31, 2020. EUGR was defined as weight below the 10th percentile at 36 weeks postmenstrual age based on the Fenton growth chart. Data were analyzed, with a p-value of less than 0.05 considered statistically significant. Multivariate regression analysis was adjusted for confounding variables.

RESULTS Among 310 eligible infants, 201 (64.8%) were diagnosed with EUGR. All of 76 SGA infants (100.0%) were EUGR. Significant risk factors included proven sepsis (OR 3.90, 95%CI 1.13-13.45, p = 0.03), diuretic use (OR 3.62, 95%CI 1.47-8.91, p = 0.005), definite NEC (OR 3.54, 95%CI 1.60-7.83, p = 0.002), maternal gestational hypertension (OR 2.36, 95%CI 1.28-4.35, p = 0.006), and multiple births (OR 1.85, 95%CI 1.04-3.28, p = 0.04). Nutritional risk factors were delayed full enteral feeding (OR 1.08, 95%CI 1.03-1.12, p = 0.001) and higher initial glucose infusion rate (GIR) in TPN (OR 1.28, 95%CI 1.11-1.48, p = 0.001). Infants with EUGR had longer hospital stays and higher hospital costs than non-EUGR infants. Multivariate analysis showed significant risks including definite NEC (OR 2.45, 95%CI 1.01-5.96, p = 0.049), maternal gestational hypertension (adjusted OR 2.79, 95%CI 1.46-5.33, p = 0.002), and multiple births (adjusted OR 2.29, 95%CI 1.24-4.24, p = 0.008).

CONCLUSIONS Multiple births, maternal gestational hypertension, SGA status, and NEC were associated with a higher risk of EUGR in preterm infants less than 32 weeks or VLBW. Providing proper antenatal care for mothers with multiple pregnancies or gestational hypertension, along with optimized postnatal care, can help improve growth outcomes and reduce the incidence of EUGR in these infants.

KEYWORDS extrauterine growth restriction, preterm infant, very low birth weight

INTRODUCTION

Over the past few decades, the survival rates of very low birth weight (VLBW) infants, those with birth weights less than 1,500 grams, have increased. However, these infants still face a risk of growth and neurodevelopmental problems

despite their higher overall survival rates (1). Extrauterine growth restriction (EUGR), particularly in VLBW preterm infants, is a prevalent issue that affects healthcare costs, length of hospital stays, and long-term morbidity, including cognitive dysfunction, behavioral problems, and metabolic diseases (2-4).

The incidence of EUGR among VLBW infants varies by country and is influenced by the quality and the competency of neonatal intensive care units (NICUs). In Asian countries, the incidence ranges from 67-72%, which is comparable to European countries where it ranges from 51-73%, but notably higher than in the U.S., where the incidence is 28% (5-9). This variation is likely due to differences in neonatal care practices, nutrition management strategies, and the availability of advanced medical technologies, all of which influence growth outcomes in preterm infants across regions.

Several biological and epidemiological factors contribute to the slower growth of Asian populations compared to Caucasians. One key factor is genetic predisposition. Studies have shown that differences in body composition, including lower lean body mass and higher fat percentage at birth, are more common in Asian infants, which may result in slower postnatal growth rates (10). Additionally, maternal nutritional status during pregnancy in many Asian countries can be suboptimal due to cultural dietary practices, economic factors, or limited access to healthcare, which can affect fetal growth and lead to smaller birth sizes (11). Furthermore, the prevalence of gestational diabetes and hypertension is higher in Asian populations, conditions known to impact fetal growth (12). Another factor is the higher incidence of preterm births in some Asian countries, which increases the likelihood of EUGR in preterm infants (13).

The Fenton growth curve is widely used to define EUGR in preterm infants, including those in Asian populations. It serves as a standardized tool for monitoring growth based on gestational age and birth weight, comparing postnatal growth to intrauterine growth patterns (14). However, the curve was developed using data predominantly from Western populations, which may not fully represent the growth characteristics of Asian infants who generally have lower birth weights and smaller body sizes at the same gestational ages compared to their Caucasian counterparts (15, 16). Despite these limitations, the Fenton growth curve remains a valuable tool for growth monitoring and continues to be used in our institution for assessing growth in VLBW infants.

Previous studies have identified several prenatal and postnatal risk factors for EUGR. Prenatal risk factors include advanced maternal age (over 35 years), multiple births, and pregnancy complications such as placental abruption, maternal gestational hypertension, and gestational diabetes (1, 17). Postnatal risk factors include general issues such as nutritional deficiencies and being small for gestational age (SGA), as well as comorbidities such as respiratory distress syndrome, patent ductus arteriosus (PDA), necrotizing enterocolitis (NEC), intraventricular hemorrhage (IVH), retinopathy of prematurity (ROP), and bronchopulmonary dysplasia (BPD) (1, 9, 18).

No study has yet examined the incidence and risk factors of EUGR in Thailand, limiting the development of strategies to prevent or reduce it. Since the incidence and risk factors for EUGR differ between countries due to population differences and healthcare practices and no data is available for Thailand, further research is needed. This study aims to identify the incidence and risk factors of EUGR in VLBW infants in Thailand.

METHOD

This retrospective cohort study utilized data gathered from electronic medical records. Participants included preterm infants with a gestational age (GA) of less than 32 weeks or a birth weight of less than 1,500 grams (very low birth weight; VLBW) who were born in a hospital or admitted within 48 hours after birth at Chiang Mai University Hospital, Thailand, a tertiary care hospital, between January 1, 2017, and December 31, 2020.

Patients with chromosomal abnormalities, major congenital malformations (including critical congenital heart conditions and surgical congenital gastrointestinal conditions), TORCH infections, and those who died before 36 weeks postmenstrual age (PMA) were excluded.

The sample size was calculated using a statistical formula based on a 95% confidence level and a 5% margin of error. This calculation was informed by the study of Peila. (8), which reported an EUGR incidence of 73% in preterm infants with a GA of

less than 30 weeks or a birth weight of less than 1,500 grams. Consequently, the required sample size for our study was determined to be 303 patients.

EUGR was diagnosed when the patient's weight at 36 weeks PMA was less than the 10th percentile according to the Fenton growth chart. Respiratory distress syndrome was diagnosed based on signs of increased work of breathing and a demonstration of fine reticular granularity of lung parenchyma with air bronchograms on chest radiography (19). PDA was diagnosed based on the presence of clinical signs plus abnormal radiographic findings, including increased pulmonary vasculature or cardiomegaly, or on echocardiographic findings of PDA which were treated medically or surgically (20). NEC was diagnosed based on clinical, radiological, and/or histopathological evidence that fulfilled stage II or III of modified Bell's criteria and was treated medically or surgically (21). IVH was detected by a radiologist and graded by Papile's classification as severe as grade III or IV (22). BPD was diagnosed using the definitions from the National Institutes of Health 2018 (23). Resuscitation in the delivery room was defined as one or more of the following procedures: positive pressure ventilation (PPV), chest compression (CPR), intubation, or continuous positive airway pressure. Proven sepsis was defined by the presence of a positive hemoculture and correlated with clinical signs of sepsis. SGA was diagnosed when the patient's birth weight was less than the 10th percentile according to the Fenton growth chart.

According to Chiang Mai University Hospital's feeding guidelines for VLBW infants, these infants are started on a standard intravenous solution containing glucose, amino acid, and calcium gluconate within 24-48 hours after birth, followed by parenteral nutrition the next day with initial fluids of 60-100 mL/kg/day, initial protein of 2-3 g/kg/day, initial glucose of 4-6 mg/kg/min, and initial lipid of 1-2 g/kg/day. Enteral nutrition is initiated within 48 hours after birth or when the infant is clinically stable, with colostrum (0.5-2 mL) used as mouth care every 8 hours, or more frequently if enteral nutrition cannot be started.

Statistical analysis

Data were analyzed using IBM SPSS statistics for Windows, version 26 (SPSS, Armonk, NY, USA). A p-value of less than 0.05 was considered statistically significant. Demographic data of infants with and without EUGR were compared using the Student's t-test for continuous variables and the Chi-square test for categorical variables, while the Mann-Whitney U test or the t-test was utilized for continuous variables in univariate analysis.

Multivariate regression analysis was used to adjust for potentially confounding variables based on significant data from the univariate logistic analysis of factors associated with EUGR. Analysis of covariance was used for continuous outcome variables, and logistic regression was used for dichotomous variables. Results are reported for both analyses if the findings were significantly different. Logistic regression analysis results are expressed as odds ratios (OR) with 95% confidence intervals (CI).

Ethical approval

The study was approved by the Research Ethic Committee Faculty of medicine, Chiang Mai University, under protocal code PED-2564-08082.

RESULTS

A total of 403 preterm infants with GA less than 32 weeks or VLBW were admitted to Chiang Mai University Hospital over four years. Ninety-three infants were excluded due to being referred at more than 48 hours of age, dying before 36 weeks PMA or discharge, having significant congenital anomalies or chromosomal abnormalities, or having a TORCH infection. This left 310 infants enrolled in the study. The data was completely reviewed without missing data.

Among the 310 eligible infants, 201 (64.8%) were diagnosed with EUGR. Additionally, all 76 SGA infants were identified with EUGR (100%). The demographic and clinical characteristics of infants with and without EUGR are shown in Table 1. Significant risk factors associated with EUGR included proven sepsis (OR 3.90, 95%CI 1.13-13.45, p = 0.030), diuretic use (OR 3.61, 95%CI 1.47-8.90, p = 0.005), definite NEC (OR 3.53, 95%CI 1.60-7.82, p = 0.002), maternal gestational hypertension (OR 2.35, 95%CI 1.27-4.34, p = 0.006), and multiple births (OR 1.84, 95%CI 1.04-3.27, p = 0.040). Nutritional risk factors included longer time to full enteral feeding (OR 1.07, 95%CI 1.02-1.12, p = 0.001) and higher GIR started in TPN (OR 1.28, 95%CI 1.10-1.48, p = 0.001). Infants with EUGR had

Table 1. Demographic and clinical characteristics of infants with and without extrauterine growth restriction (EUGR)

Factors	EUGR (n=201)	Non EUGR (n=109)	*p*-value
Male gender, n (%)	99 (49)	55 (50)	0.840
Mean gestational age, weeks (±SD)	30.5 (±2.9)	30.0 (±2.5)	0.139
Mean birth weight, grams (± SD)	1130 (±328)	1441 (±429)	< 0.001*
Antenatal factors			
Elderly gravida, n (%)	58 (29)	37 (34)	0.353
Multiple births, n (%)	59 (29)	20 (18)	0.034*
Any doses antenatal steroid, n (%)	164 (82)	92 (84)	0.533
Placenta abruption, n (%)	8 (4)	9 (8)	0.114
PROM, n (%)	53 (26)	29 (27)	0.964
Gestational diabetes, n (%)	33 (16)	22 (20)	0.407
Maternal gestational hypertension, n (%)	58 (29)	16 (15)	0.005*
Intrauterine growth restriction, n (%)	38 (19)	0 (0)	< 0.001*
Intrapartum factors			
Mean APGAR score at 5 min, score (± SD)	7 (±1)	7 (±1)	0.652
Resuscitation, n (%)	173 (86)	98 (90)	0.331
Postnatal factors			
General Postnatal factors			
- Small for gestational age, n (%)	76 (38)	0 (0)	< 0.001*
- Median NPO time, day (Range)	1 (0-106)	1 (0-21)	0.026*
- Median age at first TPN was started, hour (range)	13 (1-30)	12 (1-70)	0.213
- Mean of initial parenteral protein, gram/kg/day (± SD)	2.7 (±1.4)	2.2 (±1.0)	0.091
- Mean of initial parenteral fat, gram/kg/day (± SD)	1.1 (±0.4)	0.9 (±0.5)	0.093
- Mean of initial parenteral glucose, mg/kg/min (± SD)	5.5 (±1.4)	4.8 (±2.1)	0.001*
- Median TPN duration, day (Range)	9 (1-127)	8 (1-44)	< 0.001*
- Median time to full enteral feeding, day (range)	11 (2-126)	9 (2-45)	< 0.001*
- Breast milk as initial enteral feeding, n (%)	184 (92)	99 (91)	0.831
- Fortified breast milk, n (%)	198 (99)	102 (94)	0.019*
- Mean of max PF concentration, kcal/oz (± SD)	24 (±2)	24 (±1)	0.002*
- Mean of maximum enteral feeding total volume, mL/kg/day (± SD)	156 (±10)	154 (±8)	0.251
- Mean of maximum calories, kcal/kg/day (± SD)	128 (±8)	123 (±8)	0.891
Medication treatment			
- Post- natal steroid use, n (%)	33 (16)	6 (6)	0.060
- Diuretic drug, n (%)	35 (17)	6 (6)	0.030*
- Aminophylline, n (%)	118 (59)	65 (60)	0.874
- Median initial multivitamin, day (range)	11 (3-127)	10 (5-45)	0.003*
- Median initial iron supplement, day (range)	19 (10-140)	18 (12-52)	< 0.001*
Co-morbidities			
- RDS with surfactant, n (%)	57 (28)	36 (33)	0.392
- PDA with treatment, n (%)	72 (36)	35 (32)	0.512
- NEC, n (%)	44 (22)	8 (7)	0.001*
- Severe IVH (gr 3-4), n (%)	9 (4)	5 (5)	0.965
- BPD, n (%)	70 (35)	32 (29)	0.328
- ROP, n (%)	55 (27)	22 (20)	0.162
- Proven sepsis, n (%)	20 (10)	3 (3)	0.021*
Outcomes			
Median length of stay, day (range)	55 (16-381)	45 (7-223)	< 0.001*
Median cost, Thai baht (range)	294,833 (48,722-2,584,449)	209,079 (24,494-2,339,900)	0.001*

*Statistically significant

PROM, premature rupture of membranes; TPN, total parenteral nutrition; PF, preterm formula; RDS, respiratory distress syndrome; PDA, patent ductus arteriosus; IVH, intraventricular hemorrhage; BPD, bronchopulmonary dysplasia; ROP, retinopathy of prematurity

longer hospital stays (55 [16-381] vs 45 [7-223] days, $p < 0.001$) and higher hospital costs (294,833 [48,722-2,584,449] vs 209,079 [24,494-2,339,900] THB, $p < 0.001$) than non-EUGR infants. The significant risk factors were subsequently calculated for odds ratio, 95%CI, and p-value, as presented in Table 2.

Multivariate analysis was conducted to control for several potential confounders, as demonstrated in Table 3. The significant risk factors found to increase the risk of EUGR among infants with GA less than 32 weeks or VLBW included definite NEC (OR 2.45, 95%CI 1.004-5.98, $p = 0.049$), maternal gestational hypertension (adjusted OR 2.78, 95%CI 1.46-5.32, $p = 0.002$), and multiple births (adjusted OR 2.29, 95%CI 1.23-4.23, $p = 0.008$).

DISCUSSION

In this study, the incidence of EUGR was 64.8% in infants with GA less than 32 weeks or VLBW, which aligns with previous studies, particularly those from China, Taiwan, Spain, and Italy (1, 5, 6, 8, 9, 24). In contrast, the EUGR incidence in our study was significantly higher than in US studies (7). All 76 SGA infants were identified with EUGR (100%).

Liao (1) and Figueras-Aloy (9) found that multiple births were a risk factor for EUGR, which is consistent with our study (adjusted OR = 2.29, 95%CI 1.24-4.24). Maternal gestational hypertension was also significantly associated with EUGR (adjusted OR = 2.79, 95%CI 1.46-5.33), a finding supported by Za Zhi and Figueras-Aloy. Both factors were also associated with intrauterine growth restriction (IUGR), as found in our study.

Definite NEC was a significant risk factor for EUGR (adjusted OR = 2.45, 95%CI 1.00-5.99) because NEC causes bowel inflammation and a longer duration of NPO time. This finding is similar to those of Clark (7) and Figueras-Aloy (9). From this finding, the prevention of NEC should be more emphasized, including nutritional issues, feeding protocols for preterm infants, and reducing the prolonged use of antibiotics.

In our study, infants who received oral diuretics for more than two weeks (adjusted OR = 2.62, 95%CI 0.99-6.98, $p = 0.05$) with doses of 1-3 mg/kg/day of furosemide, spironolactone, or hydrochlorothiazide due to chronic conditions, including 74% with moderate to severe BPD and others with acyanotic congenital heart disease with increased pulmonary blood flow, were found to be significant risk factors for EUGR. Although the use of diuretics was found to be not statistically significant after further analysis, it may still impact growth outcomes. Prolonged use of diuretics, particularly loop diuretics like furosemide, can negatively affect growth outcomes. Diuretics increase the excretion of essential electrolytes

Table 2. Univariate logistic analysis of factors associated with EUGR

Risk factors	Odds ratio	95% confidence interval	p-value
Proven sepsis, n (%)	3.90	1.13-13.45	0.031
Diuretic drug, n (%)	3.61	1.47-8.90	0.005
NEC, n (%)	3.53	1.60-7.82	0.002
Maternal gestational hypertension, n (%)	2.35	1.27-4.34	0.006
Multiple births, n (%)	1.84	1.04-3.27	0.035
Mean of initial parenteral glucose, mg/kg/min (± SD)	1.28	1.10-1.48	0.001
Mean of max PF concentration, kcal/oz (± SD)	1.26	1.04-1.52	0.016
Median time to full enteral feeding, day (range)	1.07	1.02-1.12	0.001

NEC, necrotizing enterocolitis; EUGR, extrauterine growth restriction

Table 3. Multivariate logistic regression analysis of factors associated with EUGR

Risk factors	Adjusted odds ratio	95% confidence interval	p-value
Maternal gestational hypertension, n (%)	2.78	1.46-5.32	0.002
NEC, n (%)	2.45	1.004-5.98	0.049
Multiple births, n (%)	2.29	1.23-4.23	0.008

NEC, necrotizing enterocolitis; EUGR, extrauterine growth restriction

and nutrients, such as sodium, potassium, calcium, and chloride, which are critical for growth and development in preterm infants (25). Chronic diuretic therapy may lead to imbalances in these electrolytes and contribute to poor weight gain and linear growth, potentially exacerbating the risk of EUGR (26). Since oral diuretics are frequently used in our hospital, adjusting the treatment strategy to reduce their use should be encouraged.

A strength of this study is that all medical records were thoroughly reviewed using proper data gathering methods, and a standardized definition for EUGR diagnosis was applied. However, the study is limited by its retrospective design, which introduces potential bias, particularly in the definition of certain risk factors. For example, NEC was only defined as definite NEC if it met stage II or III criteria by the modified Bell's staging, whereas NEC stage I, which involves NPO management for 1-3 days, could also affect infant growth but was not included. Similarly, in cases of PDA without medical or surgical management, fluid intake may have been restricted to treat the condition, potentially impacting growth and contributing to EUGR.

Additionally, this study used the Fenton growth curve to define EUGR in the Thai population. The Fenton growth curve was developed primarily from data on Western populations, which may not accurately reflect the growth patterns of Asian infants, including Thai infants, who typically have smaller birth weights and body sizes compared to Caucasian infants (14, 15). This discrepancy could lead to an overestimation of EUGR incidence in the Thai population. Furthermore, as the Fenton curve is based on intrauterine growth patterns, it may not fully account for postnatal growth in preterm infants, especially those with complex medical conditions (16). This limitation underscores the need for population-specific growth references that better capture the growth trajectories of Thai infants as a means of improving the accuracy of EUGR diagnosis and management.

Based on our study findings, improving antenatal care to manage maternal conditions, such as gestational hypertension, and providing counseling on the risk of EUGR associated with multiple pregnancies are important. During hospitalization, special attention should be given to infants at high risk of EUGR, particularly those classified as SGA. Careful monitoring of these infants, along with adjusting feeding strategies to ensure adequate energy intake and reduce complications like NEC, is essential. Additionally, minimizing the use of diuretics is crucial to promoting better growth outcomes in VLBW infants.

CONCLUSIONS

Multiple births, maternal gestational hypertension, SGA status, and NEC are associated with a higher risk of EUGR in very preterm or VLBW infants. Providing proper antenatal care for mothers with multiple pregnancies or gestational hypertension, along with optimized postnatal care, can help improve growth outcomes and reduce the incidence of EUGR in these infants.

ACKNOWLEDGMENTS

None

FUNDING

This research received no specific grant from any funding agency in the public, commercial, or not-for-profit sectors.

CONFLICT OF INTEREST

The authors have no conflicts of interest to report.

ADDITIONAL INFORMATION

Author contribution

N.R.: contributed to concept and design the study, acquisition and analysis of the data, draft the manuscript; M.P.: contributed to concept and design the study, analysis and interpretation of the data and critically revise the manuscript. All authors approved the final manuscript as submitted.

Data availability statement

The authors confirm that the data supporting the findings of this study are available within the article.

REFERENCES

1. Liao W, Lin M, Wang T, Chen C; Taiwan Premature Infant Follow-up Network. Risk factors for postdischarge growth retardation among very-low-birth-weight infants: A nationwide registry study in Taiwan. Pediatr Neonatol. 2019;60:641-7.

2. Ruth VA. Extrauterine growth restriction: a review of the literature. Neonatal Netw. 2008;27:177-84.
3. De Curtis M, Rigo J. Extrauterine growth restriction in very-low-birthweight infants. Acta Paediatr. 2004; 93:1563-8.
4. Radmacher PG, Looney SW, Rafail ST, Adamkin DH. Prediction of extrauterine growth retardation (EUGR) in VVLBW infants. J Perinatol. 2003;23:392-5.
5. Collaborative Group for the Nutritional, Growth and Developmental Study on Very Low Birth Weight Infants. [Postnatal growth of very low birth weight infants during hospitalization]. Zhonghua Er Ke Za Zhi. 2013;51:4-11. Chinese. PubMed PMID: 23527924.
6. Hsu CT, Chen CH, Lin MC, Wang TM, Hsu YC. Correction: Post-discharge body weight and neurodevelopmental outcomes among very low birth weight infants in Taiwan: A nationwide cohort study. PLoS One. 2019;14(1):e0211526. PubMed PMID: 30682164.
7. Clark RH, Thomas P, Peabody J. Extrauterine growth restriction remains a serious problem in prematurely born neonates. Pediatrics. 2003;111:986-90.
8. Peila C, Spada E, Giuliani F, Maiocco G, Raia M, Cresi F, Bertino E, Coscia A. Extrauterine growth restriction: definitions and predictability of outcomes in a cohort of very low birth weight infants or preterm neonates. Nutrients. 2020;12(5):1224. PubMed PMID: 32357530.
9. Figueras-Aloy J, Palet-Trujols C, Matas-Barceló I, Botet-Mussons F, Carbonell-Estrany X. Extrauterine growth restriction in very preterm infant: etiology, diagnosis, and 2-year follow-up. Eur J Pediatr. 2020; 179:1469–79.
10. Victora CG, Villar J, Barros FC, Ismail LC, Chumlea C, Papageorghiou AT, et al. Anthropometric characterization of impaired fetal growth: risk factors for and prognosis of newborns with stunting or wasting. JAMA Pediatr. 2015;169:e151431. PubMed PMID: 26147058
11. Black RE, Victora CG, Walker SP, Bhutta ZA, Christian P, de Onis M, et al. Maternal and child undernutrition and overweight in low-income and middle-income countries. Lancet. 2013;382(9890):427-51.
12. Hedderson MM, Gunderson EP, Ferrara A. Gestational weight gain and risk of gestational diabetes mellitus. Obstet Gynecol. 2010;115:597-604.
13. Blencowe H, Cousens S, Oestergaard M, Chou D, Moller AB, Narwal R, et al. National, regional, and worldwide estimates of preterm birth rates in the year 2010 with time trends since 1990 for selected countries: a systematic analysis and implications. Lancet. 2012;379(9832):2162-72.
14. Fenton TR, Kim JH. A systematic review and meta-analysis to revise the Fenton growth chart for preterm infants. BMC Pediatr. 2013;13:59. PubMed PMID: 23601190
15. Villar J, Cheikh Ismail L, Victora C, Ohuma EO, Bertino E, Altman DG, et al. International standards for newborn weight, length, and head circumference by gestational age and sex: The Newborn Cross-Sectional Study of the INTERGROWTH-21st Project. Lancet. 2014;384:857-68.
16. Lee A, Kozuki N, Cousens S, Stevens G, Blencowe H, Silveira M, et al. Estimates of burden and consequences of infants born small for gestational age in low- and middle-income countries with INTERGROWTH-21st standard: analysis of CHERG datasets. BMJ. 2017;358. PubMed PMID: 28893769.
17. Tozzi M, Moscuzza F, Michelucci A, Lorenzoni F, Cosini C, Ciantelli M, et al. ExtraUterine Growth Restriction (EUGR) in preterm infants: growth patterns, nutrition, and epigenetic markers. a pilot study. Front Pediatr. 2018;6:408. PubMed PMID: 30619799.
18. Zozaya C, Avila-Alvarez A, Arruza L, García-Muñoz Rodrigo F, Fernandez-Perez C, Castro A, et al. The effect of morbidity and sex on postnatal growth of very preterm infants: a multicenter cohort study. Neonatology. 2019;115:348-54.
19. Reuter S, Moser C, Baack M. Respiratory distress in the newborn. Pediatrics In Review. 2014;35:417–29.
20. Benitz W; Committee on Fetus and Newborn, American Academy of Pediatrics. Patent ductus arteriosus in preterm infants. Pediatrics. 2016;137. PubMed PMID: 26672023.
21. Gregory KE, DeForge CE, Natale KM, Phillips M, Van Marter LJ. Necrotizing enterocolitis in the premature infant: neonatal nursing assessment, disease pathogenesis, and clinical presentation. Adv Neonatal Care. 2011;11:155–64.
22. Smith WL, McGuinness G, Cavanaugh D, Courtney S. Ultrasound screening of premature infants: longitudinal follow-up of intracranial hemorrhage. Radiology. 1983;147:445–8.
23. Gilfillan M, Bhandari A, Bhandari V. Diagnosis and management of bronchopulmonary dysplasia. BMJ. 2021;375:n1974. PubMed PMID: 34670756
24. Shan HM, Cai W, Cao Y, Fang B, Feng Y. Extrauterine growth retardation in premature infants in Shanghai: a multicenter retrospective review. Eur J Pediatr. 2009;168:1055-9.
25. Oh W, Poindexter B, Perritt R, Lemons J, Bauer C, Ehrenkranz R, et al. Association between fluid intake and weight loss during the first ten days of life and risk of bronchopulmonary dysplasia in extremely low birth weight infants. J Pediatr. 2005;147:786-90.
26. Stewart A, Brion L, Ambrosio-Perez I. Diuretics acting on the distal renal tubule for preterm infants with (or developing) chronic lung disease. Cochrane Database Syst Rev. 2011;2011:CD001817. PubMed PMID: 21901679.

Biomedical Sciences and Clinical Medicine 2025;64(2):107-125.
doi: 10.12982/BSCM.2025.10
https://he01.tci-thaijo.org/index.php/CMMJ-MedCMJ/index

Original Article

Open Access

Identification of Genomic Alterations in Chemotherapy-Related Genes: A Preliminary Study in Three Thai Adolescents with Fatal Osteosarcoma at Maharaj Nakorn Chiang Mai Hospital

Nitipum Nantasuwan[1], Sara Wattanasombat[2], Patcharawadee Thongkumkoon[3], Parunya Chaiyawat[3,4], Dumnoensun Pruksakorn[3,4,5] and Siripong Tongjai[2]

[1]Faculty of Medicine, [2]Department of Microbiology, [3]Center of Multidisciplinary Technology for Advanced Medicine (CMUTEAM), [4]Musculoskeletal Science and Translational Research (MSTR) Center, [5]Department of Orthopedics, Faculty of Medicine, Chiang Mai University, Chiang Mai, Thailand

Correspondence:
Siripong Tongjai, PhD,
Department of Microbiology,
Faculty of Medicine, Chiang Mai University, 110 Inthavaroros Rd,
Tambon Si Phum, Amphoe Muang,
Chiang Mai, 50200, Thailand.
E-mail: siripong.tongjai@cmu.ac.th

Received: April 10, 2024;
Revised: January 13, 2025;
Accepted: February 20, 2025

ABSTRACT

OBJECTIVE Osteosarcoma (OS) is the most common primary bone malignancy among adolescents and young adults. It is characterized by a high mortality rate, though it remains a relatively rare disease overall. The treatment protocols can be complex and challenging. We conducted a comparative genomic variation study to identify genes involved in the metabolism of chemotherapy drugs that are affected by various genomic alterations.

METHODS This study analyzed the germline and tumor genomes of three OS patients who responded poorly to chemotherapy, developed lung metastases, and ultimately succumbed to the disease. Genes of interest were identified through a systematic review of apoptosis, autophagy, necroptosis, and chemotherapy-related databases. Whole-genome sequencing (WGS) revealed deleterious single nucleotide polymorphisms (SNPs), copy number variations (CNVs), and structural variations (SVs) in genes linked to cancer and chemotherapy. Protein association network analyses were used to highlight both shared and unique biological processes associated with OS in these patients.

RESULTS Pathogenic SNPs were identified exclusively in patients P1 and P3. Patient P1 exhibited a missense mutation in the *PIK3CD* gene and a splice donor site mutation in the *TP53* gene, while patient P3 carried a nonsense mutation in the *MLH1* gene. The tumor genome of patient P1 showed extensive CNVs, whereas those of patients P2 and P3 displayed fewer CNV regions. *TBX4* and *PPM1D* were common genes affected in both patients P1 and P2. SVs were detected in all three tumor genomes, impacting different key genes involved in platinum drug resistance and DNA repair. Notably, all three patients shared SVs in the *TDG* and *SPECC1* genes. All identified mutated genes were correlated with clinical features of the patients.

CONCLUSIONS This study highlights the potential of genomic analysis to improve the diagnosis, treatment, and management of OS. Insights into therapy resistance mechanisms and key genomic alterations offer opportunities for developing targeted therapies and predictive biomarkers. These findings support the advancement of precision oncology in OS, as a means of paving the way for personalized treatment approaches to improve patient outcomes.

KEYWORDS osteosarcoma, genome, single nucleotide polymorphisms, copy number variations, structural variations, chemotherapy

INTRODUCTION

Osteosarcoma (OS) is the most common malignant bone tumor; it is marked by the deposition of immature osteoid matrix (1). Its prevalence varies by age, ethnicity, and genetics, with a bimodal age distribution peaking in children and adolescents and again in the elderly (2). The 5-year survival rate is approximately 60-70% (3), but the prognosis worsens if the tumor shows less than 90% necrosis after treatment (4). Treatments includes surgery, chemotherapy, and immunotherapy (3). While the pathogenesis of OS remains unclear, chromosomal abnormalities have been linked to increased susceptibility to the disease (2, 3, 5).

Genomic instability plays a critical role in tumor formation. Chromothripsis, in particular, results from the imperfect repair of fragmented chromosomes caused by clustered DNA double-strand breaks, occurring in a single event rather than gradually (6). Normally, this catastrophic rearrangement triggers apoptosis, but if apoptosis fails, the misrepaired genetic material can drive tumor development (6). Chromothripsis has been identified in OS, with studies reporting its presence in a significant number of cases (7, 8).

Chromothripsis plays a significant role in tumor development and progression by causing fragmented and rearranged chromosomes. These rearrangements can deactivate tumor suppressor genes, amplify oncogenes, and result in other genomic alterations which contribute to the cancer phenotype. Common rearrangements include structural variations (SVs) and copy number variations (CNVs). Examples include translocations impacting tumor suppressor genes like *TP53*, *RB1*, and *WWOX*, as well as CNVs such as copy number gains in *DK4* and *CCNE1* and copy number losses in *CDKN2A* and *TP53*. Additionally, *TP53* mutations are linked to early onset and higher metastatic rates in OS (9, 10). In addition, rs7591996 has been linked to increased OS risk (11). Abnormal expression of the anti-apoptotic *AKT1* gene and pro-apoptotic *BAX* gene (12), as well as autophagic and necroptotic genes like *BECN1* (13) and *RIPK1* (14), has also been observed in OS.

Platinum-based chemotherapy works by creating DNA crosslinks, leading to cytotoxicity and apoptosis. However, tumor resistance to platinum drugs can arise through mechanisms such as altered drug transport, enhanced DNA repair, modified survival pathways, pleiotropic changes, and tumor microenvironment alterations. For example, increased expression of cisplatin export modulators ATP7A and ATP7B contributes to resistance (15). Previous reports have identified 74,880 single nucleotide variants and indels, along with common CNVs, such as gains and losses in specific chromosomal regions. High expression of *PTPRQ* has been linked to poor prognosis (16). Thus, exploring CNVs in chemotherapy-related genes could potentially help develop personalized treatment strategies.

This study addresses the complexity of OS, a rare bone cancer with diverse genetic alterations that impact cell death and chemotherapy response. By analyzing genomic data from tumor and normal samples, the research aimed to identify somatic and germline mutations, focusing on structural changes in the tumor genomes of adolescents with fatal OS and poor chemotherapy outcomes, to advance understanding and treatment strategies.

METHODS

Patients

Three OS patients, all of whom had been treated at Maharaj Nakorn Chiang Mai Hospital in Chiang Mai, Thailand, were identified as P1, P2, and P3 (Table 1). Both P1 and P3 were male patients, while P2 was a female patient. All three underwent surgeries and received chemotherapy as part of their treatment. As shown in Table S1, the treatment for P1 lasted 843 days, during which time the patient received chemotherapy twice. Table S2 shows that patient P2 was scheduled to receive chemotherapy 8 times over an 836-day treatment period. The treatment for patient P3 lasted 358 days with 2 scheduled chemotherapy sessions, as shown in Table S3. Tissue/tumor biopsy specimens from the patients were collected during their first surgeries. The tissue specimens and their whole blood samples were stored at the Tissue Bank of Musculoskeletal Science and Translational Research Center, Department of Orthopaedics, Faculty of Medicine, Chiang Mai University, Chiang Mai, Thailand. Toward the end of their treatment, all three patients developed lung metastases, and all succumbed to the disease. The whole blood and tumor tissue specimens collected from the patients were extracted for

Table 1. Patients' characteristic data

Parameter	Detail
Age	15.33 years (range 11-20 years)
Gender, n (%)	
Male	2 (66.67)
Female	1 (33.33)
Osteosarcoma type, n (%)	
Conventional type	3 (100.00)
Stage at the time of diagnosis, n (%)	
IIb	3 (100.00)
Chemotherapy, n (%)	
DOX+CPT	2 (66.60)
DOX+CPT+HDMTX	1 (33.30)
Tumor necrotic percentage	64% (range 42-85%)
Metastasis status, n (%)	
Yes	3 (100.00)
No	0 (0.00)
Recurrence status, n (%)	
Yes	2 (66.67)
No	1 (33.33)
Survival duration	678 days (357-842 days)
Status, n (%)	
Death	3 (100.00)
Alive	0 (0.00)

DOX, doxorubicin; CPT, camptothecin; HDMTX, high-dose methotrexate.

germline and somatic genomic DNA for Whole Genome Sequencing (WGS), respectively.

Systematic review

A list of genes of interest was created by reviewing articles available in public databases, referencing articles (12-14, 17-60) with keywords relevant to the biological processes of interest: apoptosis, autophagy, and necroptosis. The article selection scheme, depicted in Figure 1, resulted in the selection of 63 articles. From these articles, a list of 57 genes of interest was compiled, as shown in Table S4. The gene list included PharmGKB-curated genes involved in the pharmacodynamic and pharmacokinetic pathways of chemotherapy administered to the patients (Table S1, S2, and S3), such as the Platinum pathway (pharmacokinetics/pharmacodynamics), Etoposide pathway, Ifosfamide pathway, Methotrexate pathways (pharmacokinetics, antimetabolite, and cancer), and Doxorubicin pathways (pharmacokinetics and cancer) (61-65). The gene list also encompassed genes with mutations detected in OS or cancer patients (5, 9, 10, 16). In total, 1,794 genes of interest were identified in this study, as detailed in Table S5.

Genomic DNA extraction

Tumor tissue and matched normal genomic DNA samples were extracted from whole blood and OS tissue biopsy specimens, respectively, using a modified salting-out method, as described in Supplementary Data Doc. S1.

Whole Genome Sequencing

Genomic DNA samples extracted from both the matched normal genome (white blood cells, WBC) and corresponding OS tissue met the requirements for WGS and were sent to Macrogen Korea for sequencing. WGS for the germline genomic DNA was conducted at a 30X read depth, while that of the tissue genomic DNA was performed at a 60X read depth. An Illumina NovaSeq 6000 system (Illumina, Inc., San Diego, CA, USA) was used as the sequencing platform.

Secondary NGS data analysis

WGS data from the tumor and the matched normal genomes of the three patients were analyzed using the Genome Analysis Toolkit (GATK) Best Practices (66) or single-sample short variant discovery. The human reference genome hg38 was utilized throughout the pipeline. The analysis was conducted on a Google Cloud Compute server using a custom script written in the Workflow Description Language (WDL) and managed by Cromwell (67). The pipeline includes paired-end read alignment using BWA-MEM (68). The alignment files were subsequently sorted by chromosome and by base quality score recalibration (BQSR). Known sites of indels in the human reference genome hg38 were excluded to enhance the accuracy of variant calling. Local computer servers were employed for less resource-intensive tasks, e.g., variant selection, SVs detection, and CNV estimation.

Tertiary NGS data analysis

Since the extracted variation data contained both pathologic and common variants, the common genomic variants detected or reported in both the patients and the genome database of the 1,000 Genomes Project (69) were filtered out. Notably, the 1,000 Genomes Project includes data from the Dai ethnic group in China, whose genetic background is relatively close to that of the majority of the population in Thailand (70). The variants were

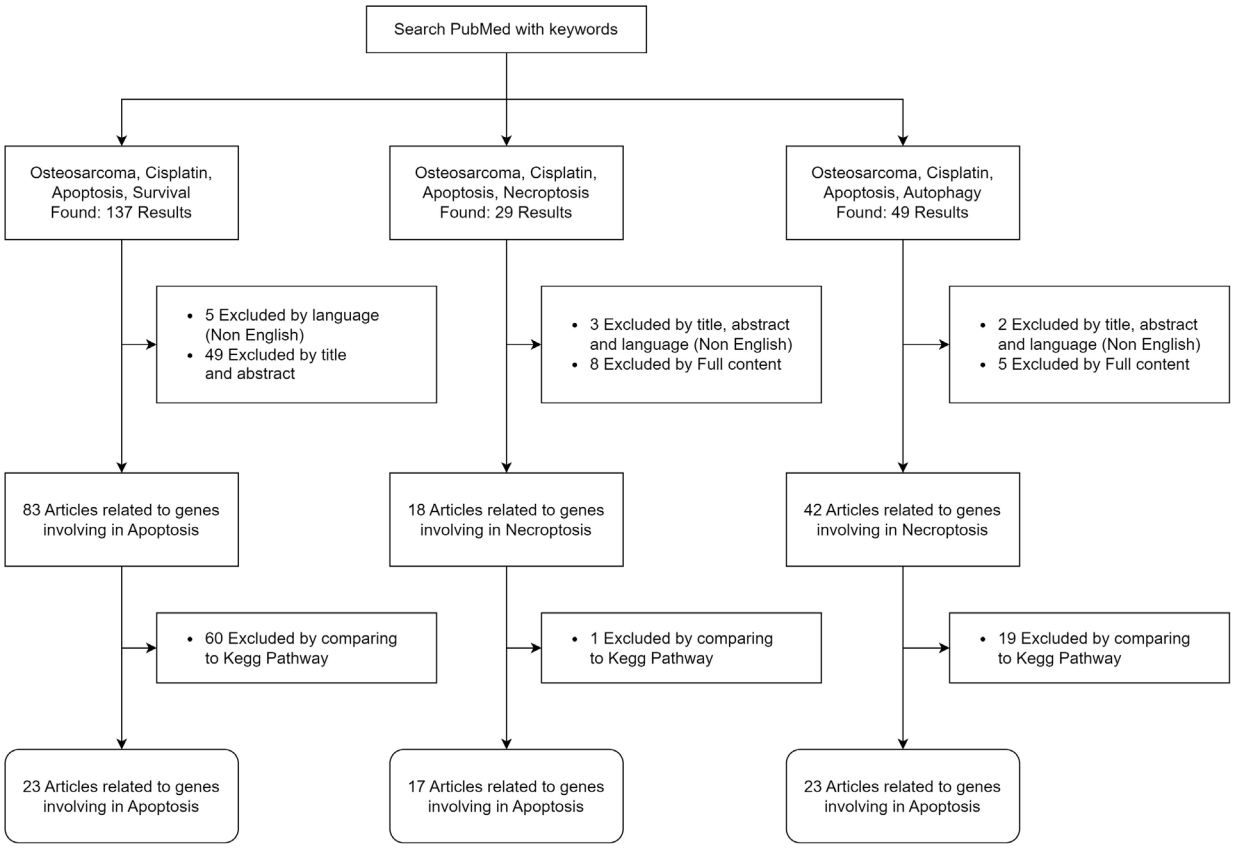

Figure 1. A selection scheme for identifying relevant PubMed articles

then annotated using the Ensembl Variant Effect Predictor (VEP) (71) as well as VarSome (72), and reported in a text-formatted file with clinically relevant information (73).

SVs in the patient dataset were identified using Manta on a binary alignment file (BAM) of a tumor genome with a matched normal genome and scored using a somatic variant model (74). CNV analysis was performed using Control-FREEC (75) on a BAM file generated from a tumor genome with a matched normal genome. The analysis provided genome-wide copy number estimates for each chromosome using a sliding window approach with a window size of 50,000 base pairs (bp). Copy number values were represented as log2 ratios to identify genomic gains and losses. For autosomes, a log2 ratio greater than 1.5 was classified as a copy number gain, while a log2 ratio below 0.5 indicated a copy number loss. For the X and Y chromosomes, a log2 ratio greater than 0.75 signified a gain, and a log2 ratio below 0.25 represented a loss. These thresholds were used to distinguish between normal and amplified or deleted genomic regions.

Data visualization and STRING analysis

SVs detected in OS genomes were visualized and reported using Circos (76). STRING (77) analyses were conducted on various lists of genes/proteins to identify their interactions and find relevant Gene Ontology (GO) terms, biological pathways, and associated diseases.

Statistical analysis

STRING analysis incorporating statistical measures, including the false discovery rate (FDR) and interaction score, were used to identify significant protein-protein interactions, pathways, and related biological processes. Interactions with an FDR of less than 0.05 were deemed statistically significant (77).

Ethics approval and consent to participate

The collection and use of the tissue specimens for the present study were approved by the Research Ethics Committee of the Faculty of Medicine, Chiang Mai University (FAC-MED-2563-07135). All subjects supplied written informed consent for participation in compliance with the Declaration of Helsinki.

RESULTS

Pathogenic mutations in key genes associated with osteosarcoma

The analysis revealed several germline and somatic mutations linked to the genes of interest in patients P1 and P3, as outlined in Table 2. Patient P1 was found to have a missense mutation (rs746943903) in the Phosphatidylinositol-4,5-Bisphosphate 3-Kinase Catalytic Subunit Delta (*PIK3CD*) gene, essential for immune response. This mutation was heterozygous in the germline but homozygous in the tumor genome, and it was assessed to have a moderate impact on the gene's function. Additionally, the tumor genome of P1 uniquely presented a homozygous somatic mutation at a splice donor site in the *TP53* gene, identified by the identifiers COSV52762386, COSV52883623, and COSV53123147. Although this mutation does not alter an amino acid, it was deemed to have a high impact and was associated with Li-Fraumeni syndrome (78). Furthermore, Patient P3's germline and tumor genomes harbored a highly pathogenic nonsense mutation (rs1575481212) in the MutL Homolog 1 (*MLH1*) gene. The *MLH1* protein is crucial for DNA mismatch repair and safeguarding against DNA damage.

Copy number variation in tumor genomes of the patients

CNV is frequently detected in tumors. The genomic regions affected by the resulted DNA imbalance may contain genes encoding essential proteins, whose altered dosage subsequently leads to oncogenesis (9, 16, 79, 80). The CNV analyses of all three tumor genomes revealed several 50,000-bp genomic regions of individual chromosomes demonstrated copy number alterations (Figures 2A – C).

Further investigations identified several affected genomic locations and genes that play important roles in chemotherapy (Table S6). As shown in Figure S1A, patient P1 exhibited copy number alterations in 6,362 regions, each spanning 50,000 base pairs (bp), including 6,275 regions with copy number gains and 87 regions with copy number losses. Among the 1,794 genes of interest, copy number gains were observed in 289 genes, whereas copy number losses were observed in 4 genes (e.g., *HLA-A*, *NF2*, *RB1*, and *WWOX*). Interestingly, both gain and loss of copy numbers were observed in the tumor suppressor and apoptotic gene WW Domain Containing Oxidoreductase (*WWOX*). Gain of copy numbers was observed in the chr16:78150001-78300000 and chr16:78350001-78450000 regions of *WWOX*, whereas loss of copy numbers was observed in the chr16:79150001-79500000 region of the gene. A complete list of genes affected by CNVs in patient P1 is presented in Table S7. The tumor genome of P1 demonstrated a copy number loss in the region of chromosome 13 (chr13:48,450,001-48,500,000), which overlaps the last 30,000 bp of

Table 2. A list of the germline and somatic mutations affecting the genes of interest.

	Patient		
	P1		P3
Gene symbol	*PIK3CD*	*TP53*	MLH1
Mutation/genotype	Germline/HET Somatic/HOM	Somatic/HOM	Germline/HET Somatic/HOM
SNP	rs746943903	COSV52762386 COSV52883623 COSV53123147	rs1575481212
Chr.	1	17	3
GRCh38 change	g.9721793G>A	g.7687376C>A	g.37014522C>A
Impact	Pathogenic Moderate	Pathogenic Strong	Pathogenic Very Strong
Consequence	Missense	Splice donor	Nonsense
Coding DNA change	*PIK3CD:c.1988G*>A	TP53:c.-29+1G>T	*MLH1*:c.768C>A
Protein change	p.Arg663His	p.?	p.Cys256Ter
RefSeq transcript ID	NM_005026.5	NM_000546.6	NM_000249.4
Ensembl Transcript ID	ENST00000377346.9	ENST00000269305.9	ENST00000231790.8

Genotypes: HET, Heterozygous; HOM, Homozygous.

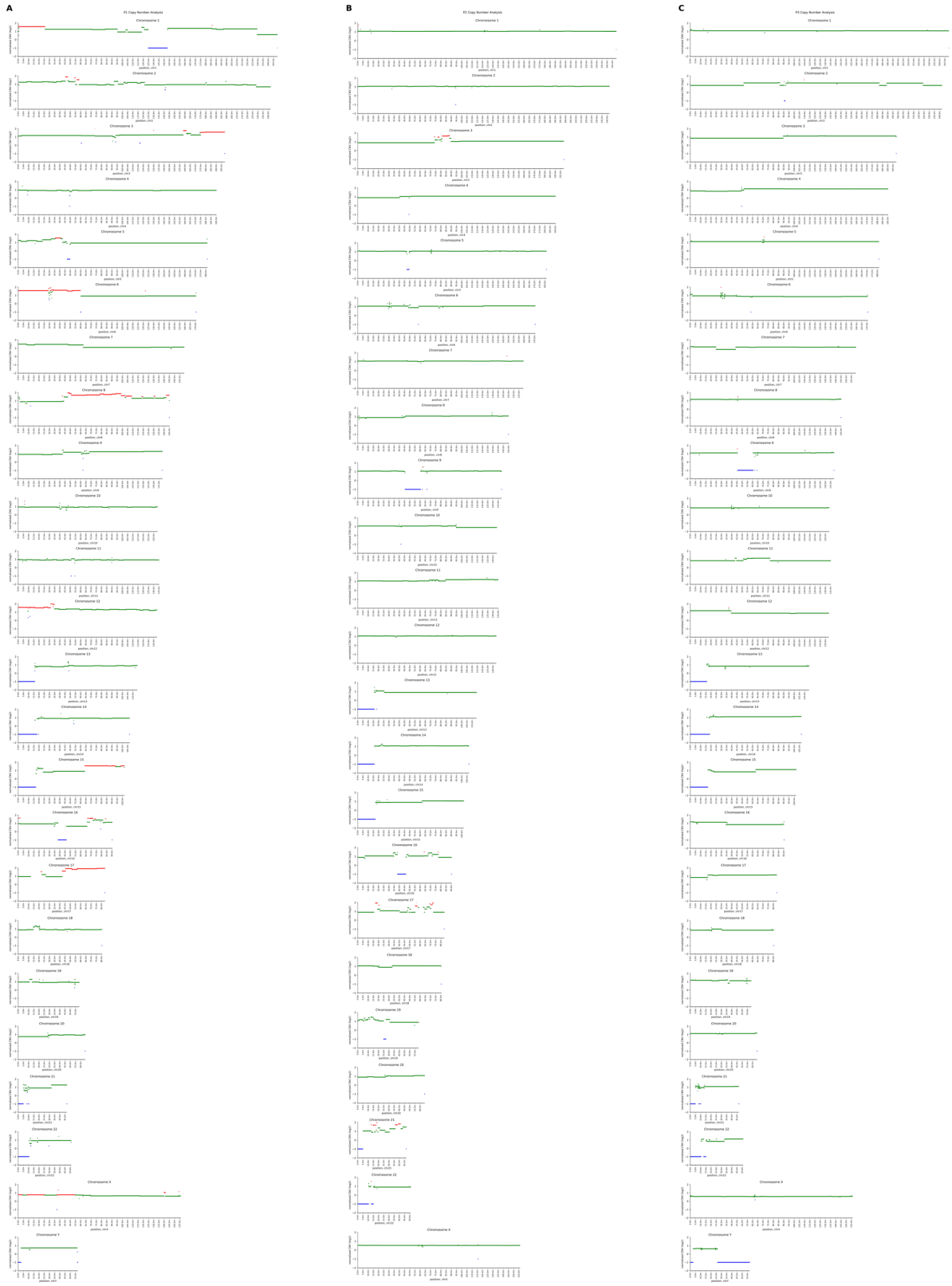

Figure 2. A comprehensive visualization of CNVs detected in the tumor genomes of patients (A) P1, (B) P2, and (C) P3 is presented. The log2 ratios reported by Control-FREEC were plotted, with the Y-axis representing the log2 ratio of copy number and the X-axis denoting the genomic positions within each chromosome. Each data point corresponds to the log2 ratio of copy number for a specific genomic window spanning 50,000 bps. Data points are color-coded for clarity: green indicates regions with a normal copy number, red represents regions with copy number gains, and blue signifies regions with copy number losses. This color scheme facilitates the identification of significant CNV events and highlights genomic regions with structural variations in the tumor genomes analyzed

the known tumor suppressor gene *RB1*. Furthermore, a copy number loss in *WWOX* is likely to affect the regulation of cell apoptosis in response to stress. Regarding platinum-based drug detoxification genes (61) in P1, *MPO* and *NQO1* exhibited gains of copy number. Additionally, copy number gains in *MSH2* and *PMS2* are likely to impact mismatch repair, whereas gains in *POLH* and *POLM* could potentially affect DNA replication. The P1 tumor genome also exhibited copy number gain of several protein-coding genes, e.g., *ABCC3*, *NQO1*, and *SLCO1B1*, which belong to the doxorubicin, etoposide, and methotrexate pathways (62, 64, 65, 81). Additionally, gains of copy number were observed in other genes belonging to the Doxorubicin pathway, including ABCC5, ABCC9, ALDH3A1, GSTA1, GSTA2, *MSH2*, and MTHFR (65). In the Methotrexate pathway, the genes that demonstrated gains in copy number included *BIRC5*, *GGH*, *MTHFR*, *MTHFS*, *SHMT1*, *SLCO1A2*, and *SLCO1B3* (64, 81).

As illustrated in Figure S1B, patient P2 exhibited copy number alterations in 821 regions, each 50,000 base pairs (bp) in size, including 742 regions with copy number gains and 79 regions with copy number losses. Specifically, copy number gains were observed in 31 genes, while a copy number loss was noted in *KIR2DL1*. A comprehensive list of genes affected by CNVs in patient P2 can be found in Table S7. The P2 tumor genome exhibited gains of copy number for *DNA* Topoisomerase II Alpha (*TOP2A*) and Serine Hydroxymethyltransferase 1 (*SHMT1*). *TOP2A* is a recognized target of the chemotherapeutic agents doxorubicin and etoposide (62, 65). On the other hand, *SHMT1* can indirectly reduce the effectiveness of methotrexate (64, 81, 82). Notably, P2 showed copy number gains in *MPO*, *NQO1*, and *SOD1*, genes implicated in reducing the intracellular concentration of platinum drugs, as documented in previous studies (61). However, the log2 ratios of tumor-to-normal copy number for these genes were below 0.585, specifically, *MPO* (0.527), *NQO1* (0.551), and *SOD1* (0.405). This reduction is attributed to the presence of normal bone marrow cells in the tumor tissue of P2.

As depicted in Fig. S1C, patient P3 was found to have copy number alterations in 11 regions, each spanning 50,000 base pairs (bp), which included 9 regions with copy number gains and 2 with copy number losses (Table S6). Interestingly, these alterations did not impact any genes associated with platinum-based drug metabolism or DNA repair mechanisms. Additionally, several regions of the P3 tumor genome could have clearly demonstrated CNVs, likely due to the diluting effect of normal bone marrow cells. In summary, copy number variation underlines the complexity and individuality of tumor genomes, as demonstrated across different patients (Figure 2).

Structural variations in tumor genomes of the patients

SV is a key process responsible for oncogenesis. The resulting genomic rearrangements, deletions, and/or amplifications can affect genomic regions ranging from a few kilobases to entire chromosomes and can subsequently lead to deleterious gene dosage alterations (8, 83-90). Analyses of SV have revealed unique patterns of genomic rearrangements in three different tumor genomes (Figure 3). The details of all SVs detected in these tumor genomes are documented in Table S8. SV has also been observed in a small number of genes with significant roles in chemotherapy.

As shown in Table 3, the patient P1 tumor genome harbored 17 genes affected by chemotherapy. The P2 tumor genome included 19 genes, whereas the P3 genome had only 7 genes. Notably, the P1 tumor genome was burdened with genomic rearrangements of genes classified as tumor suppressors, e.g., *MSH2*, *NF2*, *RB1*, and *WWOX*. SV also impacted genes involved in DNA repair, for example, *ACTL6A*, *MSH2*, *SPIDR*, and *TRIP12*. An intrachromosomal translocation of *STAT3*, a gene known to be involved in cell growth and apoptosis, was also observed.

In the patient P2 tumor genome (Table 4), structural alterations of genes caused by the DNA damage and repair mechanism were observed, including the deletion of *ASCC3*, the translocation of *CLOCK*, the duplication and translocation of *BABAM1*, the translocation of *BRIP1*, and the deletion of the *RAD51C* gene. The latter three genes also play significant roles in homologous recombination. Interestingly, SVs were also observed in genes playing vital roles in cell adhesion, e.g., *DSCAM*, *FREM2*, *ICAM1*, *ITGA3*, and *PRKCA* (91, 92).

Despite having fewer genes affected by genomic alterations (Table 5), the patient P3 tumor

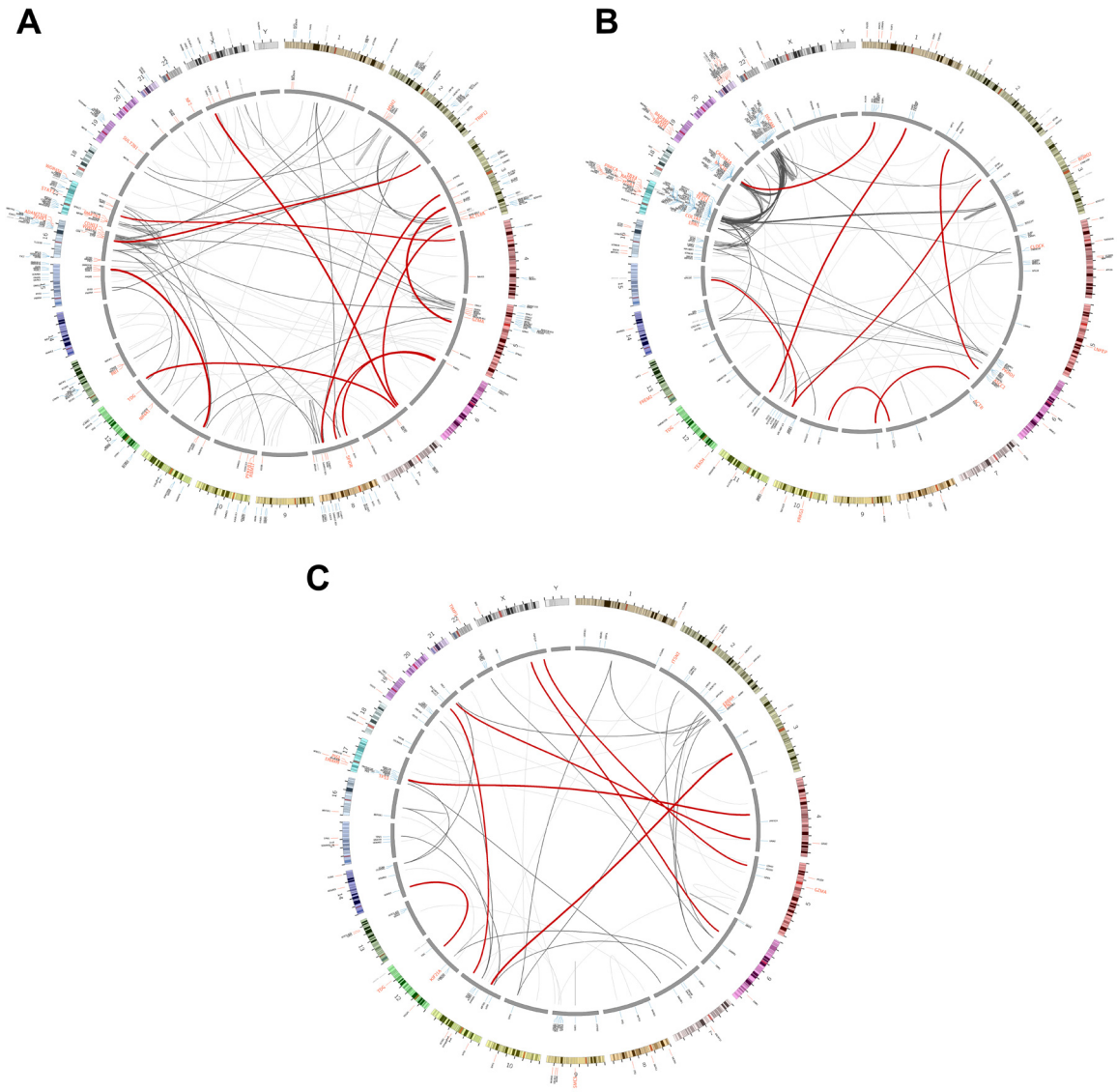

Figure 3. The CIRCOS plots visualize SVs detected in the tumor genomes of patients (A) P1, (B) P2, and (C) P3. The outer circle (first circle) depicts the cytoband of the human reference genome (GRCh38 or hg38), including the names and genomic locations of genes affected by SVs located on the plus strand. The second circle displays the names and genomic locations of genes affected by SVs on the minus strand, complementing the information provided in the outer circle. The regions harboring genes with significant roles in chemotherapy response are annotated in red. SVs, namely translocations, deletions, and duplications, are represented by lines. The red lines represent SV events that pass the filter, whereas the black and gray lines represent those that did not pass the filter. SVs, including translocations, deletions, and duplications, are depicted with lines connecting relevant genomic regions. The red lines indicate SV events that meet the predefined criteria and thus pass the filter. In contrast, the black and gray lines represent SV events that do not meet these criteria

genome exhibited an interchromosomal translocation of the tumor suppressor gene *TP53*, as well as translocations involving *ERBB4*, *FN1*, *TIMP3*, and *KIF21A*. A deletion in the *PIGL* gene was also detected in the tumor genome. These altered genes are associated with the biological pathway proteoglycan in cancer (93-96).

Functional protein association networks analysis of the affected genes

After identifying the commonly affected cancer genes in tumor genomes, their potential involvements in cancer risk, cancer development and progression, and cancer treatments were subsequently investigated for functional protein association networks. There were 312 affected genes in the P1 tumor genome. The P2 and P3

Table 3. Genes with significant roles in chemotherapy and types of SV were observed in tumor genomes of P1. Only SVs that have met the predefined criteria and thus passed the filter were included.

Gene	Description	Type	Interaction
ABHD2	Abhydrolase domain containing 2, acylglycerol lipase	Duplication	Intrachromosomal
ACTL6A	Actin like 6A	Translocation	Intrachromosomal
ADAMTS18	ADAM metallopeptidase with thrombospondin type 1 motif 18	Translocation	Intrachromosomal
CDH13	Cadherin 13	Translocation	Intrachromosomal
MAP2K4	Mitogen-activated protein kinase kinase 4	Translocation	Intrachromosomal
MSH2	MutS homolog 2	Duplication	Intrachromosomal
NF2	NF2, moesin-ezrin-radixin like (MERLIN) tumor suppressor	Deletion Translocation	Intrachromosomal Intrachromosomal
NR4A1	Nuclear receptor subfamily 4 group A member 1	Deletion Translocation	Intrachromosomal Interchromosomal
PFKFB3	6-phosphofructo-2-kinase/fructose-2,6-biphosphatase 3	Duplication	Intrachromosomal
RB1	RB transcriptional corepressor 1	Translocation	Intrachromosomal
RBM17	RNA binding motif protein 17	Duplication	Intrachromosomal
SPIDR	Scaffold protein involved in DNA repair	Translocation	Interchromosomal
STAT3	Signal transducer and activator of transcription 3	Translocation	Intrachromosomal
SULT2B1	Sulfotransferase family 2B member 1	Duplication	Intrachromosomal
TRIP12	Thyroid hormone receptor interactor 12	Translocation	Interchromosomal
WWOX	WW domain containing oxidoreductase	Translocation	Interchromosomal
ZFHX3	Zinc finger homeobox 3	Translocation Deletion Translocation Duplication	Intrachromosomal Intrachromosomal Intrachromosomal Intrachromosomal

Table 4. Genes with significant roles in chemotherapy and types of SV were observed in tumor genomes of P2. Only SVs that have met the predefined criteria and thus passed the filter were included.

Gene	Description	Type	Interaction
ACTB	Actin beta	Duplication	Intrachromosomal
ASCC3	Activating signal cointegrator 1 complex subunit 3	Deletion	Intrachromosomal
BABAM1	BRISC and BRCA1 A complex member 1	Duplication Translocation	Intrachromosomal Intrachromosomal
BRIP1	BRCA1 interacting helicase 1	Translocation	Interchromosomal
CACNA1A	Calcium voltage-gated channel subunit alpha1 A	Duplication Deletion	Intrachromosomal Intrachromosomal
CLOCK	Clock circadian regulator	Translocation	Interchromosomal
COL1A1	Collagen type I alpha 1 chain	Translocation	Interchromosomal
DSCAM	DS cell adhesion molecule	Translocation	Interchromosomal
ERN1	Endoplasmic reticulum to nucleus signaling 1	Translocation Translocation Deletion	Intrachromosomal Interchromosomal Intrachromosomal
ICAM1	Intercellular adhesion molecule 1	Translocation	Interchromosomal
ITGA3	Integrin subunit alpha 3	Translocation	Interchromosomal
PKHD1	PKHD1 ciliary IPT domain containing fibrocystin/polyductin	Deletion	Intrachromosomal
PRKCA	Protein kinase C alpha	Deletion Translocation	Intrachromosomal Intrachromosomal
RAD51C	RAD51 paralog C	Deletion	Intrachromosomal
ROBO2	Roundabout guidance receptor 2	Translocation	Intrachromosomal
TBX4	T-box transcription factor 4	Deletion	Intrachromosomal
TEAD4	TEA domain transcription factor 4	Duplication	Intrachromosomal
TEX14	Testis expressed 14, intercellular bridge forming factor	Translocation	Interchromosomal
TNFSF9	TNF superfamily member 9	Duplication	Intrachromosomal

Table 5. Genes with significant roles in chemotherapy and types of SV were observed in tumor genomes of P3. Only SVs that have met the predefined criteria and thus passed the filter were included.

Gene	Description	Type	Interaction
FN1	Fibronectin 1	Translocation	Interchromosomal
KIF21A	Kinesin family member 21A	Translocation Translocation	Interchromosomal Intrachromosomal
PIGL	Phosphatidylinositol glycan anchor biosynthesis class L	Deletion	Intrachromosomal
SMC5	Structural maintenance of chromosomes 5	Translocation	Intrachromosomal
TIMP3	TIMP metallopeptidase inhibitor 3	Translocation	Interchromosomal
TP53	Tumor protein p53	Translocation	Interchromosomal

tumor genomes carried 51 and 7 affected genes, respectively. These affected genes, identified in the tumor genome of each patient, were then subjected to STRING analysis (77). The functional enrichment analysis of protein-protein interaction networks for patient P1, P2, and P3, detailed in Tables 6, 7, and 8 respectively, identified common biological processes or pathways impacted across all patients. These include DNA damage and repair mechanisms, apoptosis (hsa04210), platinum drug resistance (hsa01524), and cancer pathways (hsa05200). Specifically, abnormal osteoclast differentiation (hsa04380) and cell death were linked to patient P1, while the tumor genome of P3 showed a correlation with proteoglycans in cancer (hsa05205), suggesting roles in cancer proliferation, cell-cell adhesion loss, angiogenesis, and metastasis. STRING analyses suggest copy number and/or SVs significantly influence OS pathogenesis, despite varying mutation burdens.

DISCUSSION

In this study, we identified pathogenic germline and somatic mutations in patients P1 and P3. Patient P1 exhibited a missense mutation in the *PIK3CD* gene, presented as a heterozygous germline mutation which evolved into a homozygous somatic mutation. Additionally, P1 exclusively possessed a somatic mutation at a splice donor site in the *TP53* gene. On the other hand, Patient P3 was found to have a nonsense mutation in the *MLH1* gene. This gene is a key component of the DNA mismatch repair mechanism, crucial for DNA damage tolerance. Notably, this nonsense mutation was observed in both the germline and tumor genomes of P3. Nonetheless, the OS genome of each patient showed a greater extent of genome rearrangements. The tumor genome of patient P1 was particularly notable for its extensive CNVs, which could lead to drastic genetic imbalances. In contrast, the tumor genomes of patients P2 and P3 demonstrated relatively moderate levels of CNVs, suggesting varied patterns of genetic alterations across different individuals. Furthermore, SVs were detected in all three tumor genomes, affecting key genes involved in mechanisms of platinum drug resistance and DNA repair. Such alterations can significantly influence the effectiveness of chemotherapy treatments and the overall prognosis of patients. Importantly, the mutated genes identified in this study were also correlated with clinical features of the patients, suggesting a direct link between specific genetic alterations and the manifestation of the disease.

OS is a primary cancer characterized by high rates of metastasis and mortality (97-99). The survival rates for OS patients who develop metastases vary significantly, reflecting the variations in severity of the disease and the effectiveness of available treatments. According to the American Cancer Society, the five-year relative survival rate for OS with distant metastases, such as those to the lungs, is approximately 24% (100). OS patients with pulmonary metastases have a five-year survival rate of 20-40%. Patients with a countable number of pulmonary lesions may have survival rates up to 40%, whereas those with recurrent OS face a five-year survival rate of 28% or less (101, 102). These statistics highlight the dire prognosis faced by patients with metastatic OS and underscore the critical need for ongoing research and improvements in therapeutic strategies. Despite its low incidence, this cancer can affect individuals of all age groups (98, 103). In Thailand,

Table 6. The result of the functional enrichment analysis of protein-protein interaction networks for osteosarcoma patient P1. Pathways or biological processes with an FDR of less than 0.05 are reported.

Biological process (gene ontology)			
GO-term	**Description**	**Strength**	**FDR**
GO:0006281	DNA repair	1.03	6.15e-51
GO:0006302	Double-strand break repair	1.1	9.52e-26
GO:0051726	Regulation of cell cycle	0.59	4.11e-18
GO:0043067	Regulation of programmed cell death	0.52	1.21e-17
GO:0000725	Recombinational repair	1.15	2.76e-17
GO:0010941	Regulation of cell death	0.49	1.92e-16
GO:0000724	Double-strand break repair via homologous recombination	1.13	1.56e-15
GO:0006282	Regulation of DNA repair	0.94	7.94e-15
GO:0008219	Cell death	0.54	2.22e-14
GO:0012501	Programmed cell death	0.55	2.33e-14
GO:0042770	Signal transduction in response to DNA damage	1.03	3.39e-13
GO:0007049	Cell cycle	0.5	5.17e-13
GO:0097190	Apoptotic signaling pathway	0.8	1.58e-12
GO:0000077	DNA damage checkpoint signaling	1.06	4.17e-11
GO:0036297	Interstrand cross-link repair	1.25	2.03e-08
GO:0006301	Post-replication repair	1.28	7.00e-08
GO:2000779	Regulation of double-strand break repair	0.9	7.26e-08
GO:0000731	DNA synthesis involved in DNA repair	1.21	2.38e-07
GO:2001233	Regulation of apoptotic signaling pathway	0.62	1.31e-06
GO:0001649	Osteoblast differentiation	0.79	2.70e-05
GO:0048705	Skeletal system morphogenesis	0.64	0.00017
GO:0000729	DNA double-strand break processing	1.22	0.00099
GO:0051302	Regulation of cell division	0.59	0.0051
GO:0033688	Regulation of osteoblast proliferation	0.98	0.0229
GO:2000819	Regulation of nucleotide-excision repair	0.98	0.0229
GO:0006298	Mismatch repair	0.95	0.0270
GO:0006289	Nucleotide-excision repair	0.76	0.0361
KEGG pathways			
Pathway	**Description**	**Strength**	**FDR**
hsa05200	Pathway in cancer	0.65	4.87e-11
hsa01524	Platinum drug resistance	1.09	9.20e-09
hsa04210	Apoptosis	0.88	6.61e-08
hsa04110	Cell cycle	0.86	8.94e-07
hsa03430	Mismatch repair	1.16	0.00025
hsa04380	Osteoclast differentiation	0.65	0.0023
hsa03410	Base excision repair	0.78	0.0398

Table 7. The result of the functional enrichment analysis of protein-protein interaction networks for osteosarcoma patient P2. Pathways or biological processes with an FDR of less than 0.05 are reported.

Biological process (gene ontology)			
GO-term	**Description**	**Strength**	**FDR**
GO:0006302	Double-strand break repair	1.31	1.04e-06
GO:0006281	DNA repair	1.01	5.46e-06
GO:0008219	Cell death	0.62	0.0094
GO:0000077	DNA damage checkpoint signaling	1.2	0.0191
GO:0010941	Regulation of cell death	0.48	0.0387
KEGG pathways			
Pathway	**Description**	**Strength**	**FDR**
hsa01524	Platinum drug resistance	1.48	0.00016
hsa04210	Apoptosis	1.11	0.0072
hsa05200	Pathways in cancer	0.69	0.0175

Table 8. The result of the functional enrichment analysis of protein-protein interaction networks for osteosarcoma patient P3. Pathways or biological processes with an FDR of less than 0.05 are reported.

Biological process (gene ontology)			
GO-term	**Description**	**Strength**	**FDR**
GO:0006302	Double-strand break repair	1.63	0.0229
KEGG pathways			
Pathway	**Description**	**Strength**	**FDR**
hsa01524	Platinum drug resistance	2.1	7.64e-06
hsa05205	Proteoglycans in cancer	1.65	0.00020
hsa05200	Pathways in cancer	1.23	0.0023
hsa04210	Apoptosis	1.52	0.0184

however, the highest incidence of OS is observed during the first 25 years of life (98). The three OS patients whose genomes were investigated in this study aptly represent this affected demographic. All three developed primary OS at a young age (average age 15.33 years, range 11-20 years) and had a poor prognosis, as indicated by the average tumor necrotic percentage being low (64%, range 42-85%), with a low degree of necrosis associated with a poor prognosis (104). Additionally, they responded poorly to chemotherapy, as evidenced by metastasis even after treatment. Furthermore, they exhibited poor survival outcomes (average 678 days, range 357-842 days) following a combination of surgery and chemotherapy. Their clinical histories seem to correlate well with resistance to platinum-based drugs, primarily arising from CNVs and SVs.

This investigation identified a nonsense mutation in *MLH1* gene in patient P3. The mutation was heterozygous in the germline genome of P3, but became homozygous in the tumor genome. This mutation may have increased the risk of OS or contributed to oncogenesis due to compromised DNA mismatch repair (105-107) and DNA damage protection mechanisms (108, 109). A homozygous splice-site donor mutation in *TP53* detected in patient P1 could have acted synergistically with earlier mutations in cancer progression through abnormal splicing of *TP53* transcripts (110-113). Despite having a few deleterious SNPs, the patients demonstrated a significant degree of genomic alterations as evidenced by CNVs and SVs. However, the patterns of these alterations varied among the patients.

An important genomic alteration observed in the P1 tumor genome was the copy number loss of *RB1*, which is a known contributor to poor prognosis in OS patients (10, 114). The tumor genome also carried copy number gains in several genes associated with resistance to Doxorubicin, Etoposide, and Methotrexate, specifically *ABCC3*, *MPO*, *NQO1*, and *SLCO1B1* (62, 64, 65, 81). In addition, the observed copy number gain of *SOX9* has been associated with a lower survival rate and poor chemotherapy response (115). The tumor genome exhibited SVs in genes associated with tumor suppression or DNA repair, namely, *RB1* (tumor suppressor), *NF2* (tumor suppressor), *WWOX* (tumor suppressor), *MSH2* (tumor suppressor and DNA repair), *ACTL6A* (DNA repair), *SPIDR* (DNA repair), and *TRIP12* (DNA repair). These genes are also collectively classified as negative regulators of cellular processes (GO:0048523).

Patient P2's history of undergoing multiple rounds of chemotherapy directed our investigation towards potential gene mutations that could result in resistance to chemotherapy. Copy number gains in *TOP2A* and *SHMT1* have been associated with reduced efficacy of Doxorubicin, Etoposide, and Methotrexate (62, 64, 65, 81, 82). Furthermore, the P2 tumor genome has demonstrated SVs in several genes associated with DNA damage, DNA repair, and homologous recombination, specifically *ASCC3* (DNA damage/repair), *CLOCK* (DNA damage/repair), *BABAM1* (DNA damage/repair and homologous recombination), *BRIP1* (DNA damage/repair and homologous recombination), and *RAD51C* (DNA damage/repair and homologous recombination). Notably, SVs in genes involved in cell adhesion (GO:0007155), e.g., *DSCAM*, *FREM2*, *ICAM1*, *ITGA3*, and *PRKCA*, could contribute to the cancer's aggressive behavior, necessitating intensive chemotherapy

treatments. Abnormal cell adhesion mechanisms contribute to oncogenesis and metastasis by disrupting normal cell-cell and cell-ECM interactions, enhancing tumor cell motility and invasion, altering interactions with the tumor microenvironment, and enabling evasion of immune surveillance (92, 116-119). These changes affecting patient P2 may have collectively facilitated the detachment of cancer cells from the primary tumor and their eventual spread to distant organs, leading to metastasis.

Patient P3, who had the poorest survival rate, exhibited interchromosomal translocations of the *TP53*, *ERBB4*, *FN1*, *TIMP3*, and *KIF21A* genes, along with a deletion in the *PIGL* gene. These genetic alterations are associated with the proteoglycan pathway in cancer, which facilitates tumor cell growth and migration by enabling interactions between proteoglycans in the tumor microenvironment and various growth factors and enzymes. The disruption of the proteoglycan pathway likely contributes to tumor progression and invasion (93-96), leading to the patient's untimely death.

Chromothripsis, marked by dozens to hundreds of DNA double-strand breaks in a localized chromosomal region in a single event, leads to faulty reassembly and complex genomic rearrangements (7, 8, 120). This accelerates tumor evolution through rapid genomic changes and mutation accumulation (79, 121, 122). Such alterations, especially in chemotherapy-related genes observed in three fetal OS patients, correlate with poor chemotherapy response and abnormal cell-cell adhesion. Comprehensive analysis of pathogenic SVs and CNVs could inform targeted cancer therapies to improve patient outcomes.

An estimated 30% of cancers possess known pathogenic SVs which are valuable for diagnosis and treatment (123-129). Moreover, 853,218 CNVs have been identified across 10,729 tumor samples belonging to 32 cancer types curated in The Cancer Genome Atlas (TCGA) database (130). Both SVs and CNVs disrupt genomic integrity, disturb gene expression, and ultimately lead to cancer development (80, 131). These large-scale genomic alterations can conveniently be observed via NGS. While Illumina's short-read sequencing technology has been the backbone of genomics because of its high accuracy and cost-effectiveness, PacBio and Oxford Nanopore's long-read sequencing technologies offer superior capabilities in detecting SVs in the human genome (132-135). These advantages make long-read sequencing more suitable for comprehensive genomic studies focused on SVs, complex genomic regions, and complete genome assembly. However, the choice of sequencing technology may depend on specific project goals, budget, and the balance between the need for depth, accuracy, and read length.

This study has several limitations. First, the small sample size of three patients limits the generalizability of the findings to the broader OS patient population. Second, the WGS approach focused solely on genetic variations, without exploring gene expression or regulatory mechanisms such as epigenetics. Furthermore, the analysis relied on gene annotations from published data, which may not fully capture population-specific variants unique to the Thai population. Addressing these limitations in future research will require larger and more diverse cohorts, the integration of multi-omics approaches, and population-specific analyses to achieve a more comprehensive understanding of genomic alterations in OS and their clinical implications.

CONCLUSIONS

This study underscores the critical role of genomic alterations in driving poor chemotherapy responses and fatal outcomes in OS. The findings reveal a convergence of genetic disruptions that collectively contribute to therapy resistance, tumor progression, and metastasis, highlighting the need for precision oncology approaches in OS treatment. Key genomic alterations include CNVs and SVs in tumor suppressor genes (e.g., *RB1*, *NF2*, and *MSH2*), DNA repair genes (e.g., *BRIP1*, *RAD51C*, and *TRIP12*), and genes involved in chemotherapy resistance (e.g., *TOP2A*, *ABCC3*, and *SOX9*). Disruptions in cell adhesion pathways further exacerbated disease progression by enabling tumor cell detachment, migration, and metastasis. Additionally, genomic changes impacting the proteoglycan pathway facilitated tumor cell growth and invasion, contributing to treatment failure. These findings demonstrate how a combination of genomic instability, resistance mechanisms, and tumor microenvironment alterations can undermine chemotherapy efficacy and accel-

erate disease progression in OS. While the study provides valuable insights for developing targeted therapies and predictive biomarkers, limitations such as the small sample size and focus on genetic alterations necessitate further investigation. Future research should integrate multi-omics approaches, larger cohorts, and population-specific analyses to enhance understanding of OS and improve patient outcomes.

ACKNOWLEDGEMENTS

The authors would like to thank Sararun Boonchuay and Pongsatorn Pisuttipunpong for initial literature reviews and data analysis. We also would like to thank The Center of Multidisciplinary Technology for Advanced Medicine (CMUTEAM), Faculty of Medicine, Chiang Mai University, Thailand for their support with computational resources and servers, as well as their administrative support.

FUNDING

This research was funded by The Faculty of Medicine Research Fund, Chiang Mai University, Grant No. 099-2563.

CONFLICT OF INTEREST

The authors have no conflicts of interest to report.

ADDITIONAL INFORMATION

Author contributions

N.N.: investigation, data validation, data curation, methodology, writing-original draft; S.W.: investigation, software, data validation, data curation, methodology, visualization, writing-original draft; P.T.: sample preparation, DNA extraction, NGS, writing – review and editing; P.C.: conceptualization, supervision, writing – review and editing; D.P.: resources, conceptualization, supervision, writing – review and editing; S.T.: conceptualization, supervision, methodology, funding acquisition, writing original draft, writing – review and editing. N.N. and S.W. contributed equally to this work and share first authorship. All authors have read and approved the final manuscript.

Patient consent for publication

Not applicable.

Data availability statement

The data supporting this study's findings are available from the corresponding author upon reasonable request.

Supplementary materials

Doc. S1 A genomic DNA extraction protocol

Figure S1 The CIRCOS plots provide a comprehensive visualization of CNVs detected in the tumor genomes of patients (A) P1, (B) P2, and (C) P3. The plots organize genomic information across multiple layers from the outermost to the innermost circle. The outer circle (first circle) depicts the cytoband of the human reference genome (GRCh38 or hg38), including the names and genomic locations of genes of interest located on the plus strand. The second circle displays the names and genomic locations of genes of interest on the minus strand, complementing the information provided in the outer circle. The third circle illustrates the CNV profiles spanning across different chromosomes. Each dot within this circle represents a 50,000-bp genomic interval, with color coding to indicate the type of copy number variation: green dots indicate copy number gains, red dots indicate copy number losses, and gray dots denote regions with no copy number alteration.

Table S1. A timeline showing the treatments, chemotherapies, and important events of patient P1 at Maharaj Nakorn Chiang Mai Hospital, Chiang Mai, Thailand

Table S2. A timeline showing the treatments, chemotherapies, and important events of patient P2 at Maharaj Nakorn Chiang Mai Hospital, Chiang Mai, Thailand

Table S3. A timeline shows the treatments, chemotherapies, and important events of patient P3 at Maharaj Nakorn Chiang Mai Hospital, Chiang Mai, Thailand

Table S4. A list of 57 genes of interest obtained from the systematic review

Table S5. A list of 1,794 genes of interest in this study

Table S6. Copy number variations observed in each chromosome in tumor genomes of (A) P1, (B) P2, and (C) P3

Table S7. A list of the selected genes of interest affected by CNVs in tumor genomes of all three patients

Table S8. Structural variations detected in the tumor genomes of patient P1, P2, and P3

Supplementary data are available at https://doi.org/10.6084/m9.figshare.25514878.v2 (136)

REFERENCES

1. Yücetürk G, Sabah D, Keçeci B, Kara AD, Yalçinkaya S. Prevalence of bone and soft tissue tumors. Acta Orthop Traumatol Turc. 2011;45:135-43.
2. Sadykova LR, Ntekim AI, Muyangwa-Semenova M, Rutland CS, Jeyapalan JN, Blatt N, et al. Epidemiology and Risk Factors of Osteosarcoma. Cancer Investigat. 2020;38:259-69.
3. Jafari F, Javdansirat S, Sanaie S, Naseri A, Shamekh A, Rostamzadeh D, et al. Osteosarcoma: A comprehensive review of management and treatment strategies. Ann Diagn Pathol. 2020;49:151654. PubMed PMID: 33130384.
4. Chaiyawat P, Klangjorhor J, Settakorn J, Champattanachai V, Phanphaisarn A, Teeyakasem P, et al. Activation status of receptor tyrosine kinases as an early predictive marker of response to chemotherapy in osteosarcoma. Transl Oncol. 2017;10:846-53.
5. Rickel K, Fang F, Tao J. Molecular genetics of osteosarcoma. Bone. 2017;102:69-79.
6. Rode A, Maass KK, Willmund KV, Lichter P, Ernst A. Chromothripsis in cancer cells: An update. Int J Cancer. 2016;138(10):2322-33.
7. Cortes-Ciriano I, Lee JJ, Xi R, Jain D, Jung YL, Yang L, et al. Comprehensive analysis of chromothripsis in 2,658 human cancers using whole-genome sequencing. Nat Genet. 2020;52:331-41.
8. Stephens PJ, Greenman CD, Fu B, Yang F, Bignell GR, Mudie LJ, et al. Massive genomic rearrangement acquired in a single catastrophic event during cancer development. Cell. 2011;144:27-40.
9. Smida J, Xu H, Zhang Y, Baumhoer D, Ribi S, Kovac M, et al. Genome-wide analysis of somatic copy number alterations and chromosomal breakages in osteosarcoma. International Journal of Cancer. 2017;141:816-28.
10. Sayles LC, Breese MR, Koehne AL, Leung SG, Lee AG, Liu H-Y, et al. Genome-informed targeted therapy for osteosarcoma. Cancer Discov. 2019;9:46-63.
11. Zhang C, Hansen HM, Semmes EC, Gonzalez-Maya J, Morimoto L, Wei Q, et al. Common genetic variation and risk of osteosarcoma in a multi-ethnic pediatric and adolescent population. Bone. 2020;130:115070. PubMed PMID: 31525475.
12. Wei X, Xu L, Jeddo SF, Li K, Li X, Li J. MARK2 enhances cisplatin resistance via PI3K/AKT/NF-kB signaling pathway in osteosarcoma cells. Am J Transl Res. 2020;12:1807-23.
13. Garcia-Ortega DY, Cabrera-Nieto SA, Caro-Sánchez HS, Cruz-Ramos M. An overview of resistance to chemotherapy in osteosarcoma and future perspectives. Cancer Drug Resist. 2022;5:762-93.
14. Li L, Luo C, Song Z, Reyes-Vargas E, Clayton F, Huang J, et al. Association of anti-HER2 antibody with graphene oxide for curative treatment of osteosarcoma. Nanomedicine. 2018;14:581-93.
15. Huang D, Savage SR, Calinawan AP, Lin C, Zhang B, Wang P, et al. A highly annotated database of genes associated with platinum resistance in cancer. Oncogene. 2021;40(46):6395-405.
16. Pires SF, Barros JS, Costa SSD, Carmo GBD, Scliar MO, Lengert AVH, et al. Analysis of the mutational landscape of osteosarcomas identifies genes related to metastasis and prognosis and disrupted biological pathways of immune response and bone development. Int J Mol Sci. 2023;24(13). PubMed PMID: 37445641.
17. Yarapureddy S, Abril J, Foote J, Kumar S, Asad O, Sharath V, et al. ATF6α activation enhances survival against chemotherapy and serves as a prognostic indicator in osteosarcoma. Neoplasia. 2019;21:516-32.
18. Tsai H-C, Huang C-Y, Su H-L, Tang C-H. CCN2 enhances resistance to cisplatin-mediating cell apoptosis in human osteosarcoma. PLoS ONE. 2014;9(3):e90159. PubMed PMID: 24637722.
19. Iwata S, Tatsumi Y, Yonemoto T, Araki A, Itami M, Kamoda H, et al. CDK4 overexpression is a predictive biomarker for resistance to conventional chemotherapy in patients with osteosarcoma. Oncology Reports. 2021;46:135. PubMed PMID: 34036394.
20. Campbell KJ, Witty JM, Rocha S, Perkins ND. Cisplatin mimics ARF tumor suppressor regulation of relA (p65) nuclear factor-κB transactivation. Cancer Res. 2006;66:929-35.
21. Davaadelger B, Duan L, Perez RE, Gitelis S, Maki CG. Crosstalk between the IGF-1R/AKT/mTORC1 pathway and the tumor suppressors p53 and p27 determines cisplatin sensitivity and limits the effectiveness of an IGF-1R pathway inhibitor. Oncotarget. 2016;7:27511-26.
22. He C, Sun J, Liu C, Jiang Y, Hao Y. Elevated H3K27me3 levels sensitize osteosarcoma to cisplatin. Clinical Epigenetics. 2019;11:8. PubMed PMID: 30651137.
23. Sun X, Wei Q, Cheng J, Bian Y, Tian C, Hu Y, et al. Enhanced Stim1 expression is associated with acquired chemo-resistance of cisplatin in osteosarcoma cells. Human Cell. 2017;30:216-25.
24. Kim M, Kim D. GFRA1: A novel molecular target for the prevention of osteosarcoma chemoresistance. Int J Mol Sci. 2018;19(4):1078. PubMed PMID: 29617307.
25. Duan L, Perez RE, Hansen M, Gitelis S, Maki CG. Increasing cisplatin sensitivity by schedule-dependent inhibition of AKT and Chk1. Cancer Biol Ther. 2014;15:1600-12.
26. Dai G, Deng S, Guo W, Yu L, Yang J, Zhou S, et al. Notch pathway inhibition using DAPT, a γ-secretase inhibitor (GSI), enhances the antitumor effect of cisplatin in resistant osteosarcoma. Mol Carcinog. 2019;58:3-18.
27. Xi X, Bao Y, Zhou Y, Chen Y, Zhong X, Liao J, et al. Oncogenic gene TRIM10 confers resistance to cisplatin in osteosarcoma cells and activates the NF-κB signaling pathway. Cell Biol Int. 2021;45:74-82.
28. Fellenberg J, Kunz P, Sähr H, Depeweg D. Overexpression of inosine 5′-monophosphate dehydro-

genase type ii mediates chemoresistance to human osteosarcoma cells. PLoS ONE. 2010;5(8):e12179. PubMed PMID: 20808934.
29. Huang Z, Huang Y, He H, Ni J. Podocalyxin promotes cisplatin chemoresistance in osteosarcoma cells through phosphatidylinositide 3-kinase signaling. Mol Med Rep. 2015;12:3916-22.
30. Woessmann W, Chen X, Borkhardt A. Ras-mediated activation of ERK by cisplatin induces cell death independently of p53 in osteosarcoma and neuroblastoma cell lines. Cancer Chemother Pharmacol. 2002;50: 397-404.
31. Zou J, Gan M, Mao N, Zhu X, Shi Q, Yang H. Sensitization of osteosarcoma cell line SaOS-2 to chemotherapy by downregulating survivin. Arch Med Res. 2010; 41:162-9.
32. Zhang Z, Yu L, Dai G, Xia K, Liu G, Song Q, et al. Telomerase reverse transcriptase promotes chemoresistance by suppressing cisplatin-dependent apoptosis in osteosarcoma cells. Scientific Reports. 2017;7: 7070. PubMed PMID: 28765565.
33. Zhou Y, Zang X, Huang Z, Zhang C. TWIST interacts with endothelin-1/endothelin A receptor signaling in osteosarcoma cell survival against cisplatin. Oncology Lett. 2013;5:857-61.
34. Vianello C, Cocetta V, Catanzaro D, Dorn GW, De Milito A, Rizzolio F, et al. Cisplatin resistance can be curtailed by blunting Bnip3-mediated mitochondrial autophagy. Cell Death Dis. 2022;13:398. PubMed PMID: 35459212.
35. Yang C, Gao R, Wang J, Yuan W, Wang C, Zhou X. High-mobility group nucleosome-binding domain 5 increases drug resistance in osteosarcoma through upregulating autophagy. Tumor Biol. 2014;35:6357-63.
36. Feng H, Zhang Q, Zhao Y, Zhao L, Shan B. Leptin acts on mesenchymal stem cells to promote chemoresistance in osteosarcoma cells. Aging. 2020;12:6340-51.
37. Zhan H, Xiao J, Wang P, Mo F, Li K, Guo F, et al. Exosomal CTCF confers cisplatin resistance in osteosarcoma by promoting autophagy via the IGF2-AS/miR-579-3p/MSH6 Axis. J Oncol. 2022;2022:1-18.
38. Huang J, Ni J, Liu K, Yu Y, Xie M, Kang R, et al. HMGB1 promotes drug resistance in osteosarcoma. Cancer Res. 2012;72:230-8.
39. Huang J, Liu K, Yu Y, Xie M, Kang R, Vernon PJ, et al. Targeting HMGB1-mediated autophagy as a novel therapeutic strategy for osteosarcoma. Autophagy. 2012;8:275-7.
40. Jiang K, Zhang C, Yu B, Chen B, Liu Z, Hou C, et al. Autophagic degradation of FOXO3a represses the expression of PUMA to block cell apoptosis in cisplatin-resistant osteosarcoma cells. Am J Cancer Res. 2017;7:1407-22.
41. Kim M, Jung J-Y, Choi S, Lee H, Morales LD, Koh J-T, et al. GFRA1 promotes cisplatin-induced chemoresistance in osteosarcoma by inducing autophagy. Autophagy. 2017;13:149-68.
42. Usman RM, Razzaq F, Akbar A, Farooqui AA, Iftikhar A, Latif A, et al. Role and mechanism of autophagy-regulating factors in tumorigenesis and drug resistance. Asia Pac J Clin Oncol. 2021;17:193-208.
43. Gao S, Wang K, Wang X. miR-375 targeting autophagy-related 2B (ATG2B) suppresses autophagy and tumorigenesis in cisplatin-resistant osteosarcoma cells. Neoplasma. 2020;67:724-34.
44. Mukherjee S, Dash S, Lohitesh K, Chowdhury R. The dynamic role of autophagy and MAPK signaling in determining cell fate under cisplatin stress in osteosarcoma cells. PLOS ONE. 2017;12(6):e0179203. PubMed PMID: 28598976.
45. Xiao X, Wang W, Li Y, Yang D, Li X, Shen C, et al. HSP90AA1-mediated autophagy promotes drug resistance in osteosarcoma. J Exp Clin Cancer Res. 2018;37(1):201. PubMed PMID: 30153855
46. Miao X-D, Cao L, Zhang Q, Hu X-Y, Zhang Y. Effect of PI3K-mediated autophagy in human osteosarcoma MG63 cells on sensitivity to chemotherapy with cisplatin. Asian Pac J Trop Med. 2015;8:731-8.
47. Zhang Z, Shao Z, Xiong L, Che B, Deng C, Xu W. Expression of Beclin1 in osteosarcoma and the effects of down-regulation of autophagy on the chemotherapeutic sensitivity. J Huazhong Univ Sci Technolog Med Sci. 2009;29:737-40.
48. Liu B, Feng C, Liu Z, Tu C, Li Z. A novel necroptosis-related lncRNAs signature effectively predicts the prognosis for osteosarcoma and is associated with immunity. Front Pharmacol. 2022;13:944158. PubMed PMID: 36105232.
49. Passeri G, Northcote-Smith J, Perera R, Gubic N, Suntharalingam K. An osteosarcoma stem cell potent nickel(II)-Polypyridyl Complex Containing Flufenamic Acid. Molecules. 2022;27(10):3277. PubMed PMID: 35630754.
50. Li J, Yang Z, Li Y, Xia J, Li D, Li H, et al. Cell apoptosis, autophagy and necroptosis in osteosarcoma treatment. Oncotarget. 2016;7:44763-78.
51. Hua L, Lei P, Hu Y. Construction and validation model of necroptosis-related gene signature associates with immunity for osteosarcoma patients. Sci Rep. 2022; 12(1):15893. PubMed PMID: 36151259.
52. Xiao H, Jensen PE, Chen X. Elimination of osteosarcoma by necroptosis with graphene oxide-associated Anti-HER2 antibodies. Int J Mol Sci. 2019;20(18):4360. PubMed PMID: 31491952.
53. Sun M, Zhou C, Zeng H, Puebla-Osorio N, Damiani E, Chen J, et al. Hiporfin-mediated photodynamic therapy in preclinical treatment of osteosarcoma. Photochem Photobiol. 2015;91:533-44.
54. Coupienne I, Fettweis G, Piette J. RIP3 expression induces a death profile change in U2OS osteosarcoma cells after 5-ALA-PDT: Lasers in Surg Med. 2011;43: 557-64.
55. Qian C, Wu D, Du J. RIPK3 modulates sarcoma through immune checkpoint HAVCR2. Oncol Lett. 2022;24(5):381. PubMed PMID: 36238358.
56. Li S, Zhang T, Xu W, Ding J, Yin F, Xu J, et al. Sarcoma-targeting peptide-decorated polypeptide nanogel intracellularly delivers shikonin for upregulated

osteosarcoma necroptosis and diminished pulmonary metastasis. Theranostics. 2018;8:1361-75.
57. Tong X, Tang R, Xiao M, Xu J, Wang W, Zhang B, et al. Targeting cell death pathways for cancer therapy: recent developments in necroptosis, pyroptosis, ferroptosis, and cuproptosis research. J Hematol Oncol. 2022;15(1):174. PubMed PMID: 36482419.
58. Fu Z, Deng B, Liao Y, Shan L, Yin F, Wang Z, et al. The anti-tumor effect of shikonin on osteosarcoma by inducing RIP1 and RIP3 dependent necroptosis. BMC Cancer. 2013;13(1):580. PubMed PMID: 24314238.
59. Eskandari A, Flamme M, Xiao Z, Suntharalingam K. The bulk osteosarcoma and osteosarcoma stem cell activity of a necroptosis-inducing nickel(II)–phenanthroline complex. chembiochem. 2020;21:2854-60.
60. Dai W, Cheng J, Leng X, Hu X, Ao Y. The potential role of necroptosis in clinical diseases (Review). Int J Mol Med. 2021;47(5):89. PubMed PMID: 33786617
61. Marsh S, McLeod H, Dolan E, Shukla SJ, Rabik CA, Gong L, et al. Platinum pathway. Pharmacogenet Genomics. 2009;19:563-4.
62. Yang J, Bogni A, Schuetz EG, Ratain M, Dolan ME, McLeod H, et al. Etoposide pathway. Pharmacogenet Genomics. 2009;19:552-3.
63. Lowenberg D, Thorn CF, Desta Z, Flockhart DA, Altman RB, Klein TE. PharmGKB summary: ifosfamide pathways, pharmacokinetics and pharmacodynamics. Pharmacogenet Genomics. 2014;24:133-8.
64. Mikkelsen TS, Thorn CF, Yang JJ, Ulrich CM, French D, Zaza G, et al. PharmGKB summary: methotrexate pathway. Pharmacogenet Genomics. 2011;21:679-86.
65. Thorn CF, Oshiro C, Marsh S, Hernandez-Boussard T, McLeod H, Klein TE, et al. Doxorubicin pathways: pharmacodynamics and adverse effects. Pharmacogenet Genomics. 2011;21:440-6.
66. Poplin R, Ruano-Rubio V, DePristo MA, Fennell TJ, Carneiro MO, Van Der Auwera GA, et al. Scaling accurate genetic variant discovery to tens of thousands of samples [preprint]. Genomics; 2017. https://doi.org/10.1101/201178
67. Auwera Gvd, O'Connor BD. Genomics in the cloud: using Docker, GATK, and WDL in Terra. Sebastopol, CA: O'Reilly Media; 2020 2020. p. 467.
68. Li H. Aligning sequence reads, clone sequences and assembly contigs with BWA-MEM [preprint]. Genomics; 2013. https://doi.org/10.48550/arXiv.1303.3997.
69. Fairley S, Lowy-Gallego E, Perry E, Flicek P. The International Genome Sample Resource (IGSR) collection of open human genomic variation resources. Nucleic Acids Res. 2020;48(D1):D941-D7.
70. Kutanan W, Liu D, Kampuansai J, Srikummool M, Srithawong S, Shoocongdej R, et al. Reconstructing the human genetic history of Mainland Southeast Asia: insights from genome-wide data from Thailand and Laos. Mol Biol Evol. 2021;38:3459-77.
71. McLaren W, Gil L, Hunt SE, Riat HS, Ritchie GRS, Thormann A, et al. The ensembl variant effect predictor. Genome Biol. 2016;17(1):122. PubMed PMID: 27268795
72. Kopanos C, Tsiolkas V, Kouris A, Chapple CE, Albarca Aguilera M, Meyer R, et al. VarSome: the human genomic variant search engine. Bioinformatics. 2019;35(11):1978-80.
73. Richards S, Aziz N, Bale S, Bick D, Das S, Gastier-Foster J, et al. Standards and guidelines for the interpretation of sequence variants: a joint consensus recommendation of the American College of Medical Genetics and Genomics and the Association for Molecular Pathology. Genet Med. 2015;17:405-24.
74. Chen X, Schulz-Trieglaff O, Shaw R, Barnes B, Schlesinger F, Källberg M, et al. Manta: rapid detection of structural variants and indels for germline and cancer sequencing applications. Bioinformatics. 2016;32:1220-2.
75. Boeva V, Popova T, Bleakley K, Chiche P, Cappo J, Schleiermacher G, et al. Control-FREEC: a tool for assessing copy number and allelic content using next-generation sequencing data. Bioinformatics. 2012;28:423-5.
76. Krzywinski M, Schein J, Birol İ, Connors J, Gascoyne R, Horsman D, et al. Circos: An information aesthetic for comparative genomics. Genome Res. 2009;19:1639-45.
77. Szklarczyk D, Kirsch R, Koutrouli M, Nastou K, Mehryary F, Hachilif R, et al. The STRING database in 2023: protein–protein association networks and functional enrichment analyses for any sequenced genome of interest. Nucleic Acids Res. 2023;51(D1):D638-D46.
78. Verselis SJ, Rheinwald JG, Fraumeni JF, Jr., Li FP. Novel p53 splice site mutations in three families with Li-Fraumeni syndrome. Oncogene. 2000;19:4230-5.
79. Shoshani O, Brunner SF, Yaeger R, Ly P, Nechemia-Arbely Y, Kim DH, et al. Chromothripsis drives the evolution of gene amplification in cancer. Nature. 2021;591(7848):137-41.
80. Shao X, Lv N, Liao J, Long J, Xue R, Ai N, et al. Copy number variation is highly correlated with differential gene expression: a pan-cancer study. BMC Med Genet. 2019;20:175. PubMed PMID: 31706287.
81. Whirl-Carrillo M, Huddart R, Gong L, Sangkuhl K, Thorn CF, Whaley R, et al. An Evidence-Based Framework for Evaluating Pharmacogenomics Knowledge for Personalized Medicine. Clin Pharmacol Ther. 2021;1100:563-72.
82. Garcia-Canaveras JC, Lancho O, Ducker GS, Ghergurovich JM, Xu X, da Silva-Diz V, et al. SHMT inhibition is effective and synergizes with methotrexate in T-cell acute lymphoblastic leukemia. Leukemia. 2021;35:377-88.
83. Bignell GR, Santarius T, Pole JC, Butler AP, Perry J, Pleasance E, et al. Architectures of somatic genomic rearrangement in human cancer amplicons at sequence-level resolution. Genome Res. 2007;17:1296-303.
84. Lee JA, Carvalho CM, Lupski JR. A DNA replication mechanism for generating nonrecurrent rearrangements associated with genomic disorders. Cell. 2007;131:1235-47.

85. Campbell PJ, Yachida S, Mudie LJ, Stephens PJ, Pleasance ED, Stebbings LA, et al. The patterns and dynamics of genomic instability in metastatic pancreatic cancer. Nature. 2010;467(7319):1109-13.
86. Zhang CZ, Spektor A, Cornils H, Francis JM, Jackson EK, Liu S, et al. Chromothripsis from DNA damage in micronuclei. Nature. 2015;522(7555):179-84.
87. Maciejowski J, Li Y, Bosco N, Campbell PJ, de Lange T. Chromothripsis and kataegis induced by telomere crisis. Cell. 2015;163:1641-54.
88. Liu P, Yuan B, Carvalho CMB, Wuster A, Walter K, Zhang L, et al. An organismal CNV mutator phenotype restricted to early human development. Cell. 2017;168:830-42 e7.
89. Menghi F, Barthel FP, Yadav V, Tang M, Ji B, Tang Z, et al. The tandem duplicator phenotype is a prevalent genome-wide cancer configuration driven by distinct gene mutations. Cancer Cell. 2018;34:197-210 e5.
90. Li Y, Roberts ND, Wala JA, Shapira O, Schumacher SE, Kumar K, et al. Patterns of somatic structural variation in human cancer genomes. Nature. 2020;578(7793):112-21.
91. Hanahan D, Weinberg RA. Hallmarks of cancer: the next generation. Cell. 2011;144:646-74.
92. Janiszewska M, Primi MC, Izard T. Cell adhesion in cancer: Beyond the migration of single cells. J Biol Chem. 2020;295:2495-505.
93. Iozzo RV. Matrix proteoglycans: from molecular design to cellular function. Annu Rev Biochem. 1998;67:609-52.
94. Nikitovic D, Berdiaki A, Spyridaki I, Krasanakis T, Tsatsakis A, Tzanakakis GN. Proteoglycans-biomarkers and targets in cancer therapy. Front Endocrinol (Lausanne). 2018;9:69. PubMed PMID: 29559954.
95. Vitale D, Kumar Katakam S, Greve B, Jang B, Oh ES, Alaniz L, et al. Proteoglycans and glycosaminoglycans as regulators of cancer stem cell function and therapeutic resistance. FEBS J. 2019;286(15):2870-82.
96. Ahrens TD, Bang-Christensen SR, Jorgensen AM, Loppke C, Spliid CB, Sand NT, et al. The role of proteoglycans in cancer metastasis and circulating tumor cell analysis. Front Cell Dev Biol. 2020;8:749. PubMed PMID: 32984308
97. Mirabello L, Pfeiffer R, Murphy G, Daw NC, Patino-Garcia A, Troisi RJ, et al. Height at diagnosis and birth-weight as risk factors for osteosarcoma. Cancer Causes Control. 2011;22:899-908.
98. Pruksakorn D, Phanphaisarn A, Pongnikorn D, Daoprasert K, Teeyakasem P, Chaiyawat P, et al. AgeStandardized incidence rates and survival of osteosarcoma in Northern Thailand. Asian Pac J Cancer Prev. 2016;17:3455-8.
99. Bielack SS, Kempf-Bielack B, Delling G, Exner GU, Flege S, Helmke K, et al. Prognostic factors in high-grade osteosarcoma of the extremities or trunk: an analysis of 1,702 patients treated on neoadjuvant cooperative osteosarcoma study group protocols. J Clin Oncol. 2002;20:776-90.
100. team ACSmae. Osteosarcoma Early Detection, Diagnosis, and Staging: American Cancer Society; 2020 [updated March 1st, 2023]. [cited 2024 Mar 19]. Available from: https://www.cancer.org/cancer/types/osteosarcoma/detection-diagnosis-staging/survival-rates.html
101. Meazza C, Scanagatta P. Metastatic osteosarcoma: a challenging multidisciplinary treatment. Expert Rev Anticancer Ther. 2016;16:543-56.
102. Xie L, Xu J, Li X, Zhou Z, Zhuang H, Sun X, et al. Complete remission of metastatic osteosarcoma using combined modality therapy: a retrospective analysis of unselected patients in China. BMC Cancer. 2021;21(1):337. PubMed PMID: 33789614.
103. Mirabello L, Troisi RJ, Savage SA. Osteosarcoma incidence and survival rates from 1973 to 2004: data from the surveillance, epidemiology, and end results program. Cancer. 2009;115:1531-43.
104. Richardson SM, Wurtz LD, Collier CD. Ninety percent or greater tumor necrosis is associated with survival and social determinants of health in patients with osteosarcoma in the national cancer database. Clin Orthop Relat Res. 2023;481:512-22.
105. Dowty JG, Win AK, Buchanan DD, Lindor NM, Macrae FA, Clendenning M, et al. Cancer risks for *MLH1* and *MSH2* mutation carriers. Hum Mutat. 2013;34:490-7.
106. Bonadona V, Bonaiti B, Olschwang S, Grandjouan S, Huiart L, Longy M, et al. Cancer risks associated with germline mutations in *MLH1*, *MSH2*, and MSH6 genes in Lynch syndrome. JAMA. 2011;305:2304-10.
107. Ramsoekh D, Wagner A, van Leerdam ME, Dooijes D, Tops CM, Steyerberg EW, et al. Cancer risk in *MLH1*, *MSH2* and MSH6 mutation carriers; different risk profiles may influence clinical management. Hered Cancer Clin Pract. 2009;7:17. PubMed PMID: 20028567.
108. Huang KK, Jang KW, Kim S, Kim HS, Kim SM, Kwon HJ, et al. Exome sequencing reveals recurrent REV3L mutations in cisplatin-resistant squamous cell carcinoma of head and neck. Sci Rep. 2016;6:19552. PubMed PMID: 26790612
109. Huang F, Tanaka H, Knudsen BS, Rutgers JK. Mutant POLQ and POLZ/REV3L DNA polymerases may contribute to the favorable survival of patients with tumors with POLE mutations outside the exonuclease domain. BMC Med Genet. 2020;21(1):167. PubMed PMID: 32838755
110. Escobar-Hoyos LF, Penson A, Kannan R, Cho H, Pan CH, Singh RK, et al. Altered RNA splicing by mutant p53 activates oncogenic RAS signaling in pancreatic cancer. Cancer Cell. 2020;38:198-211 e8.
111. Smeby J, Sveen A, Eilertsen IA, Danielsen SA, Hoff AM, Eide PW, et al. Transcriptional and functional consequences of *TP53* splice mutations in colorectal cancer. Oncogenesis. 2019;8(6):35. PubMed PMID: 31092812
112. Chen J, Zhang D, Qin X, Owzar K, McCann JJ, Kastan MB. DNA-Damage-Induced Alternative Splicing of p53. Cancers (Basel). 2021;13(2). PubMed PMID: 33445417
113. Chen Z, Guo J, Zhang K, Guo Y. *TP53* mutations and survival in osteosarcoma patients: a meta-analysis of

published data. Dis Markers. 2016;2016:4639575. PubMed PMID: 27239089
114. Ren W, Gu G. Prognostic implications of *RB1* tumour suppressor gene alterations in the clinical outcome of human osteosarcoma: a meta-analysis. Eur J Cancer Care (Engl). 2017;26(1). PubMed PMID: 26503016
115. Zhu H, Tang J, Tang M, Cai H. Upregulation of SOX9 in osteosarcoma and its association with tumor progression and patients' prognosis. Diagn Pathol. 2013;8:183. PubMed PMID: 24188461
116. Genda T, Sakamoto M, Ichida T, Asakura H, Hirohashi S. Loss of cell-cell contact is induced by integrin-mediated cell-substratum adhesion in highly-motile and highly-metastatic hepatocellular carcinoma cells. Lab Invest. 2000;80:387-94.
117. Christofori G. Changing neighbours, changing behaviour: cell adhesion molecule-mediated signalling during tumour progression. EMBO J. 2003;22:2318-23.
118. Moh MC, Shen S. The roles of cell adhesion molecules in tumor suppression and cell migration: a new paradox. Cell Adh Migr. 2009;3:334-6.
119. Laubli H, Borsig L. Altered cell adhesion and glycosylation promote cancer immune suppression and metastasis. Front Immunol. 2019;10:2120. PubMed PMID: 31552050
120. Voronina N, Wong JKL, Hubschmann D, Hlevnjak M, Uhrig S, Heilig CE, et al. The landscape of chromothripsis across adult cancer types. Nat Commun. 2020;11(1):2320. PubMed PMID: 32385320
121. Zhang CZ, Leibowitz ML, Pellman D. Chromothripsis and beyond: rapid genome evolution from complex chromosomal rearrangements. Genes Dev. 2013; 272513-30.
122. Luijten MNH, Lee JXT, Crasta KC. Mutational game changer: Chromothripsis and its emerging relevance to cancer. Mutat Res Rev Mutat Res. 2018;777:29-51.
123. Vogelstein B, Kinzler KW. Cancer genes and the pathways they control. Nat Med. 2004;10:789-99.
124. Aplan PD. Causes of oncogenic chromosomal translocation. Trends Genet. 2006;22:46-55.
125. Sudmant PH, Rausch T, Gardner EJ, Handsaker RE, Abyzov A, Huddleston J, et al. An integrated map of structural variation in 2,504 human genomes. Nature. 2015;526(7571):75-81.
126. Group PTC, Calabrese C, Davidson NR, Demircioglu D, Fonseca NA, He Y, et al. Genomic basis for RNA alterations in cancer. Nature. 2020;578(7793):129-36.
127. Mitelman F, Johansson B, Mertens F. The impact of translocations and gene fusions on cancer causation. Nat Rev Cancer. 2007;7:233-45.
128. Ho SS, Urban AE, Mills RE. Structural variation in the sequencing era. Nat Rev Genet. 2020;21:171-89.
129. van Belzen I, Schonhuth A, Kemmeren P, Hehir-Kwa JY. Structural variant detection in cancer genomes: computational challenges and perspectives for precision oncology. NPJ Precis Oncol. 2021;5(1):15. PubMed PMID: 33654267
130. Harbers L, Agostini F, Nicos M, Poddighe D, Bienko M, Crosetto N. Somatic copy number alterations in human cancers: an analysis of publicly available data from the cancer genome atlas. Front Oncol. 2021;11:700568. PubMed PMID: 34395272
131. Scott AJ, Chiang C, Hall IM. Structural variants are a major source of gene expression differences in humans and often affect multiple nearby genes. Genome Res. 2021;31:2249-57.
132. Ameur A, Kloosterman WP, Hestand MS. Single-molecule sequencing: towards clinical applications. Trends Biotechnol. 2019;37:72-85.
133. Amarasinghe SL, Su S, Dong X, Zappia L, Ritchie ME, Gouil Q. Opportunities and challenges in long-read sequencing data analysis. Genome Biol. 2020;21(1):30. PubMed PMID: 32033565
134. Adewale BA. Will long-read sequencing technologies replace short-read sequencing technologies in the next 10 years? Afr J Lab Med. 2020;9(1):1340. PubMed PMID: 33354530.
135. Chen Z, He X. Application of third-generation sequencing in cancer research. Med Rev (2021). 2021;1: 150-71.
136. Tongjai S, Wattanasombat S, Nantasuwan N, Thongkumkoon P, Chaiyawat P, Pruksakorn D. 3OS ChemoGenes Supplementary Data. figshare [Internet]. 2024 [cited 2024 Apr 1]. Available frome: https://doi.org/10.6084/m9.figshare.25514878.v1

Biomedical Sciences and Clinical Medicine 2025;64(2):126-136.
doi: 10.12982/BSCM.2025.15
https://he01.tci-thaijo.org/index.php/CMMJ-MedCMJ/index

BSCM
Biomedical Sciences and Clinical Medicine

Original Article

Open Access

Male Victims of Family Physical Violence and Associated Forensic Aspects

Puimek Kasemtavornsin

Department of Forensic Medicine, Nakornping Hospital, Chiang Mai, Thailand

Correspondence:
Puimek Kasemtavornsin, MD, Department of Forensic Medicine, Nakornping Hospital, 159 Village No.10, Donkaew, Maerim, Chiang mai 50180, Thailand.
E-mail: pinkybeamy@hotmail.com

Received: November 17, 2024;
Revised: February 20, 2025;
Accepted: March 3, 2025

ABSTRACT

OBJECTIVE This study aimed to study the characteristics of violence against men aged 18 and over who were physically assaulted by family members and issues related to forensic aspects.

METHODS A retrospective analytic study of 225 male patients aged 18 or over who had been physically abused by family members and had received treatment or were autopsied at the forensic department of Nakornping Hospital during the six-year period from June 2018 through May 2024.

RESULTS Of the 225 individuals included in the study, 218 had been injured and 7 had died of their injuries. The highest incidence occurred in the 30-39 age group. The plurality of perpetrators of physical violence, a total of 65 individuals, was intimate partners, (28.89%). Weapons or other objects were used in 164 cases (72.89%), with knives being the most common, used in 92 cases (40.89%). The most frequently damaged parts of the body were the head, face, and arms, affected in 147 cases (65.33%). Most victims sustained injuries to multiple parts of the body. A total of 180 injured individuals (80.00%) were hospitalized. Only 65 victims (28.89%) reported the incidents to the police. Most of the victims of violence by relatives were either age 30-39 or over 60. The majority of the perpetrators were men, and the violence typically resulted in injuries to the upper part of the body.

CONCLUSIONS Male victims of family physical violence account for one-third of all domestic assaults. Individuals in their 30s are the most often abused. Injuries tended to be quite severe, often requiring hospitalization. This violence strains the healthcare system, the justice process budget and results in a loss of labor in the economy. Appropriate guidelines for assisting patients who are victims of domestic violence should ensure that treatment is provided without discrimination and with equality of human rights for both men and women.

KEYWORDS family violence, domestic violence, male abuse, physical violence

INTRODUCTION

According to reports from the Centers for Disease Control and Prevention of the United States, during their lifetime 41% of women and 26% of men have been victims of domestic violence (1) Domestic violence can take many forms, including physical abuse, sexual abuse, verbal abuse, emotional abuse, neglect of children or the elderly, stalking, or even financial coercion (2-4). However, most cases involve physical abuse (5-7). The consequences of being subjected to domestic violence can range from physical injuries,

post-traumatic stress disorder, low self-esteem, sexually transmitted infections. Additionally, children who witness parental violence are more likely to become perpetrators themselves when they grow up. The worst situations may lead to suicide or death (8-10). Generally, people think that victims of violence are primarily women and children. However, in reality, men can also be victims of domestic violence. Studies have found that violence against men is as prevalent as violence against women (11-14). Other studies have reported more male victims of domestic violence than females (15). Male victims of domestic violence often keep it a secret and do not seek help from hospitals, government agencies, or even the police (3). In general, previous studies of domestic violence have mostly focused on women rather than men. Due to the patriarchal nature of Thai society, the general public may think that Thai family members rarely harm men. Studies of male victims of domestic violence in Thailand are still scarce (9). In today's society, however, people are becoming more aware of gender equality (8, 16). The one-stop crisis center (OSCC) of Nakornping Hospital, which initially assisted only children and women, has since June 2018 included family violence in its policy in response to an increase in the number of men being abused by family members. Most of the violence reported at OSCC was physical abuse, for which there was obvious evidence. This study was conducted based on this principle and reasoning and aimed to study the characteristics of violence against men aged 18 and older who were physically assaulted by family members as well as issues related to forensic aspects of violence in those who received hospital treatment or who were examined by the forensic department of Nakornping Hospital over the of 6-year period from June 2018 through May 2024.

According to the Domestic Violence Victim Protection Act. B.E.2550 (2007 A.D.) Section 3, family violence refers to "any act intended to cause harm to the body, mind, or health, or an act done with the intention that it is likely to cause harm to the body, mind, or health of family members, or to compel or use undue influence to make family members act, refrain from acting, or accept any action improperly, but does not include negligent acts".

Family members refers to "spouses, former spouses, individuals who live or have lived together as husband and wife without being legally married, children, adopted children, family members, and any individuals who depend on and live in the same household".

METHODS

Study design

Retrospective analytic study

Population and Sample

Data was collected from a total of 225 male patients aged 18 and over who had been physically abused by family members and who had received treatment or been autopsied at the Forensic Medicine Department of Nakornping Hospital over a period of 6 years, from June 2018 through May 2024 (Figure 1).

Data collection

Data was collected from Out-patient Department records, forensic report forms, OSCC records, autopsy reports, and other medical reports, selecting all male cases who had been physically assaulted by family members, whether they had been examined at the clinical forensic medicine clinic or were deceased and underwent autopsy in the forensic department.

This study collected data in five areas 1) information on the victims and the perpetrators, 2) information on the physical assault, 3) the type of injury, 4) medical treatment, and 5) legal proceedings.

Data analysis

The characteristics of the sample group are described using descriptive statistics including numbers, percentages, means, and standard deviations. Data was analyzed using SPSS for descriptive statistics and group relationships were determined using the Chi-Square test or Fisher's exact test, with the statistical significance level set at 0.05.

Ethical statement

This study was approved for human research by Nakornping Hospital on June 27, 2024 (ethics approval number NKP No.106/67).

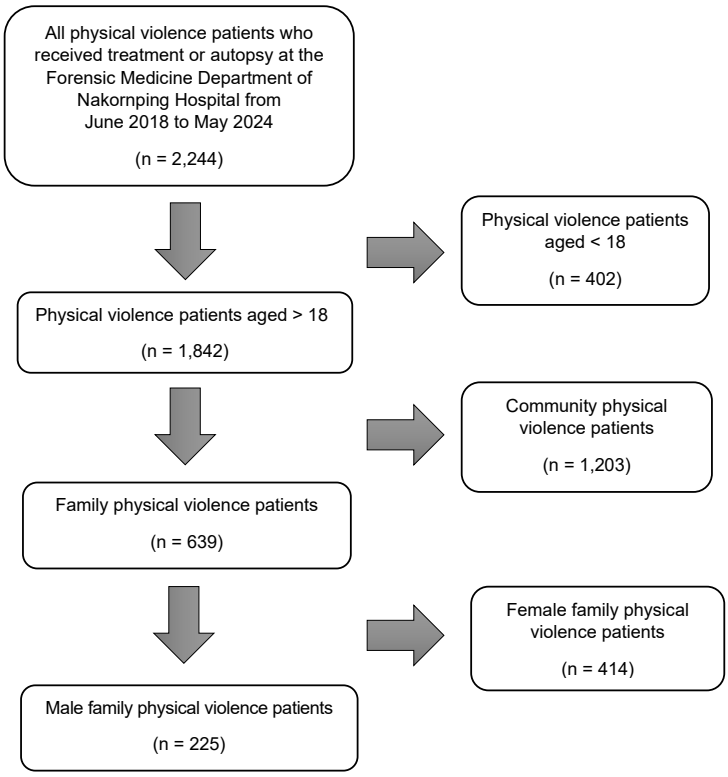

Figure 1. Flow chart of the patient selection process

RESULTS

This study was conducted at the Forensic Medicine Department of Nakornping Hospital, which provides physical examinations for legal case patients and performs autopsies on individuals who die an unnatural death. Data was collected from June 1, 2018 through May 31, 2024. There was a total of 1,759 patients over the age of 18 who had been physically assaulted, comprising 1,203 males (68.39%) and 556 females (31.61%). Among those, 625 individuals had been physically assaulted by family members, accounting for 35.53% of all assaulted patients. Among the autopsies of individuals over the age of 18 who had died from physical assaults, there were 83 cases over the six-year data collection period, consisting of 73 males (87.95%) and 10 females (12.05%). There were 14 cases of individuals murdered by family members, accounting for 16.87% of all assault-related deaths. In this study, there were a total of 225 males aged 18 and over who were physically assaulted by family members and who underwent medical treatment or autopsy at the forensic medicine department at Nakornping Hospital between June 2018 and May 2024 (Figure 2).

Victim and perpetrator characteristics

The average age of the 225 men aged 18 and over who were physically abused by family members was 44.07 ± 14.97 years. The youngest was 18 years old, punched by his father and the oldest was 84 years old. There were two cases involving a son pushing his father and a grandson slapping his grandfather. The age group most frequently abused by family members was 30-39 years, with 61 cases (27.11%). Most of the perpetrators were male, totaling 135 (60.00%). In cases involving intimate partners, most of the perpetrators were female 63 cases or 96.92%, with only two cases involving same-sex couples. Most perpetrators acted alone (215 cases or 95.50%), while eight involved more than one perpetrator, half of whom were family members and half outsiders (Table 1). The perpetrators included intimate partners in 65 cases (28.89%), other relatives in 159 cases (70.67%) and one case involving an action by a wife with a son (Figure 3).

Mechanism of injuries from family physical violence

This study found that male victims of domestic violence are often harmed by either weapons or household items, with 164 cases (72.89%) involving

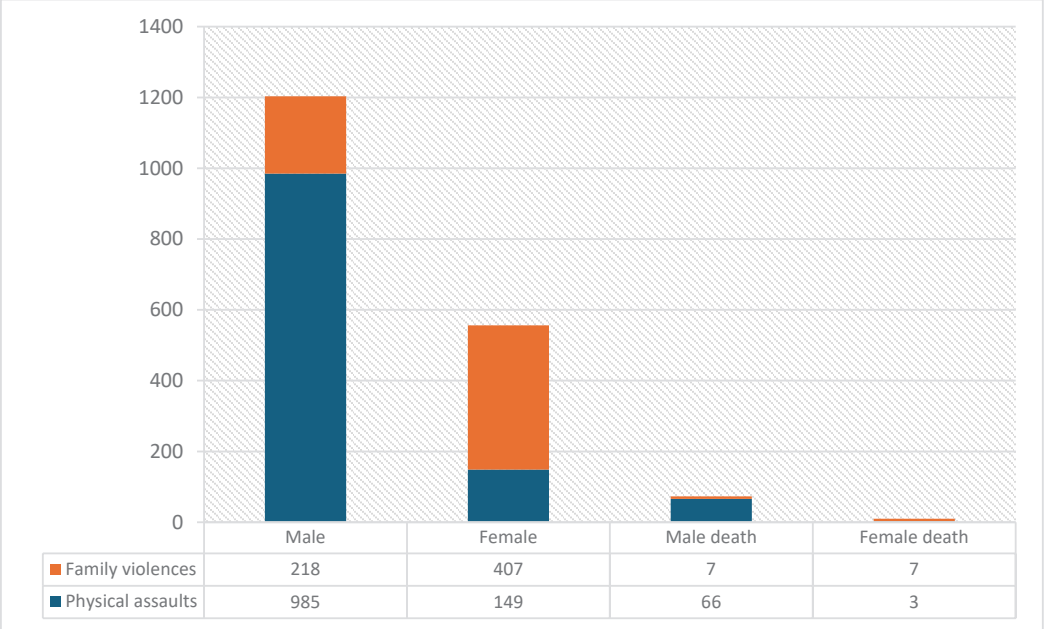

Figure 2. The total number of patients who were physically assaulted or murdered over a period of 6 years, from June 2018 through May 2024

Table 1. Information about male victims and family violence perpetrators

		n=225 (100%)
Victims	Age, n (%)	
	18-29 years	42 (18.67)
	30-39 years	61 (27.11)
	40-49 years	44 (19.56)
	50-59 years	35 (15.55)
	≥60 years	43 (19.11)
Perpetrators	Gender, n (%)	
	Male	135 (60.00)
	Female	74 (32.89)
	Both male & female	4 (1.78)
	N/A	12 (5.33)
	Number of perpetrator (s), n (%)	
	1	215 (95.56)
	>1	8 (3.55)
	N/A	2 (0.89)
	Relationship, n (%)	
	IPV	65 (28.89)
	Non-IPV	159 (70.67)
	IPV & non-IPV	1 (0.44)

N/A, not available; IPV, intimate partner violence; non-IPV, non-intimate partner violence

weapons and 58 cases (25.78%) involving bodily harm without weapons. Weapons were used seven times as often as household items, with 140 cases (85.37%) involving weapons and only 20 cases (12.20%) involving household items (Table 2). There were one case involving the use of gasoline to set the male victim on fire and one case of running over the victim with a car. Most physical violence involved punching, hitting, slapping, and kicking. The study found that injuries from sharp objects were the most common at 46.66%, and almost all victims had visible wounds and other injuries, with only 2 cases showing no visible injuries (Table 3).

In cases where females were the perpetrators, the use of weapons or other equipment was found in 59 cases (79.73%), with 58 individuals (78.38%) admitted to the hospital but only 17 individuals (22.97%) reported the incident to the police. In cases where males were the perpetrators, the use of weapons or other equipment was found in relatively fewer cases, specifically 94 individuals (69.63%), with 112 individuals (82.96%) admitted to the hospital, but a larger proportion (44 individuals or 32.59%) reporting to the police.

Autopsy of victims of family physical violence

The physical violence against males by family members in this study involved 218 injured individuals (96.89%) of whom 7 men (3.11%) died. Details of the deceased are shown in Table 4.

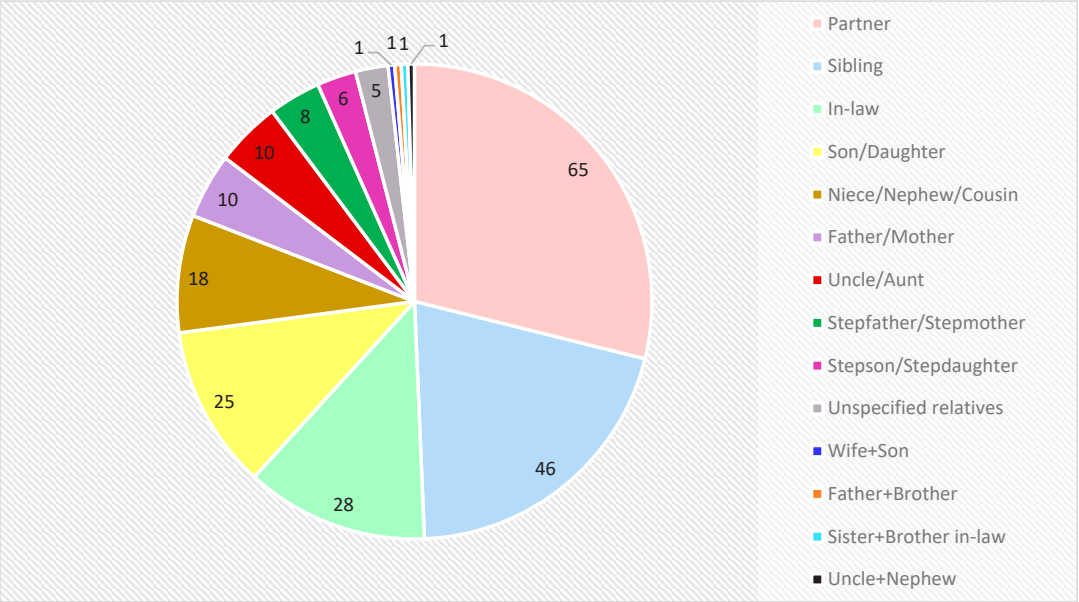

Figure 3. The number of men who were physically assaulted by family members

Table 2. Weapons and household items used by family members to physically assault men

Weapons	Cases	Household items	Cases
Knife	92	Bottle	9
Wood	16	Bamboo	4
Gun	11	Stone	3
Scissor	6	Bicycle pump	1
Hammer	5	Fan	1
Axe	5	Fork	1
Metal rod	5	Tray	1
Hoe	3	Guitar	1
Brass knuckle	2	Mortar	1
Sickle	1		

Table 3. Mechanisms of physical violence of male victims by family members

	Cases, n (%)
Instrument	164 (72.89)
Weapon	140 (62.22)
Household item	20 (8.89)
Weapons & household item	2 (0.89)
Others	2 (0.89)
Physical violence alleged	58 (25.78)
Barehanded (punches, kicks, slapping)	56 (24.89)
Shoving	9 (4.00)
Strangling	7 (3.11)
Grabbing	6 (2.67)
Scratching	6 (2.67)
Biting	4 (1.78)
Throwing objects	3 (1.33)
Injuries caused by	167 (74.22)
Sharp object	104 (46.22)
Blunt object	50 (22.22)
Gunshot injury	10 (4.46)
Gunshot & sharp object	1 (0.44)
Burn	1 (0.44)

Forensic examination of the injuries of family physical violence

Most of the injuries were found in the upper body, including the head and face, neck, chest, and arms, a total of 111 cases (49.33%). Injuries in the lower body alone, including the abdomen, back, genitals and anus, and legs, were found in only 20 cases. There were 94 cases of injuries in both the upper and lower body. The most frequently injured areas were the head/face and the arms, with 147 cases (65.33%). The least frequently injured areas were the genitals and anus, with only 3 cases. Most patients had injuries in more than one area, a total of 150 cases (66.67%), with the most extensive injuries involving six areas in one case where a female partner used a bottle to inflict harm. Among the injured who received treatment at the hospital, most had to be admitted for treatment, a total of 180 cases (80.00%). The most common diagnosis for male victims of family physical violence was soft tissue injury. Details of the diagnoses are shown in Table 5. There were differences in injuries from bodily force, blunt objects, and sharp object trauma as shown in Table 6. In terms of treatment, the

Table 4. Autopsy findings of male victims who died from physical violence by a family member

Autopsy	Age	Relation	Weapon	Findings
1	44	Father	Hammer	Basal subarachnoid hemorrhage, fracture maxilla & mandible
2	49	Mother	Knife	Hemoperitoneum, left carotid artery, lung & diaphragm tear
3	50	Wife	Gun	Hemothorax, hemoperitoneum, aorta, heart, both lungs, liver & right diaphragm tear
4	60	Sibling	Gun	Hemothorax, heart, right lung & liver tear, multiple left ribs fracture
5	32	Sibling	Knife	Hemothorax, left lung tear, fracture left 5th rib
6	56	Sibling	Axe	Diastatic fracture, bilateral frontal subarachnoid hemorrhage, multiple ribs fracture, right kidney tear
7	64	Daughter-in-law	Gun	Hemoperitoneum, aorta, right kidney & small intestine tear

Table 5. Diagnoses of male victims of family physical violence

Diagnosis	Cases	Diagnosis	Cases
Soft tissue injury	79	Bone fracture & tendon injury	51
Abrasion	47	Tendon, vessel, and nerve injuries	23
Contusion	39	Carpal bone	13
Cut	26	Ulnar	9
Laceration	19	Radius	4
Stab	8	Humerus	4
Fingernail	4	Scapular	3
Bite	3	Elbow	2
Burn	1	Shoulder	2
Head & face injury	77	Spine	1
Intracranial hemorrhage	40	Pelvis	1
Skull fracture	29	Femur	1
Fracture orbit	16	Foot	1
Fracture nasal	15	Abdominal injury	21
Fracture zygoma	11	Thoracic injury	21
Fracture mandible	9	Blindness	1
Fracture maxilla	3	Paralysis	1
Fracture facial sinus	3		

Table 6. Comparison between injuries from bodily force, blunt object, and sharp object trauma

	Bodily force	Blunt object trauma	Sharp object trauma
Location	Upper body	Upper body	Throughout body
Injured area	Head & face	Head & face	Arm
Diagnosis	Soft tissue injury	Head & face injury	Bone & tendon injury
Treatment	Medication	Medication	Debridement & suture
Admission rate	65.52%	80.00%	88.46%

most common was debridement and suturing the wound, with 88 cases (39.11%), most of whom were admitted for 1-3 days; no cases were admitted for more than 1 month.

Most victims did not report the violence to the police: 160 people (71.11%). Only 65 people (28.89%) reported the incident, with the majority of those reporting being relatives of the victim (50 cases). In only 15 cases were the people involved classified as intimate partners.

Differences among characteristics in cases involving intimate partner violence (IPV) and non-intimate partner violence (non-IPV) offenders and the results of statistical group comparison

When comparing the group of males who were abused by their partners with the ones who were abused by relatives, a significant factor difference

is age. Abused individuals in both groups were mostly in the age range of 30-39 years, but in cases of abuse by relatives, it was more common to find individuals over 60 years old as well. The perpetrators in the intimate partner group were mostly female, while in the relative group they were usually male. The injury locations in the former group often included both upper and lower parts of the body, while in the latter group, most were only in the upper body (Table 7).

DISCUSSION

This study found the male family physical violence rate to be 35.21%. Violence often comes from intimate partners rather than other relatives. Among relatives, siblings were found to be the most violent towards each other, possibly due to their proximity, which makes conflicts more likely. The rate of IPV was 15.55%. Two studies in France found IPV rates of 11.39% (6) and 11.00% (17), while a study in Portugal found a rate of 11.51% (18). In Australia, the rate involving an intimate partner was similar at 12.00% (19). This contrasts with studies in Arab countries, where the deeply rooted patriarchal culture showed much lower rates of male IPV. In Turkey, the rate was 1.30% (20), and 1.40% in Jordan (21). Most of the physical violence against men in the current study involved heterosexual partners, with only 3.08% involving same-sex partners. Despite increasing openness about homosexuality, some still consider it shameful, do not want their families to know, fear social stigma, or worry about bias and discrimination from law enforcement. This has led to even less disclosure of violence between same-sex partners. Studies of violence between same-sex partners are still rare, but one study in the U.S., a country with sexual freedom, found a rate of 13.80% (3). A study in Germany found a similar rate of 8.40% (22).

The age group where male physical abuse occurred most frequently was 30-39 years, which aligns with most studies (6, 8, 23). This may be due to high stress levels related to work and finances, potentially affecting family relationships. As for abuse by relatives, it is most commonly found in two age groups: 30-39 and over 60 years. In the over-60 age group, the abuse is often perpetrated by children, with issues of alcohol or drug addiction.

As to the issue of reporting to the police, our study found that 28.89% of cases involved reporting family members, while only 23.08% involved reporting intimate partners. A study in Germany found reporting rates as high as 78.40% (22), and France the rate was 58.40% (6). However, a study in Australia found a lower reporting rate of 8.10% (19). Most male victims of physical abuse tend to confide in friends, relatives, neighbors, or even strangers on social media rather than consulting a doctor, who received the lowest number of consultations (3). When it comes to reporting to the police, victims stated that the police provided the least amount of help due to various factors, particularly the patriarchal nature of Thai society. Male victims feared being blamed for weakness, for not being trustworthy, being ridiculed by society, being falsely accused of being the aggressor, losing custody of their children, or because their injuries were minor and they hoped their partner would change their attitude and they could reunite as a family (3, 4, 8, 24).

In IPV, injuries are often found throughout the body, both upper and lower parts. This may be due to the incidents occurring in private homes where there are no witnesses to assist. During a scuffle, injuries can occur to all parts of the body in a non-specific manner. The most commonly injured areas are the arms (69.23%), followed by the head and face (41.54%). Similarly, in studies in France and Germany (18, 22), the upper limbs were the most frequently injured areas. In two other studies conducted in France (6, 25), the head and neck were the most commonly injured areas (71.70% and 61.00%, respectively). Arm injuries are rampant due to defensive actions, while the head and face are easily accessible areas for harm. In cases of violence by other relatives, injuries are often found only in the upper body rather than the entire body.

Most studies have found that men are more often subjected to violence in the form of blunt force rather than sharp force. For example, a study in France found the incidence of blunt force to be 79.00% and of sharp force to be 12.00% (22). Another study in Bulgaria similarly found the former more than the latter (97.20% vs. 2.80%) (23). Two other studies from France found that blunt objects were used more than sharp objects, with 15.00% versus 11.10% (6) and 16.60% versus 2.30%

Table 7. Differences in characteristics among cases involving intimate partner violence and other relative offenders and results of statistical group comparison

	IPV=65 (100%)	Non-IPV=159 (100%)	Total=224 (100%)	*p*-value
Age, n (%)				0.042[a*]
18-29 years	14 (21.54)	28 (17.61)	42 (18.75)	
30-39 years	24 (36.92)	37 (23.27)	61 (27.23)	
40-49 years	14 (21.54)	29 (18.24)	43 (19.20)	
50-59 years	7 (10.77)	28 (17.61)	35 (15.62)	
≥60 years	6 (9.23)	37 (23.27)	43 (19.20)	
Sex, n (%)				0.000[b*]
Male	2 (3.08)	133 (83.65)	135 (60.27)	
Female	61 (93.84)	13 (8.17)	74 (33.03)	
Male & Female	2 (3.08)	1 (0.63)	3 (1.34)	
N/A	0 (0.00)	12 (7.55)	12 (5.36)	
Number of perpetrator(s), n (%)				1.000[b]
1	63 (96.92)	152 (95.60)	215 (95.98)	
>1	2 (3.08)	6 (3.77)	8 (3.57)	
N/A	0 (0.00)	1 (0.63)	1 (0.45)	
Instrument, n (%)				0.165[b]
Weapon	42 (64.61)	98 (61.63)	140 (62.50)	
Household item	6 (9.23)	14 (8.81)	20 (8.93)	
Weapon & household item	2 (3.08)	0 (0.00)	2 (0.89)	
No	13 (20.00)	45 (28.30)	58 (25.90)	
Others	1 (1.54)	1 (0.63)	2 (0.89)	
N/A	1 (1.54)	1 (0.63)	2 (0.89)	
Injuries caused by, n (%)				0.128[b]
Sharp object	38 (58.46)	66 (41.51)	104 (46.43)	
Blunt object	12 (18.46)	38 (23.90)	50 (22.32)	
Body	13 (20.00)	44 (27.67)	57 (25.45)	
Gunshot injury	1 (1.54)	9 (5.66)	10 (4.45)	
Gunshot & sharp object	0 (0.00)	1 (0.63)	1 (0.45)	
Burn	0 (0.00)	1 (0.63)	1 (0.45)	
N/A	1 (1.54)	0 (0.00)	1 (0.45)	
Severity, n (%)				0.676[b]
Injury	64 (98.46)	153 (96.23)	217 (96.88)	
Death	1 (1.54)	6 (3.77)	7 (3.12)	
Location, n (%)				0.018[a*]
Upper body	24 (36.92)	87 (54.72)	111 (49.55)	
Lower body	10 (15.39)	10 (6.29)	20 (8.93)	
Upper & Lower	31 (47.69)	62 (38.99)	93 (41.52)	
Admit, n (%)				0.182[a]
IPD	49 (75.38)	131 (82.39)	180 (80.36)	
OPD	15 (23.08)	22 (13.84)	37 (16.52)	
Death	1 (1.54)	6 (3.77)	7 (3.12)	
Length of stay, n (%)				0.378[b]
1-3 day(s)	28 (43.08)	58 (36.48)	86 (38.39)	
4-10 days	17 (26.15)	56 (35.22)	73 (32.59)	
10 days – 1 month	2 (3.08)	9 (5.66)	11 (4.91)	
Refer	2 (3.08)	8 (5.03)	10 (4.46)	
OPD	15 (23.07)	22 (13.84)	37 (16.52)	
Death	1 (1.54)	6 (3.77)	7 (3.13)	
Police, n (%)				0.210[a]
Yes	15 (23.08)	50 (31.45)	65 (29.02)	
No	50 (76.92)	109 (68.55)	159 (70.98)	

[a]Chi square test, [b]Fisher's exact test, [*]Statistically significant ($p < 0.05$)

N/A, not available; IPD, In-patient Department; IPV, intimate partner violence; non-IPV, non-intimate partner violence; OPD, Out-patient Department

(18). In contrast, our study frequently found male family physical violence using sharp objects. In cases of IPV, sharp objects were used in 58.46% of the cases, followed by the use of the body as a weapon in 20.00%. The use of blunt objects was the least frequent, at 18.46%. Similarly, another study in France found that sharp objects were used more frequently than blunt objects, with sharp objects at 12.60% and blunt objects at only 5.20% (25). Another point that our study found to be different from previous studies is that in our study weapons were often used, accounting for 63.11% of cases. In cases involving intimate partners, weapons were used 67.69% of the time, with knives being the most common weapon. This study found that knives were used in 53.85% of intimate partner cases. This may be due to the context of Thai society, where the belief that men are the dominant figures persists even today. If there is no extreme fear or anger, women rarely physically harm men. When they do choose to act, they often need weapons or tools to defend themselves because men have greater physical strength, and women still primarily handle household chores. Knives are commonly found in every household, making them a familiar weapon that can be easily thought of and grabbed in urgent situations. However, in most studies, male victims were more often harmed through direct physical force (6, 17, 18, 22, 25) In most cases, no weapons or other tools were involved. But in cases where tools were used, they were often used with male victims more than female victims, and they were usually household objects (6, 26). A study in France found that women used objects to physically harm men more than men did to harm women (33.00% vs. 19.00%) (17). Another study in Germany found that 55.70% of men physically harmed by their partners had no weapons or tools, and if they did, they were usually objects rather than weapons (65.80%). The most commonly used weapon was a knife (22).

When considering the severity of injuries in our study, it was found that serious injuries were more common in IPV, at 52.31%, while minor injuries, which include skin abrasions, were at 47.69%. From past studies comparing men and women in a family who had been physically abused, it was found that men often sustained more severe injuries than women (16, 25). This is because women often use weapons or tools in the abuse, resulting in more severe trauma compared to cases where men are the perpetrators. Similarly, a study in Turkey found that male victims often experienced major trauma more frequently than female victims, with a mortality rate of 56.30% versus 12.30% for women (20). However, reports of several studies differ, indicating that the severity of injuries in men is often minor, e.g., skin abrasions, bruises, and hematomas (6, 8, 18). For example, a study from France found that while injuries in men were more frequent, they were not as severe as those found in women, with severe injuries like fractures occurring in only 5.00% of cases (17). Another study in France also found that superficial skin injuries were more common in men, with only 2.40% of male victims sustaining fractures (25). Regarding mortality rates, our study found that more men than women died from family violence, with rates of 3.11% and 1.69%, respectively.

When domestic violence occurs, seeking medical help is often a rare occurrence. A study in Portugal found that only 8.10% sought medical assistance (18). In the United States, agencies that assist men who have experienced violence found that men most frequently used counseling services, followed by the police, with medical services being third. This study found that one in three men reported having had negative experiences with medical services after being assaulted (3). In an Australian study, only 26.10% of male victims sought health services (19), while another American study found that only 18.10% of male victims visited a doctor (27). Research has shown that medical personnel often lack knowledge and awareness of male violence (28), and some places lack counselors for men who have experienced domestic violence. In this study, the proportion of men who were physically abused by their partners and required hospitalization was found to be quite high, up to 75.38%, because they are often attacked with sharp weapons violently, although most usually recover in the hospital in no more than 3 days, which is different from 3 studies in France that found only 7.00% (17), 3.10% (6) and 2.10% (25) of patients needed hospitalization and that most treatment involved medication and observation, while surgery was required in only 7.50% of cases. In contrast, our study found that 20.00% of male patients required surgery.

Limitations

Firstly, as this is a retrospective study, there are limitations regarding the completeness and accuracy of the data. Some patient information may have been missing or inadequately recorded, such as the perpetrator's gender, the number of perpetrators, the familial relationship, or the weapons used, which could affect the data analysis. Another limitation is that patients may have reported false or incorrect accusations of abuse to the hospital. Additionally, this study only collected data from patients receiving treatment at Nakornping Hospital in Chiang Mai Province, which may have different social characteristics and values than the general population. Therefore, this sample cannot be considered representative of the general population of Thailand. Future studies should involve a larger population, potentially at the provincial, regional, or national level, and should further investigate the causes of physical abuse, repeated victimization, and the psychological state of the victims. It should also include assessments of the perpetrators and family members affected in order to better understand the social context surrounding men who are abused by family members, and to prevent and reduce the number of people experiencing family physical violence in the future. Healthcare professionals should implement policies that promote understanding of male victims of domestic violence, without gender bias. Legal enforcement should emphasize that abuse victims, regardless of gender, should not be ignored. There should be a shift away from patriarchal values that enforce the idea that men must be family leaders, as sometimes men can also be victims of domestic abuse just like women.

CONCLUSIONS

Since the OSCC began collecting data, a period of 6 years, it has been found that male victims of family physical violence account for one-third of all physical domestic violence. In reality, the number is likely higher, as those who do not visit doctors if not severely injured or who are unwilling to inform the police, often keep the abuse a secret. Among men who are abused by family members, only about 1 in 4 report it to the police. The age group most often abused is the 30s, the working age, leading to both a loss of labor and income. The most frequent perpetrators are female partners, which can make children witnesses and can lead to a chain reaction of ongoing impacts. This study found that physical abuse of males tends to be quite severe, often involving sharp weapons, resulting in injuries that require hospitalization, surgery, casts, or sutures. This strains the healthcare budget and leads to a loss of labor in the economy. Additionally, expenditures for the justice process are affected. Collaboration between forensic examinations and the OSCC can provide more assistance to male victims of violence, including screening for those in need of help, preventing repeated violence, treating injuries, and rehabilitating both physically and mentally, as well as providing legal assistance. This comprehensive approach to preventing family violence should be non-discriminatory, ensuring equality in human rights for both men and women.

ACKNOWLEDGMENTS

The author would like to thank the Social Work Department of Nakornping Hospital for helping to gather patient information.

FUNDING

This research received no specific grant from any funding agency in the public, commercial, or not-for-profit sectors.

CONFLICTS OF INTEREST

The author has no conflicts of interest to report.

REFERENCES

1. CDC [Internet]. Atlanta: Centers for Disease Control and Prevention; c1996. Intimate partner violence prevention; [updated 2024 May 16; cited 2024 Oct 20]; [about 1 screen]. Available from: https://www.cdc.gov/intimate-partner-violence/about/index.html
2. Phantong W, Thapsongsang P, Pluplatong T. "Man don't cry": Male victims of domestic violence and abuse in family. J Buddhist Psychol. 2022;7:99-114.
3. Tsui V. Male victims of intimate partner abuse: Use and helpfulness of services. Soc work 2014;59:121-30.
4. Perryman SM, Appleton JV. Male victims of domestic abuse: implications for health visiting practice. Int J Res Nurs. 2016;21:386-414.
5. Taft A, Hegarty K, Flood M. Are men and women equally violent to intimate partners?. Aust N Z J Public Health. 2001;25:498-500.
6. Dumont N, Martrille L, Albuisson E, Baland-Peltre K, Marchand E. Examining men as victims of intimate

partner violence in a French forensic department. Forensic Sci Int. 2022;337:111368. PubMed PMID: 35809544.
7. Chuemchit M, Perngparn U. Intimate Partner Violence: Thailand Situation and Intervention Programme. IJSSH. 2014;4:275-8.
8. Kolbe V, Büttner A. Domestic violence against men-prevalence and risk factors. Dtsch Arztebl Int. 2020;117:534-41.
9. Kulachai W, Chitsawang S. A causal model analysis of violence committed by women against their intimate partners. J Public Adm Polit. 2023;12:20-41.
10. Lee M, Stefani KM, Park E. Gender-specific differences in risk for intimate partner violence in South Korea. BMC Public Health. 2014;14:415. PubMed PMID: 24885985
11. Archer J. Sex differences in aggression between heterosexual partners: A meta-analytic review. Psychol Bull. 2000;126:651-80.
12. Graham-Kevan N. The re-emergence of male victims. Int J Men's Health 2007;6:3–6.
13. Gass JD, Stein DJ, Williams DR, Seedat S. Gender differences in risk for intimate partner violence among South African adults. J Interpers Violence. 2011;26: 2764-89.
14. Ansara D, Hindin M. Exploring gender differences in the patterns of intimate partner violence in Canada: a latent class approach. J Epidemiol Community Health. 2009;64:849-54.
15. Leung P, Cheung M. A prevalence study on partner abuse in six Asian-American ethnic groups in the United States. Int Soc Work. 2008;51:635-49.
16. Mahyut SMB, Dhillon G. Story of domestic violence against men: the truth, untold and complicated. JMPHSS. 2017;1:24-30.
17. Thureau S, Le Blanc-Louvry I, Thureau S, Gricourt C, Proust B. Conjugal violence: a comparison of violence against men by women and women by men. J Forensic Leg Med. 2015;31:42-6.
18. Carmo R, Grams A, Magalhães T. Men as victims of intimate partner violence. J Forensic Leg Med. 2011;18: 355-9.
19. Grande ED, Hickling J, Taylor A. Domestic violence in South Australia: a population survey of males and females. Aust N Z J Public Health. 2003;27:543-50.
20. Kavak N, Kavak RP, Özdemir M, Sever M, Ertan N, Suner A. A 10-year retrospective analysis of intimate partner violence patients in the emergency department. Ulus Travma Acil Cerrahi Derg. 2022;28:796-804.
21. Alsawalqa RO. A qualitative study to investigate male victims' experiences of female-perpetrated domestic abuse in Jordan. Curr Psychol. 2023;42:5505-20.
22. Wörmann X, Wilmes S, Seifert D, Anders S. Males as victims of intimate partner violence -results from a clinical forensic medical examination centre. Int J Legal Med. 2021;135:2107-15.
23. Kiryakova T, Alexandrov A. Forensic aspects of domestic violence: men as victims of intimate partner violence. Med Biol Stud. 2022;6:5-12.
24. Walker A, Lyall K, Silva D, Craigie G, Mayshak R, Costa B, et al. Male victims of female-perpetrated intimate partner violence, help-seeking, and reporting behaviors: a qualitative study. Psychol Men Mascul. 2019;21:213-23.
25. Savall F, Lechevalier A , Hérin C, Vergnault M, Telmon N, Bartoli C. A ten-year experience of physical Intimate partner violence (IPV) in a French Forensic Unit. J Forensic Leg Med. 2017;46:12-5.
26. Drijber BC, Reijnders UJL, Ceelen M. Male victims of domestic violence. J Fam Viol. 2013;28:173-8.
27. Douglas EM, Hines DA. The helpseeking experiences of men who sustain intimate partner violence: an overlooked population and implications for practice. J Fam Violence. 2011;26:473-85.
28. Barber CF. Domestic violence against men. Nurs Stand. 2008;22:35-9.

Biomedical Sciences and Clinical Medicine 2025;64(2):137-149.
doi: 10.12982/BSCM.2025.11
https://he01.tci-thaijo.org/index.php/CMMJ-MedCMJ/index

Original Article

Open Access

Evaluation of Various Resolutions for Optimization and Dose Calculation in VOLO™ Ultra of the Tomo Therapy Treatment Planning System

Sirirad Tongta[1,2], Anirut Watcharawipha[2], Wannapha Nobnop[2], Somsak Wanwilairat[2] and Warit Thongsuk[2]

[1]Medical Physics Program, [2]Division of Radiation Oncology, Department of Radiology, Faculty of Medicine, Chiang Mai University, Chiang Mai, Thailand

Correspondence:
Anirut Watcharawipha, PhD,
Division of Radiation Oncology,
Faculty of Medicine, Chiang Mai University. 110 Inthavarorot Rd,
Tambon Si Phum, Amphur Muang,
Chiang Mai, 50200, Thailand.
E-mail: anirut.watch@cmu.ac.th

Received: 26 September, 2024;
Revised: December 14, 2024;
Accepted: January 7, 2025

ABSTRACT

OBJECTIVE Helical tomotherapy can deliver a radiation dose using modulated intensity. This delivery technique requires inverse treatment planning for dose distribution. The specific parameters include the resolution of optimization and dose calculation. The highest resolution provided a high plan quality in a previous study, but that plan would increase the calculation time. This study investigated the quality of plans using various resolutions of optimization and dose calculation in VOLO™ Ultra. The exploration aimed to determine the optimal resolution to inform the treatment planning process in nasopharyngeal carcinoma (NPC).

METHODS Forty-one cases of NPC who had been previously treated using helical therapy were randomly recruited between January 2022 and December 2023. Nine treatment planning scenarios were created using the VOLO™ Ultra planning system using a combination of optimization and calculated resolution. Three different levels of resolutions were chosen: high (H), medium (M) and low (L). The different resolution combinations were expressed as, e.g., H/H for high resolution optimization and dose calculation. The dosimetric parameters of the planning target volumes (PTVs), organs at risk (OARs), and plan quality index, such as dose coverage ($D_{98\%}$, Dose at 98% target volume), conformity index (CI) and homogeneity index (HI), were evaluated.

RESULTS The PTVs revealed an increasing dose value when the dose calculation resolution was increased. In contrast, the study found an increasing dose value when the resolution was decreased. A similar trend was also found in the conformity index value in the optimization process. The OARs demonstrated similar dose levels, with the exception of the spinal cord and both parotid glands.

CONCLUSIONS This study illustrates that the resolution of M/H and M/M scenarios is a specific choice of interest. These scenarios provide higher dose coverage, have a mild impact on OAR dose, a moderate impact on conformity and a shorter treatment planning time.

KEYWORDS tomotherapy, dose optimization, dose calculation, nasopharyngeal carcinoma, resolution

INTRODUCTION

Radiotherapy in the head and neck region (H&N) presents a significant challenge for treatment planning. The complexity of treatment planning is heightened by the proximity of critical organs such as the brainstem, parotids, and spinal cord to target area. For those reasons, intensity modulated radiotherapy (IMRT) plays a crucial role (1) in sparing normal organs (2) while delivering the prescribed dose to the target. Inverse planning (3) is necessary for this treatment technique, which requires dose constraints, photon fluence optimization and dose calculation. Tomotherapy is a treatment modality that provides intensity modulation using both a static gantry IMRT and a rotating gantry (Intensity Modulated Arc Therapy, IMAT). By utilizing a Binary Multi-Leaf Collimator (BiMLC) and overlapping helical fan beam rotation (helical tomotherapy, HT), this treatment offers beneficial beam modulation diversity (4).

When employing HT, the treatment planning system (TPS) requires specific parameters consisting of a field width (FW), a pitch factor (PF), and a modulation factor (MF) (5). FW is the width of the radiation fan beam which can be selected based on the length of the target. PF can be determined by couch travel/FW. This parameter can be specified by the irregular shape of the target. In MF, this parameter is calculated by the ratio of the maximum leaf open time and the average leaf open time. The value of MF depends on the shape and location of the target. These parameters can improve the plan quality, particularly in the case of cancers in the H&N region. Treatment planning can be performed using two platforms in this TPS: the Classic treatment planning platform and the VOLO™ Ultra platform. The VOLO™ Ultra uses fewer specific parameters than the classic platform to create a treatment plan, e.g., there is no PF or MF requirement. Using the VOLO™ Ultra platform is convenient and user friendly, especially for nasopharyngeal carcinoma (NPC) treatment planning. However, there are other parameters that are required in both platforms, including the grid spacing or resolution of dose optimization and the dose calculation for each plan, both of which might impact plan quality. Although previous publications (5-10) have reported on the impact of resolution in dose optimization and dose calculation, this impact has not yet been demonstrated in tomotherapy, particularly VOLO™ Ultra treatment planning. The resolution in tomotherapy TPS can be selected from four different levels; however, the selection is also dependent on the size of the field of view (FOV). The resolution of HT is classified not only by an image pixel number, e.g., very low (64×64 pixels), low (128×128 pixels), medium (256×256 pixels) and high (512×512 pixels), but is also determined by the FOV/image pixel number, e.g. 500/512 or 600/512. For a high quality treatment plan, it is necessary to determine appropriate values for treatment parameters (11) and to use the highest resolution of the optimization and dose calculation. Although the central processing unit (CPU) technology has been highly developed, choosing the highest resolution may increase the computational time (5-7, 12).

By various the resolution in the optimization and dose calculation, this study aimed to investigate the impact of different resolution levels on plan quality and to determine the optimal resolution selection, including the optimal FOV for NPC. While there are four resolution levels available, this study focused on three levels: low, medium and high resolution, for both fluence optimization and dose calculation.

METHODS

Ethical clearance

This retrospective study recruited 41 NPC patients who had been treated between January 2022 and December 2023 and included 31 males and 10 females. The research proposal was approved by the Research Ethics Committee of the Faculty of Medicine at Chiang Mai University (Study code: RAD-2566-0556) in November 2023.

Patient selection and data preparation

The helical tomotherapy treatment plans for the 41 NPC patients were randomly selected during the period January 2022 through December 2023. All the treatment plans had been performed on computed tomography (CT) image sets acquired by a CT simulator (SOMATOM definition AS, Siemens Healthineers, Inc., Erlangen, Germany). Although the slice thickness of the image set was set at 3 mm, the size of FOV was harmonized with the body of the patients. In this study, the image planning acquisition had 3 sizes of FOV, specifically, 500

mm, 550 mm and 650 mm. The S-type thermoplastic mask (Klarity White™, Klarity®, Guangzhou, China) was used for the immobilization of all the selected cases.

All recruited treatment plans consisted of three planning target volumes (PTVs) at dose levels of 70.0 Gy, 59.4 Gy and 54.0 Gy. These zones were expanded by 5 mm from the clinical target volume (CTV). In cases of skin involvement with the CTV, the PTVs were cropped by 3 mm from the surface. The simultaneous integrated boost (SIB) technique was employed on all PTVs across 33 fractions. Other structures and organs at risk (OARs), considered in the radiation dose plan included the brainstem, spinal cord, parotid glands, optic chiasm, optic nerves and globes.

Treatment planning scenarios

All treatment plans were replanned using the TPS of Tomotherapy (Precision® version 3.3.0.1, Accuray Inc., Sunnyvale, California, USA). Although the previous plans had been performed, they were re-optimized and re-dose calculated utilizing the VOLO™ Ultra (Precision® version 3.3.0.1, Accuray Inc., Sunnyvale, California, USA). The treatment plans were created in 9 scenarios by a single planner, which were a combination of various resolutions of optimization and dose calculations. The resolution of the previous treatment plan was selected as the template for a new treatment plan, including the beam geometries such as treatment techniques, FW, etc. The treatment plans for each patient then had nine scenarios with different combinations of resolution between fluence optimization and dose calculation. The resolution of the optimization and dose calculation (Opt/Cal) varied between high-resolution (H), medium-resolution (M) and low-resolution (L). The abbreviation of each scenario is expressed as H/H for high-resolution optimization/high-resolution dose calculation, M/L for medium-resolution optimization/low-resolution dose calculation, etc. Using the VOLO™ Ultra, the treatment system automatically calculated the optimum PF and MF. Although the PF was calculated automatically, the value was then fixed in all treatment scenarios for each case. Only the MF could not be adjusted using this option. These plan parameters are summarized in Table 1.

The constraints of the targets followed the guidelines of the International Commission on Radiation Units and Measurements (ICRU) number 83 (13), specifically: 1) 98% of the target volume received at least 95% of the prescribed dose ($D_{98\%}$ ≥ 95% of the prescribed dose), 2) the prescribed dose was delivered to 50% of the target volume ($D_{50\%}$ = prescribed dose) and 3) less than 107% of the prescribed dose was delivered to 2% of the target volume ($D_{2\%}$ ≤ 107% of the prescribed dose). However, the structures of $PTV_{59.4}$ contained the $PTV_{70.0}$ and were superior to the isolated structure of $PTV_{54.0}$. The dose of $D_{2\%}$ was then constrained only on the $PTV_{70.0}$. Table 2 summarizes the dose constraints both for the targets and also for each organ of OAR.

Dosimetric parameters, indexes and planning time

All treatment plan scenarios were evaluated regarding targets and the OARs by dosimetric parameters and indexes. The indexes were evaluated regarding the PTV which consisted of a

Table 1. Mean, standard deviation (SD) of patient characteristics and treatment planning parameters in tomotherapy

PTV size (cc)	
PTV70.0 Gy	209.41 (95.23)
PTV59.4 Gy	639.19 (145.13)
PTV54.0 Gy	138.20 (82.14)
Pitch	0.41 (0.06)
Modulation factor	1.49 (0.22)
Field width (mm)	4.39 (1.09)
Field of view (mm)	600 (55.90)

PTV, planning target volume

Table 2. Dose constraints of target and organs at risk of nasopharyngeal carcinoma

Structures	Parameter	Dose constraints
Target		
$PTV_{70.0}$	$D_{98\%}$	≥ 95% of prescribed dose
	$D_{50\%}$	= prescribed dose
	$D_{2\%}$	≤ 107% of prescribed dose
$PTV_{59.4}$	$D_{98\%}$	≥ 95% of prescribed dose
	$D_{50\%}$	= prescribed dose
$PTV_{54.0}$	$D_{98\%}$	≥ 95% of prescribed dose
	$D_{50\%}$	= prescribed dose
Organs at risk		
Brainstem	$D_{2\%}$	≤ 54 Gy
Spinal cord	$D_{2\%}$	≤ 45 Gy
Optic chiasm	$D_{2\%}$	≤ 54 Gy
Optic nerve	$D_{2\%}$	≤ 54 Gy
Parotid	$D_{50\%}$	≤ 30 Gy
Globe	D_{mean}	≤ 35 Gy

PTV, planning target volume

conformity index (12) (CI_{ICRU}) and a homogeneity index (12) (HI). The CI_{ICRU} and HI were employed using the ICRU no. 83 formula as recommended. The CI_{ICRU} was calculated by PIV/PTV, where PIV is the prescribed isodose volume. The HI was calculated by $(D_{2\%} - D_{98\%})/D_{50\%}$ where $D_{x\%}$ is the dose level at x% volume. Other structures for evaluation were the OARs. The dose constraints described in Table 2 were normalized on the organs in the treatment plan scenarios as an evaluation tool.

Treatment planning time was also used to compare the computation time of the plan scenarios. However, this measurement was not included in the time of dose constraints adjustment of each organ. The optimization was set at 20 iterations per round for each of 3 rounds. The dose calculation time was then added to the time of the optimization process.

Statistical analysis

Statistical analysis was conducted using SPSS version 27.0.1 (IBM SPSS Statistics, IBM Co., Armonk, New York, USA). This analysis assessed the significant differences between the plan quality parameters and dosimetric indexes, CI_{ICRU} and HI, of PTVs as well as the dose levels on the OARs. The planning time and the differences in FOV were also analyzed. The Shapiro-Wilk test was employed to assess the normality of the data. A Wilcoxon sign-rank test was used for significant difference analysis between the highest resolution scenario (H/H resolution scenario) and each of the others at a 95% confidence interval ($p < 0.05$).

RESULTS

The results of the various resolutions and the optimization and dose calculations of the treatment planning were assembled. The results were classified in terms dosimetric parameters of the target and OARs, treatment planning time and dosimetric parameters of various FOV.

Dosimetric parameters on the targets and OARs

The dosimetric parameters of the $PTV_{70.0}$, $PTV_{59.4}$ and $PTV_{54.0}$ are reported in Table 3. The values are expressed as mean percentage dose difference (standard deviations: SD) compared to dose constraints. The relative values of the nine scenarios were normalized by the dose constraints as listed in Table 2. Figure 1 shows the plots of PTV dosimetric results of all scenarios.

Table 3. Mean percentage dose difference (SD) compared to dose constraint of target parameters in various resolutions of optimization and dose calculation.

Target	Parameter	Optimization/calculation resolution scenario (%)								
		H/H	H/M	H/L	M/H	M/M	M/L	L/H	L/M	L/L
PTV_{70}	$D_{2\%}$	96.92 (0.74)	96.54 (0.73)	95.98 (0.77)	97.21 (0.68)	96.78 (0.67)	96.16 (0.68)	97.88 (0.70)	97.42 (0.66)	96.73 (0.72)
	$D_{50\%}$	100.64 (0.46)	100.46 (0.43)	100.03 (0.50)	100.98 (0.43)	100.79 (0.44)	100.35 (0.43)	101.24 (0.44)	101.5 (0.42)	100.64 (0.42)
	$D_{98\%}$	97.84 (5.44)	97.51 (5.36)	96.69 (5.16)	98.30 (5.53)	98.01 (5.45)	97.19 (5.23)	98.34 (5.62)	98.12 (5.54)	97.49 (5.37)
CI		15.42 (9.04)	14.20 (10.46)	9.70 (9.46)	19.30 (11.75)	16.89 (11.26)	11.79 (10.21)	26.09 (13.87)	23.54 (13.43)	18.56 (12.27)
HI		10.71 (5.09)	10.61 (5.03)	10.84 (4.78)	10.53 (5.16)	10.37 (5.07)	10.53 (4.84)	11.17 (5.28)	10.91 (5.17)	10.81 (4.95)
$PTV_{59.4}$	$D_{50\%}$	105.15 (4.11)	104.94 (4.04)	104.49 (3.93)	105.49 (4.25)	105.24 (4.18)	104.76 (4.00)	106.31 (4.33)	06.05 (4.25)	105.53 (4.14)
	$D_{98\%}$	100.17 (1.30)	99.84 (1.36)	98.96 (1.43)	100.77 (1.24)	100.50 (1.38)	99.62 (1.44)	100.61 (1.34)	100.23 (1.86)	99.78 (1.49)
PTV_{54}	$D_{50\%}$	100.36 (0.51)	100.14 (0.52)	99.72 (0.56)	100.54 (0.76)	100.44 (0.46)	100.00 (0.46)	100.83 (0.53)	100.66 (0.53)	100.21 (0.58)
	$D_{98\%}$	101.68 (1.00)	101.35 (1.16)	100.39 (1.30)	102.48 (1.15)	102.16 (1.15)	101.15 (1.20)	102.27 (0.94)	102.11 (1.03)	101.48 (1.13)

H, high resolution; M, medium resolution; L, low resolution; PTV, planning target volume; CI, conformity index; HI, homogeneity index and Dx%, dose at x% volume

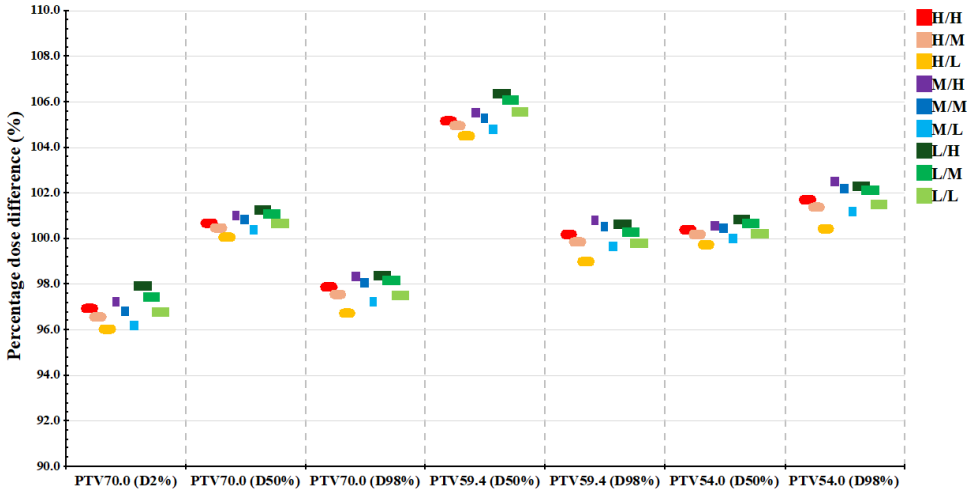

Figure 1. Mean percentage dose difference compared to the dose constraint of PTVs dosimetric parameters in various resolutions of optimization and dose calculation

Table 4. Statistical analysis (*p*-value) of target dosimetric parameters in various resolutions of optimization and dose calculation using the highest resolution scenario (H/H resolution scenario) benchmark

Target	Parameter	Optimization/calculation resolution scenario (%)								
		H/H	H/M	H/L	M/H	M/M	M/L	L/H	L/M	L/L
PTV_{70}	$D_{2\%}$	Benchmark	$p < 0.001$	$p < 0.001$	$p < 0.001$	$p = 0.004$	$p < 0.001$	$p < 0.001$	$p < 0.001$	$p < 0.001$
	$D_{50\%}$		$p < 0.001$	$p < 0.001$	$p < 0.001$	$p < 0.001$	$p < 0.001$	$p < 0.001$	$p < 0.001$	-
	$D_{98\%}$		$p < 0.001$	$p < 0.001$	$p < 0.001$	$p < 0.001$	$p < 0.001$	$p < 0.001$	$p < 0.001$	$p < 0.001$
	CI		$p < 0.001$	$p < 0.001$	$p < 0.001$	$p = 0.015$	$p < 0.001$	$p < 0.001$	$p < 0.001$	$p < 0.001$
	HI		$p < 0.001$	$p < 0.001$	$p = 0.008$	$p < 0.001$	$p = 0.024$	$p < 0.001$	$p < 0.001$	$p = 0.014$
$PTV_{59.4}$	$D_{50\%}$		$p < 0.001$	$p < 0.001$	$p < 0.001$	-	$p < 0.001$	$p < 0.001$	$p < 0.001$	$p < 0.001$
	$D_{98\%}$		$p < 0.001$	$p < 0.001$	$p < 0.001$	$p < 0.001$	$p < 0.001$	$p < 0.001$	$p = 0.001$	$p < 0.001$
PTV_{54}	$D_{50\%}$		$p < 0.001$	$p < 0.001$	$p < 0.001$	$p = 0.024$	$p < 0.001$	$p < 0.001$	$p < 0.001$	$p < 0.001$
	$D_{98\%}$		$p < 0.001$	$p < 0.001$	$p < 0.001$	$p < 0.001$	$p < 0.001$	$p < 0.001$	$p < 0.001$	$p = 0.007$

H, high resolution; M, medium resolution; L, low resolution; PTV, planning target volume; CI, conformity index; HI, homogeneity index and Dx%, dose at x% volume
p-value was expressed only the data that had *p*-value less than 0.05

At the $PTV_{70.0}$, all scenarios had a mean percentage dose difference of $D_{2\%}$ lower than 100%. This means that all plans had a high dose lower than 2% of $PTV_{70.0}$. In comparison, all scenarios showed a significant difference when compared to the highest resolution scenario ($p \leq 0.004$). At the target dose, the $D_{50\%}$ of PTVs had a value of over a hundred percent which shows all PTVs received the prescribed dose, with the exception of the $PTV_{54.0}$ in the H/L scenario. Although $PTV_{54.0}$ in this scenario received a dose lower than the prescription, the range of prescribed doses was acceptable. The dosimetric parameters were statistically analyzed as shown in Table 4. This analysis demonstrated a significant difference between the H/H scenario and all scenarios of $PTV_{70.0}$ ($p <$ 0.004), $PTV_{59.4}$ ($p \leq 0.001$) and $PTV_{54.0}$ ($p \leq 0.024$), with the exception of the L/L scenario of $PTV_{70.0}$ and M/M scenario of $PTV_{59.4}$. These results revealed a percentage of $D_{98\%}$ lower than a hundred in all scenarios of $PTV_{70.0}$ and $PTV_{54.0}$. On the other hand, the $PTV_{59.4}$ received a dose of $D_{98\%}$, lower than the hundred in the H/M, H/L, M/L and L/L scenarios. Statistical analysis showed a significant difference among all scenarios of $PTV_{70.0}$ ($p < 0.004$), $PTV_{59.4}$ ($p \leq 0.001$) and $PTV_{54.0}$ ($p \leq 0.007$).

The CI_{ICRU} and HI were also observed in this study. The percentages are presented in Figure 2a. The results show the lowest and highest values of CI_{ICRU} in the H/L and L/H scenarios, respectively. On the HI, the lowest value was the M/M scenario, whereas the highest value was the L/H

Table 5. Mean percentage dose difference (SD) compared to dose constraint of organs at risks parameters in various resolutions of optimization and dose calculation

Organs at risk	Parameter	Optimization/calculation resolution scenario (%)								
		H/H	H/M	H/L	M/H	M/M	M/L	L/H	L/M	L/L
Brainstem	$D_{2\%}$	91.28 (9.76)	91.29 (9.65)	91.43 (9.44)	91.59 (9.75)	91.55 (9.65)	91.68 (9.40)	92.13 (10.18)	92.05 (10.15)	92.09 (9.94)
Spinal cord	$D_{2\%}$	68.01 (12.27)	68.48 (12.09)	69.93 (12.20)	67.92 (12.20)	68.45 (12.37)	69.70 (12.35)	66.13 (13.21)	66.48 (13.28)	67.66 (13.27)
Lt parotid	$D_{50\%}$	105.95 (37.71)	106.97 (36.94)	108.92 (35.46)	105.88 (38.06)	106.94 (37.23)	108.23 (35.52)	106.13 (38.86)	107.08 (38.05)	108.91 (36.49)
Rt parotid	$D_{50\%}$	104.18 (37.33)	105.26 (36.68)	107.26 (35.40)	104.56 (37.56)	105.46 (37.05)	108.07 (35.85)	104.32 (39.20)	105.43 (38.56)	107.38 (37.22)
Optic chiasm	$D_{2\%}$	74.56 (32.90)	75.03 (32.97)	74.63 (33.30)	74.58 (32.76)	74.82 (32.94)	75.44 (33.36)	74.48 (32.87)	73.71 (32.85)	74.93 (33.26)
Lt optic nerve	$D_{2\%}$	79.07 (30.38)	79.38 (30.53)	79.86 (30.82)	78.78 (30.16)	79.09 (30.32)	79.69 (30.67)	79.10 (30.53)	79.28 (30.54)	79.48 (30.69)
Rt optic nerve	$D_{2\%}$	77.32 (28.72)	77.69 (28.87)	78.32 (29.17)	76.06 (29.07)	77.76 (28.78)	78.24 (29.01)	77.75 (29.02)	77.79 (29.04) $p = 0.003$	78.04 (29.10) $p < 0.001$
Lt globe	D_{mean}	37.81 (20.00)	37.97 (20.18)	38.28 (20.34)	38.08 (20.35)	38.28 (20.42)	38.64 (20.60)	36.45 (19.38)	36.59 (19.42)	37.02 (19.63)
Rt globe	D_{mean}	38.02 (17.73)	38.32 (17.75)	38.66 (17.91)	38.19 (17.69)	38.33 (17.74)	38.80 (17.92)	37.27 (17.34)	37.44 (17.37)	37.83 (17.52)
Opt and calc time	Sec	377.35 (96.99)	337.94 (90.69)	328.38 (89.26)	161.37 (49.60)	121.89 (38.21)	110.89 (36.03)	121.89 (27.56)	80.67 (16.07)	70.92 (14.01)

H, high resolution; M, medium resolution; L, low resolution; D_{mean}, mean dose; $D_{x\%}$, dose at x% volume; Opt, optimization and calc, calculation; Lt, letf; Rt, right; Sec, second

Table 6. Statistical analysis (p-value) of organs at risk and time with various resolutions of optimization and dose calculation using the highest resolution scenario (H/H resolution scenario) as a benchmark

Organs at risk	Parameter	Optimization/calculation resolution scenario (%)								
		H/H	H/M	H/L	M/H	M/M	M/L	L/H	L/M	L/L
Brainstem	$D_{2\%}$	Benchmark	-	-	$p = 0.005$	$p = 0.014$	$p = 0.005$	$p < 0.001$	$p < 0.001$	$p < 0.001$
Spinal cord	$D_{2\%}$		$p < 0.001$	$p < 0.001$	-	$p = 0.013$	$p < 0.001$	$p < 0.001$	$p < 0.001$	-
Lt parotid	$D_{50\%}$		$p < 0.001$	$p < 0.001$	-	$p < 0.001$	$p < 0.001$	-	$p = 0.011$	$p < 0.001$
Rt parotid	$D_{50\%}$		$p < 0.001$	$p < 0.001$	-	$p < 0.001$	$p < 0.001$	-	$p = 0.012$	$p < 0.001$
Optic chiasm	D2%		$p = 0.036$	$p = 0.008$	-	-	$p = 0.01$	-	-	-
Lt optic nerve	$D_{2\%}$		$p < 0.001$	$p < 0.001$	-	-	$p = 0.002$	-	-	-
Rt optic nerve	$D_{2\%}$		$p < 0.001$	$p < 0.001$	-	$p < 0.001$	$p < 0.001$	-	$p = 0.003$	$p < 0.001$
Lt globe	D_{mean}		$p < 0.001$	$p < 0.001$	-	-	$p = 0.015$	$p = 0.002$	$p = 0.002$	-
Rt globe	D_{mean}		$p < 0.001$	$p < 0.001$	-	-	$p < 0.001$	-	-	-
Opt and calc time	Sec		$p < 0.001$	$p < 0.001$	$p < 0.001$	$p < 0.001$	$p < 0.001$	$p < 0.001$	$p < 0.001$	$p < 0.001$

H, high resolution; M, medium resolution; L, low resolution; D_{mean}, mean dose; $D_{x\%}$, dose at x% volume; Lt, letf; Rt, right; Opt, optimization; Sec, second

p-value was expressed only the data that had p-value less than 0.05

scenario. A significant difference was found in all scenarios on both the CI_{ICRU} ($p \leq 0.015$) and HI ($p \leq 0.024$).

Table 5 summarizes the data on OARs expressed as mean percentage (SD) dose by the organ dose constraints normalization. Figure 3 shows the percentage dose level of the normal organs of interest. All OARs had a percentage lower than a hundred percent. This means these OARs met the criteria of the organ dose, with the exception of both parotid glands. A significant difference in OARs was also observed as shown in Table 6. The analysis shows that there was no significant difference in the H/M and H/L ($p > 0.05$) on the

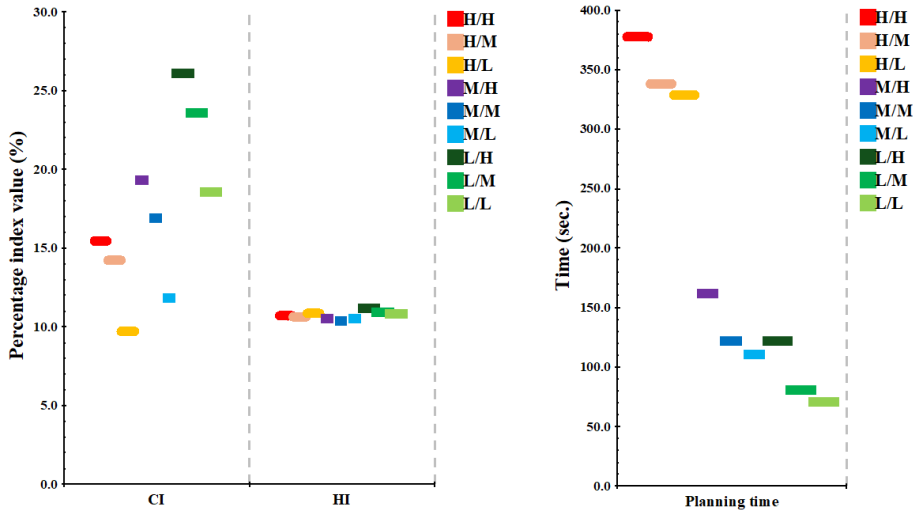

(a) (b)

Figure 2. Percentage value difference of $PTV_{70.0}$ dosimetric indexes and treatment planning time in various resolutions of the optimization and dose calculation. (a) Percent difference of CI_{ICRU} and HI and (b) Treatment planning time.

brainstem, whereas there was a significant difference (p = 0.005) in the M/H. Two scenarios, M/M and L/M, almost had a significant difference ($p \leq 0.014$) in similar organs. However, the L/M scenario showed one additional organ with a significant difference (p = 0.002) in the left globe. The L/H scenario showed a significant difference on the brainstem ($p < 0.001$), spinal cord ($p < 0.001$) and left globe (p = 0.002). The L/L scenario showed a significant difference ($p < 0.001$) regarding the brainstem, both the parotid and right optic nerve. Only the M/L scenario was significantly different on all OARs ($p \leq 0.015$).

Treatment planning time

The planning time is presented on the rows labelled Opt and Cal time in Table 5. The planning time was the longest in the highest resolution of the optimization, whereas the lowest resolution had the lowest computational time. In Table 6, The results show a significant difference ($p <$ 0.001) between the highest resolution and other scenarios. The planning time in each resolution scenario is shown in Figure 2b.

Dosimetric parameters by various FOV

The mean percentage difference compared to dose constraint of the target for each FOV is summarized in Table 7. The results show that the $D_{98\%}$ of $PTV_{70.0}$ in the FOV 500 mm provided the highest dose level, whereas the highest dose level was observed in the $D_{50\%}$ of $PTV_{59.4}$ in the FOV 650 mm. Other dosimetric parameters showed similar results. The different dose levels for each FOV are shown in Figure 4. As shown in Table 8, for most scenarios there were no significant differences in dose parameters.

DISCUSSION

This study explored the impact of treatment plan quality using various resolutions of both dose calculation and optimization. Nine treatment plan scenarios with different resolutions were created for the investigation. In the inverse treatment planning, the photon fluence was determined in the first step (14). This compromised the photon fluence between the dose on the target and OARs as those were constraints (14). Since the constraints were accepted, the final dose calculation determined the dosage (15). This means that the photon optimization and dose calculation were separate processes, thus the resolution can differ between these two steps.

Dosimetric parameters of the targets and OARs

In PTVs, the results showed an increasing dose level when the dose calculation resolution was increasing. These results show the same pattern as those observed by Srivastava et al. (10), Kim et al. (6) and Kawashima et al. (5). In contrast, the opposite results were observed in optimization resolution. Resolutions presented with an increasing dose level when the resolution was decreased. The main impact would be raised by number of

Table 7. Mean percentage difference (SD) compared to dose constraint of target parameters in various fields of view (FOV), resolution of optimization and dose calculation

Target	Parameter	Optimization/calculation resolution scenario (%)								
		H/H	H/M	H/L	M/H	M/M	M/L	L/H	L/M	L/L
FOV 500 mm										
Opt resolution (mm)		0.98	0.98	0.98	1.95	1.95	1.95	3.91	3.91	3.91
Cal resolution (mm)		0.98	1.95	3.91	0.98	1.95	3.91	0.98	1.95	3.91
PTV_{70}	$D_{2\%}$	96.82 (0.45)	96.51 (0.45)	96.58 (1.03)	97.14 (0.62)	96.81 (0.64)	96.28 (0.64)	97.62 (0.59)	97.30 (0.60)	96.74 (0.65)
	$D_{50\%}$	100.83 (0.22)	100.69 (0.25)	100.72 (0.84)	101.06 (0.49)	100.92 (0.49)	100.60 (0.51)	101.42 (0.20)	101.28 (0.20)	100.95 (0.24)
	$D_{98\%}$	100.17 (0.60)	99.89 (0.60)	99.60 (0.31)	100.52 (0.51)	100.24 (0.44)	99.50 (0.27)	100.69 (0.79)	100.46 (0.82)	99.81 (0.90)
$PTV_{59.4}$	$D_{50\%}$	105.03 (3.77)	104.83 (3.70)	105.09 (4.61)	105.13 (3.81)	104.93 (3.74)	104.56 (3.65)	105.91 (4.10)	105.72 (4.07)	105.30 (3.96)
	$D_{98\%}$	100.39 (0.91)	100.15 (0.82)	99.80 (0.22)	100.84 (1.07)	100.64 (0.96)	99.94 (0.81)	101.05 (1.27)	100.86 (1.20)	100.32 (1.01)
PTV_{54}	$D_{50\%}$	100.58 (0.28)	100.42 (0.25)	100.36 (0.59)	101.02 (0.10)	100.89 (0.10)	100.57 (0.11)	100.84 (0.22)	100.74 (0.23)	100.48 (0.24)
	$D_{98\%}$	102.71 (0.70)	102.51 (0.77)	102.14 (1.40)	103.14 (1.15)	102.97 (1.22)	102.37 (1.45)	103.02 (0.47)	102.92 (0.54)	102.50 (0.81)
FOV 550 mm										
Opt resolution (mm)		1.07	1.07	1.07	2.15	2.15	2.15	4.30	4.30	4.30
Cal resolution (mm)		1.07	2.15	4.30	1.07	2.15	4.30	1.07	2.15	4.30
PTV_{70}	$D_{2\%}$	96.59 (0.70)	96.27 (0.71)	95.68 (0.72)	96.88 (0.54)	96.50 (0.52)	95.91 (0.53)	97.57 (0.60)	97.16 (0.61)	96.49 (0.64)
	$D_{50\%}$	100.56 (0.51)	100.40 (0.50)	99.98 (0.51)	100.83 (0.44)	100.65 (0.44)	100.27 (0.45)	101.11 (0.47)	100.95 (0.47)	100.56 (0.47)
	$D_{98\%}$	96.94 (6.71)	96.65 (6.60)	96.00 (6.27)	97.32 (6.86)	97.05 (6.78)	96.41 (6.45)	97.39 (6.94)	97.21 (6.83)	96.66 (6.57)
$PTV_{59.4}$	$D_{50\%}$	104.42 (3.20)	104.27 (3.17)	103.84 (3.09)	104.78 (3.28)	104.56 (3.25)	104.12 (3.16)	105.60 (3.45)	105.37 (3.43)	104.89 (3.35)
	$D_{98\%}$	100.01 (1.47)	99.66 (1.50)	98.85 (1.54)	100.41 (1.39)	100.15 (1.60)	99.40 (1.63)	100.37 (1.53)	99.69 (2.46)	99.62 (1.60)
PTV_{54}	$D_{50\%}$	100.50 (0.45)	100.28 (0.45)	99.88 (0.43)	100.46 (1.07)	100.51 (0.41)	100.10 (0.40)	100.91 (0.47)	100.77 (0.46)	100.28 (0.62)
	$D_{98\%}$	101.83 (0.78)	101.50 (1.11)	100.66 (1.15)	102.45 (1.34)	102.14 (1.31)	101.30 (1.32)	102.36 (0.92)	102.20 (0.99)	101.65 (1.09)
FOV 650 mm										
Opt resolution (mm)		1.27	1.27	1.27	2.54	2.54	2.54	5.08	5.08	5.08
Cal resolution (mm)		1.27	2.54	5.08	1.27	2.54	5.08	1.27	2.54	5.08
PTV_{70}	$D_{2\%}$	97.18 (0.71)	96.73 (0.73)	96.12 (0.73)	97.47 (0.70)	96.98 (0.73)	96.33 (0.74)	98.14 (0.70)	97.63 (0.65)	96.90 (0.76)
	$D_{50\%}$	100.67 (0.44)	100.47 (0.39)	99.98 (0.39)	101.07 (0.41)	100.88 (0.42)	100.38 (0.40)	101.31 (0.42)	101.10 (0.40)	100.65 (0.39)
	$D_{98\%}$	98.17 (4.77)	97.82 (4.70)	96.81 (4.59)	98.72 (4.79)	98.39 (4.71)	97.44 (4.60)	98.72 (4.90)	98.47 (4.85)	97.78 (4.75)
$PTV_{59.4}$	$D_{50\%}$	105.71 (4.77)	105.43 (4.69)	104.89 (4.48)	106.06 (4.96)	105.78 (4.88)	105.24 (4.65)	106.88 (4.99)	106.58 (4.88)	106.03 (4.75)
	$D_{98\%}$	100.27 (1.25)	99.93 (1.34)	98.92 (1.45)	101.01 (1.14)	100.73 (1.25)	99.73 (1.39)	100.72 (1.23)	100.53 (1.32)	99.83 (1.49)
PTV_{54}	$D_{50\%}$	100.23 (0.56)	99.99 (0.57)	99.52 (0.55)	100.54 (0.50)	100.33 (0.48)	99.85 (0.46)	100.77 (0.60)	100.57 (0.60)	100.12 (0.58)
	$D_{98\%}$	101.42 (1.09)	101.07 (1.15)	99.95 (1.19)	102.40 (1.01)	102.06 (1.04)	100.88 (1.01)	102.11 (0.96)	101.93 (1.07)	101.21 (1.13)

Opt, optimization; Cal, calculation; H, high resolution; M, medium resolution; L, low resolution; PTV, planning target volume and $D_{x\%}$, dose at x% volume

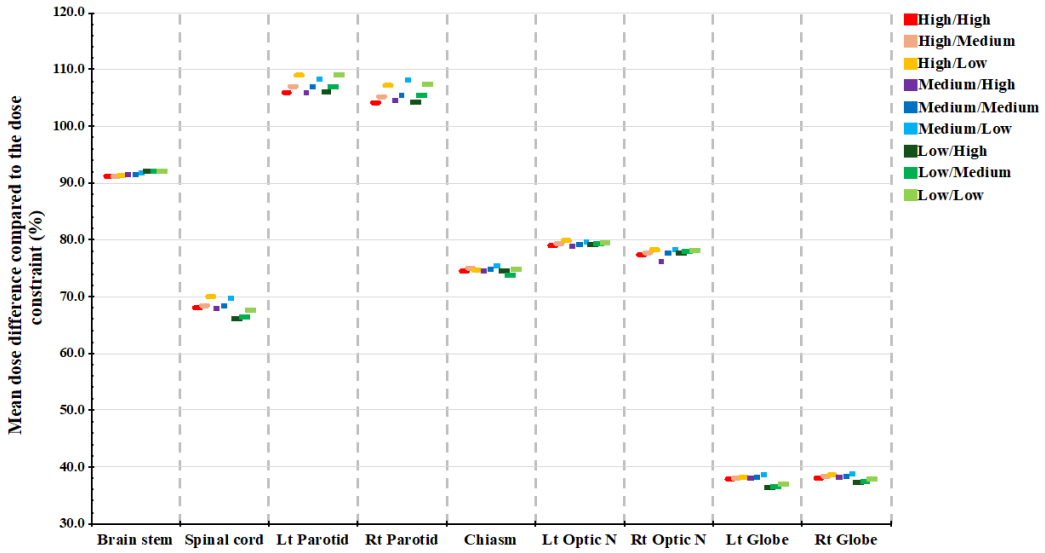

Figure 3. Comparison of percentage dose differences with dose constraint of organs at risk and dosimetric parameters in various resolutions of optimization and dose calculation.

Table 8. Statistical analysis (*p*-value) of target dosimetric parameters in various FOV

Target	Parameter	Optimization/calculation resolution scenario (%)								
		H/H	H/M	H/L	M/H	M/M	M/L	L/H	L/M	L/L
FOV 500 mm vs FOV 550 mm (*p*-value)										
PTV_{70}	$D_{2\%}$	-	-	-	-	-	-	-	-	-
	$D_{50\%}$	-	-	-	-	-	-	-	-	-
	$D_{98\%}$	-	-	-	-	-	-	-	-	-
$PTV_{59.4}$	$D_{50\%}$	-	-	-	-	-	-	-	-	-
	$D_{98\%}$	-	-	-	-	-	-	-	-	-
PTV_{54}	$D_{50\%}$	-	-	-	-	-	0.044	-	-	-
	$D_{98\%}$	-	-	-	-	-	-	-	-	-
FOV 550 mm vs FOV 650 mm (*p*-value)										
PTV_{70}	$D_{2\%}$	0.026	-	-	0.009	0.033	-	0.023	-	-
	$D_{50\%}$	-	-	-	-	-	-	-	-	-
	$D_{98\%}$	-	-	-	-	-	-	-	-	-
$PTV_{59.4}$	$D_{50\%}$	-	-	-	-	-	-	-	-	-
	$D_{98\%}$	-	-	-	-	-	-	-	-	-
PTV_{54}	$D_{50\%}$	-	-	0.048	-	-	-	-	-	-
	$D_{98\%}$	-	-	-	-	-	-	-	-	-
FOV 500 mm vs FOV 650 mm (*p*-value)										
PTV_{70}	$D_{2\%}$	-	-	-	-	-	-	-	-	-
	$D_{50\%}$	-	-	-	-	-	-	-	-	-
	$D_{98\%}$	-	-	-	-	-	-	-	-	-
$PTV_{59.4}$	$D_{50\%}$	-	-	-	-	-	-	-	-	-
	$D_{98\%}$	-	-	-	-	-	-	-	-	-
PTV_{54}	$D_{50\%}$	-	-	0.036	0.049	0.03	0.024	-	-	-
	$D_{98\%}$	-	0.037	0.024	-	-	-	-	-	-

FOV, field of view; H, high resolution; M, medium resolution; L, low resolution; PTV, planning target volume and Dx%, dose at x% volume.
p-value was expressed only the data that had *p*-value less than 0.05

elements contained in each structure volume, particularly around the boundary of the structure. The elements at the object boundary are taken into account differently in the structures, depending on each TPS. In the optimization process of VOLO™ Ultra, a whole voxel was included in the PTVs if its partial volume was involved (15). Additionally, an accelerated optimization method was used to decrease the planning time. This method employed a lower resolution level in the optimization step (15). However, this down sampling was used only on the first or second optimization round (15). The enlargement of the target could be observed in this process and was dependent on the chosen resolution. The voxel of the optimization increased the size of the target volume when the low resolution was selected. This impact can be observed in Figure 1. However, the results found differences in the $PTV_{59.4}$ and $PTV_{54.0}$ at the level $D_{98\%}$. These results showed the radiation dose was reduced when a low resolution of optimization was used. As the IMRT technique was employed in this study, the concept of target enlargement also applied across all targets, i.e., $PTV_{70.0}$, $PTV_{59.4}$ and $PTV_{54.0}$. Although all targets were enlarged, the $PTV_{59.4}$ and $PTV_{54.0}$ lost a number of voxels due to the overlap and the adjacent region between each target, respectively.

The results demonstrated that there was a significant difference in almost all resolution scenarios when compared to the highest resolution. These differences were within 2.5%, which would indicate no significant difference in clinics. However, the coverage of $PTV_{70.0}$ ($D_{98\%}$) was found to be under 100% in all scenarios. This illustrates that the $PTV_{70.0}$ receives a lower dose than the constraints due to the partial adjacency of the brainstem. This demonstrates that the enlargement of the PTVs might have less impact on the adjacent normal organ as shown by the dose values on brainstems in Figure 3. Although the TPS calculated the dose using a similar dose constraint, the performance of M/H, M/M, L/H and L/M scenarios showed a higher dose coverage than the H/H scenario. As part of the H/H scenario, these might be candidates of interest.

With regard to conformity, the results showed that the CI_{ICRU} value was similar in pattern to the $PTV_{70.0}$. The volume of a radiation dose is the numerator in this formula. These calculations confirm the assumption that the PTVs are enlarged by the increasing CI_{ICRU} value when the resolution of the optimization is decreased. The dose calculation resolution demonstrated that the volume of radiation was rapidly decreased by decreasing the resolution. By the binary numeric based calculation, the voxel of deposited dose would be enlarged by 2n as well. Although the concept of optimization might differ between each TPS, this tendency of the dose calculation resolution also confirms the work of Srivastava et al. (10), Kim et. al. (6) and Chow et al. (16) In contrast, this was not observed in the HI value. As the formula for HI focused on the dose level, this study found a similar level of value in all resolution scenarios. However, this also revealed that all resolution scenarios would provide a similar dose range between $D_{98\%}$ and $D_{2\%}$ dose levels. In Figure 2a, the CI_{ICRU} value of a low optimization resolution presented with the highest value. This might indicate a limitation of using this resolution in the optimization step.

On the OARs, similar dose levels were also observed among some resolution scenarios. Similar dose levels were found on the brainstem, optic chiasm, both optic nerves and both globes. In the craniocaudal direction, an axial fan beam of the tomotherapy might involve a less inferior volume to these organs. This could be a reason that these organs were less impacted by various resolution scenarios. This is in contrast with the work of Srivastava et al. (10) that investigated using the C-arm based linear accelerator. The impact may increase with the size of the MLC. In our study, two other organs impacted by the various resolution scenarios were the spinal cord and both parotids. This result also confirms the work of Srivastava et al. (10). These three structures are located close to all PTVs. The increase in PTVs voxels must impact the volume of these structures. However, all OARs met the acceptance criteria, with the exception of both parotids. Due to the overlapping structures of the PTVs, the parotids might not have been kept within the criteria of the study, but this could be acceptable in clinics. Although all organs met the criteria, with the exception of both parotid glands, no significant differences were found regarding the resolution between the H/H and M/H scenarios. This scenario might represent an interesting resolution in clinical practice.

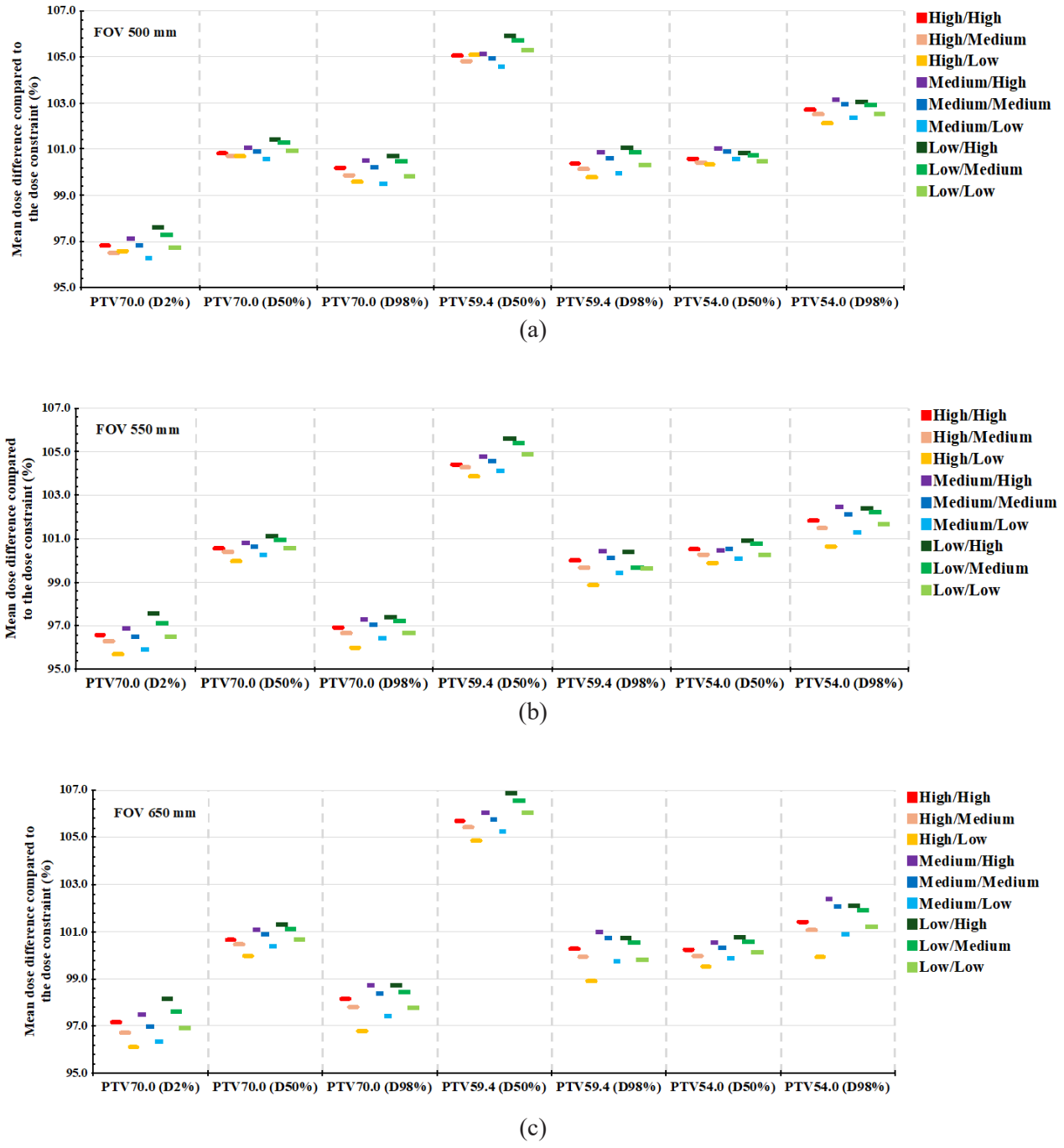

Figure 4. Mean percentage dose difference compared to dose constraint of PTVs dosimetric parameters in various resolutions of optimization and dose calculation and field of view (FOV). (a) Mean dosimetric parameters in FOV500 mm, (b) Mean dosimetric parameters in FOV550 mm and (c) Mean dosimetric parameters in FOV650 mm.

Treatment planning time

Regarding treatment planning time, other publications (5-7, 12) report that the most time-consuming practice was with the highest resolution. The present study found similar results. The treatment planning time would be higher for the optimization process than for the dose calculation process. Anchoring the optimization time, the treatment planning time was average regards the optimization group. This showed that the planning time would decrease from high resolution to low resolution by the steps of the binary numeric base which were 347.89 sec (~ 2^8 sec), 131.38 sec (~ 2^7 sec) and 91.16 sec (~2^6 sec) for high, medium and low resolution, respectively.

Table 9. Summary of the target and organs at risk dose impact using various optimization and dose calculation grid resolution.

Grid resolution		PTVs dose			OARs dose*	
Optimization	Calculation	$PTV_{70.0}$	$PTV_{59.4}$	$PTV_{54.0}$	Spinal cord	Parotids
Increase	Fixed		Decrease		No difference	
Decrease	Fixed		Increase		No difference	
Fixed	Increase		Increase		Decrease	
Fixed	Decrease		Decrease		Increase	

*Dose on other OARs were not dependent on various resolution both the optimization and dose calculation

Dosimetric parameters by various FOV

The FOV was one of the factors investigated in this study. In most scenarios, no significant differences were observed among the dosimetric PTVs parameters. Although the resolution of optimization and dose calculation were dependent on the FOV, the difference in the voxel size did not exceed 2.54 mm when the high and medium resolutions were applied. For these ranges of the FOV, the low-resolution level is not recommended.

The influence of optimization and dose calculation resolution on the targets and OARs dose is summarized in Table 9. The highest resolution of the optimization and dose calculation are recommended for the treatment planning. This resolution requires a longer planning time for generating the treatment plan. However, that may not impact centers that have a smaller number of patients. In many treatment centers the lower resolution can reduce the treatment planning time while maintaining optimal quality. Although the VOLO™ Ultra is a new technology in tomotherapy treatment planning and has an algorithm of accelerated optimization, the resolution can be selected for the optimization and dose calculation process. The selection of the lower resolution (medium resolution) can provide a shorter treatment planning time while retaining a plan quality equal to the highest resolution.

This study observed the impact of optimization and dose calculation resolution in the VOLO™ Ultra only for the high to low resolution. In this TPS, a very low resolution can be selected, a resolution that was not included in this study. This might be a limitation of this investigation. On the other hand, the accelerated optimization method was integrated in this program but not on the classic Precision® which might be an area of interest in future research.

CONCLUSIONS

This study investigated the impact on plan quality of using various resolutions of optimization and dose calculation. The results show that the resolution of M/H and M/M are of particular interest. These scenarios provide a higher dose coverage, have a mild impact on OARs and a moderate impact on conformity. The most beneficial of these scenarios can reduce the treatment planning time by 37.8% without a modification in the dose constraint. In this study, the plan quality was found to have had no impact with various FOVs of the CT image.

ACKNOWLEDGMENTS

This article has no acknowledgments.

FUNDING

This article has no support or funding.

CONFLICTS OF INTEREST

The authors have no conflicts of interest to report.

ADDITIONAL INFORMATION

Author contributions

S.T.: conceptualization, data curation, investigation, formal analysis, writing – original draft, writing – review and editing; A.W.: conceptualization, formal analysis, writing – review and editing, supervision; W.N.: formal analysis, writing – review and editing; S.W.: formal analysis, writing – review and editing; W.T.: formal analysis.

REFERENCES

1. De Felice F, Cattaneo C, Franco P. Radiotherapy and Systemic Therapies: Focus on Head and Neck Cancer. Cancers (Basel). 2023;15:4232. PubMed PMID: 37686508

2. Taylor A, Powell M. Intensity-modulated radiotherapy--what is it? Cancer Imaging. 2004;4:68-73.
3. Chui C, Spirou S. Inverse planning algorithms for external beam radiation therapy. Med Dosim. 2001;26: 189-97.
4. Rong Y, Welsh J. Dosimetric and clinical review of helical tomotherapy. Expert Rev Anticancer Ther. 2011;11:309-20.
5. Kawashima M, Kawamura H, Onishi M, Takakusagi Y, Okonogi N, Okazaki A, et al. The impact of the grid size on tomotherapy for prostate cancer. J Med Phys. 2017;42:144-50.
6. Kim K, Chung J, Suh T, Kang S, Kang S, Eom K, et al. Dosimetric and radiobiological comparison in different dose calculation grid sizes between Acuros XB and anisotropic analytical algorithm for prostate VMAT. PLoS One. 2018;13:e0207232. PubMed PMID: 30419058
7. Park J, Kim S, Park H, Lee J, Kim Y, Suh T. Optimal set of grid size and angular increment for practical dose calculation using the dynamic conformal arc technique: a systematic evaluation of the dosimetric effects in lung stereotactic body radiation therapy. Radiat Oncol. 2014;9:5. PubMed PMID: 24387278
8. Snyder Karen C, Liu M, Zhao B, Huang Y, Ning W, Chetty I, et al. Investigating the dosimetric effects of grid size on dose calculation accuracy using volumetric modulated arc therapy in spine stereotactic radiosurgery. J Radiosurg SBRT. 2017;4:303-13.
9. Spirou S, Fournier-Bidoz N, Yang J, Chui C, Ling C. Smoothing intensity-modulated beam profiles to improve the efficiency of delivery. Med Phys. 2001;28: 2105-12.
10. Srivastava S, Cheng C, Das I. The dosimetric and radiobiological impact of calculation grid size on head and neck IMRT. Pract Radiat Oncol. 2017;7:209-17.
11. Yawichai K, Chitapanarux I, Wanwilairat S. Helical tomotherapy optimized planning parameters for nasopharyngeal cancer. Journal of Physics: Conference Series. 2016;694:012002.
12. Park J, Park S, Kim J, Carlson J, Kim J. The influence of the dose calculation resolution of VMAT plans on the calculated dose for eye lens and optic pathway. Australas Phys Eng Sci Med. 2017;40:209-17.
13. International Commission on Radiation Units and Measurements. J ICRU. 2014;14:Np.
14. Oelfke U, Bortfeld T. Inverse planning for photon and proton beams. Med Dosim. 2001;26:113-24.
15. Incorporated. A. Radixact Physics Essential Course Workbook 1058101.K2022.
16. Chow J, Jiang R. Dose-volume and radiobiological dependence on the calculation grid size in prostate VMAT planning. Med Dosim. 2018;43:383-9.

Biomedical Sciences and Clinical Medicine 2025;64(2):150-157.
doi: 10.12982/BSCM.2025.14
https://he01.tci-thaijo.org/index.php/CMMJ-MedCMJ/index

Original Article

Open Access

Effect of Tranexamic Acid Infusion to Reduce Intraoperative Blood Loss in Large Meningioma: A Prospective Randomized Control Study (Preliminary Report)

Pathomporn Pin-on, Ananchanok Saringkarinkul, Prangmalee Leurcharusmee, Settapong Boonsri and Kevin Chotinaruemol

Department of Anesthesiology, Faculty of Medicine, Chiang Mai University, Chiang Mai, Thailand

Correspondence:
Pathomporn Pin-on, MD, Department of Anesthesiology, Faculty of Medicine, Chiang Mai University, 110 Inthavarorot Rd, Amphur Muang, Chiang Mai 50200, Thailand.
E-mail: pinon.pathomporn@gmail.com

Received: May 1, 2024;
Revised: January 27, 2025;
Accepted: March 3, 2025

ABSTRACT

OBJECTIVE Resection of intracranial meningioma has been related to significant blood loss. Intravenous tranexamic acid (TXA) has been shown to successfully attenuated blood loss and transfusion in various surgical procedures. However, the evidence has been limited in the surgical management of brain tumors. This study aims to evaluate the efficacy of intravenous TXA in reducing intraoperative blood loss and the need for blood transfusion during the surgical resection of intracranial meningiomas.

METHODS We conducted a prospective, randomized double-blind controlled study aiming for a sample size of 44 patients. In this preliminary report, twenty-five patients aged 18-60 years with large intracranial meningioma undergoing elective meningioma resection were enrolled and randomized to receive either TXA or a placebo. "Large meningioma" was defined as a radiographic finding of a tumor with a diameter > 5 cm in at least 2 dimensions. The TXA group was administered TXA at 20 mg/kg over 20 minutes, prior to the operation, followed by an infusion of 1 mg/kg/hr until the end of the operation. The primary outcome measure was volume of intraoperative blood loss. Continuous variables were analyzed with Student's t-test or the Mann-Whitney U-test depending upon the distribution of the data. Fisher's exact test was used to compare categorical variables.

RESULTS Twenty-five patients were randomized with 12 in the TXA group and 13 in the placebo group. Baseline characteristics of the patients in the two groups were similar. The median intraoperative blood loss volume was 1,925 mL (IQR=1,575) in the TXA group and 1,500 mL (IQR=1,700) in the placebo group (p = 0.904). The median of intraoperative packed red cells (PRC) transfusion volume was 801.5 mL (IQR=825.5) in the TXA group and 493 mL (IQR=856) in the placebo group (p = 0.883). There was no significant difference in blood transfusion volumes between the groups in first 24 hours after surgery (p = 0.581). The incidence of thromboembolic events was similar in the two groups (p = 1.0). No postoperative seizures occurred in either group during the study.

CONCLUSIONS TXA did not reduce intraoperative blood loss, the intraoperative transfusion requirement, and the transfusion requirements during the first 24 hours after surgery in patients who underwent large intracranial meningioma resection.

KEYWORDS tranexamic acid; meningioma; blood loss; blood transfusion

INTRODUCTION

Meningioma is the most common primary central nervous system (CNS) tumor, accounting for one-third of primary brain tumors. Its histology is usually benign and presents with intracranial, extra-axial, and dural attachment lesions. Meningioma has been found in 53.3% of all CNS non-malignant tumors (1-3). Neurological symptoms develop in only 8.1% of patients due to the tumor's slow-growing nature which allows adequate time for cerebral auto-regulation and cerebral compensation. For that reason, most patients presenting to the neurosurgeon have a large meningioma (3, 4). Meningioma contains more tissue plasminogen activator (tPA) than normal brain tissue which causes hyperfibrinolysis during resection of the meningioma resulting from release of tPA into the blood circulatory system. The degree of hemostatic disturbance from tPA is directly associated with the volume of the meningioma and the extent of the resection (5-7).

Surgical removal of meningioma is associated with a large volume of blood loss which causes hemodynamic instability and usually requires allogeneic blood transfusion. Massive blood transfusion, however, increases morbidity and mortality due to prolonged use of a ventilator, a longer postoperative Intensive Care Unit (ICU) stay and hospital stay, a higher incidence of 30-day major complications, and coagulation disturbance (8, 9). Minimizing bleeding during meningioma resection is primarily in the surgeons' hands and their expertise. Various strategies have been developed to decrease intra-operative blood loss and transfusion requirements, e.g., preoperative embolization of the arterial supply of the tumor, preoperative autologous blood transfusion, preoperative erythropoietin administration, acute normovolemic hemodilution, and a blood cell saver. Those methods are currently practiced, but they are not routine (10) and none of those strategies are considered a standard technique.

Tranexamic acid (TXA), an anti-fibrinolytic agent, binds to lysine receptors on plasmin and blocks the binding of plasmin to fibrin, inhibiting fibrinolysis (11). TXA has been shown to reduce perioperative blood loss and transfusion in various surgical procedures. In the neurosurgical field, large sample size trial of TXA have been limited to traumatic brain injury (TBI) and subarachnoid hemorrhage patients (12, 13). There is only very limited evidence of TXA being used in a craniotomy to remove a brain tumor. To fill this knowledge gap, we studied the effect of TXA in large meningioma surgery because of TXA's inhibitory effect on the fibrinolysis pathway.

The primary purpose of this study is to determine efficacy of TXA in reducing intraoperative blood loss. Secondary objectives are to assess the efficacy of TXA in attenuation of intraoperative and 24 hours post-surgery blood transfusion requirements. Adverse effects of TXA, focusing on thromboembolic events and convulsions, are also recorded.

METHODS

Study design

This was a single-center, prospective, double-blind, placebo-controlled, randomized study conducted between August 2020 and January 2022 at the Maharaj Nakorn Chiang Mai Hospital, Thailand.

Methodology

The Research Ethics Committee No.2 of the Faculty of Medicine, Chiang Mai University, authorized the study protocol (ANE-2563-07307). This permission allows the execution of human research in full accordance with the study protocol. The ClinicalTrials.gov ID was NCT04386642. After obtaining ethics committee approval and written informed consent from patients, twenty-five individuals aged 18 to 60 years who were diagnosed with intracranial meningioma with a radiographic finding of a tumor diameter > 5 cm in at least 2 dimensions were included (14-16). All the patients were scheduled for elective craniotomy to remove the tumor. The exclusion criteria were patients who refused to participate in this study, patients with recurrent tumors, an intracranial tissue biopsy, a history of TXA allergy, pregnancy, a history of significant thromboembolic episodes, or significant renal dysfunction (GFR ≤ 50 mL/min).

Sample size calculation

The sample size was calculated based on a previous study of TXA effects to reduce blood loss during intracranial meningioma removal (14). The average blood loss in large meningioma remov-

al in our institution is 800 mL. The mean loss in the experimental group was 500 mL. The sample size, calculated using continuous outcome for the superiority trial, was 44 patients (22 patients per group). This sample size had a power of 90%, a significance level of 5%, and standard deviation of outcome of 300. Due time limitations, we were not able to achieve the expected number participants. For that reason, this study presents the preliminary results of 25 patients.

Randomization and blinding

We used a computer-generated permuted block of 4 randomization. The random assignments were concealed in opaque, sealed envelopes. The envelopes were sent to the central pharmaceutical unit for preparation of the study drugs. The pharmacist opened the concealed envelopes and prepared the drug in clear 50 mL syringes. Patients in the TXA group received a TXA 20 mg/kg loading over 20 minutes before the skin incision, followed by a maintenance infusion of 1 mg/kg/hr until the end of operation (17, 18). The patients randomized to a placebo group received 0.9% normal saline. All the patients, attending anesthesiologists, neurosurgeons, data collectors and outcome assessors were blinded to the randomization. This blinding process was reliable as the research drug and placebo were prepared by a pharmacist who was not involved in the study. The investigational drug and the placebo were contained in a 50 mL clear syringe as a transparent solution.

Surgical procedure

The standard treatment for large meningioma is surgical removal. Surgical approaches are determined by the tumor's size, location, and vascular supply. This research focused exclusively on tumors situated within the supratentorial compartment. Total resection is the objective for neurosurgeons; however, this must be balanced against factors such as blood loss, brain edema, injury to adjacent normal brain tissue, and the patient's overall condition. A craniotomy for the removal of a large meningioma typically requires over six hours of surgical intervention and is associated with considerable blood loss.

Anesthetic protocols

A standard anesthetic protocol was followed with all the patients. At the operating theatre, patients received total intravenous anesthesia (TIVA) with propofol infusion via target-controlled infusion (TCI) following the Schneider pharmacokinetic model. Propofol TCI was set at an effect site concentration (Ce) of 4-6 mcg/mL. Fentanyl 2 mcg/kg and Cis-atracurium 0.15 mg/kg were administered during the induction period. Anesthesia was maintained by propofol TCI titration to the Bi-Spectral Index (BIS) value of 40-60. Ventilation was controlled with an air-oxygen mixture (FiO_2 0.4-0.5) with 2 L/min fresh gas flow. An arterial line and central venous line (if needed) were cannulated after induction of anesthesia. The blinded study drug was loaded at 0.5 mL/kg 20 mins prior to skin incision followed by 0.025 mL/kg/hr (1 mg/kg/hr) continuously infused to the end of operation. Propofol TCI tailed off when closing the dura mater was started. In-operating-theater extubation was discussed with the surgeons, and considered the patient's preoperative condition as well as anesthetic and surgical aspects. When to turn off the propofol infusion and whether to switch to a volatile anesthetic was determined by the attending anesthesiologist. Fentanyl was intermittently supplemented (25-50 mcg) during the surgery as needed.

Intraoperative fluid management was guided by pulse pressure variation (PPV). For the patients who had a central venous catheterization, PPV could be augmented by central venous pressure as a guided fluid administration. Arterial waveform analysis showing a PPV greater than 13% suggests the blood pressure is likely responsive to volume administration, classifying the patient as a volume responder. Serial arterial blood gas (ABG) analysis was done to assess the acid-base status, oxygenation, ventilation, hemoglobin (Hb) and hematocrit (Hct) and blood glucose. The types and volume of blood transfusion were decided by an anesthesiologist based on significant hemodynamic changes and the degree of anemia. The perioperative transfusion triggers in our institute are Hct < 30% for packed RBCs, INR > 1.5 for fresh frozen plasma (FFP) and platelet counts < 100,000/mm^3 for platelet transfusion. The volume of transfused packed RBCs, FFP and platelets were recorded. The visual estimation of intraoperative blood loss was done by estimating the amount of blood in surgical sponges and the

operative field, then subtracting the amount of irrigation fluid used from the total volume blood and fluid in the scaled suction canisters.

Following surgery, the patients were admitted to the neurosurgical ICU. Intubation and ventilation assistance was continued for variable periods depending on intraoperative events and the patient's neurological condition. The patients were transferred to a normal ward when their neurological status and hemodynamic were stable. Postoperative imaging is not routinely done in our institution. The radiologist was consulted urgently if the patient developed a new neurological deficit, pupils had either unequal responsiveness or total unresponsiveness to light or a worsening Glasgow Coma Scale (GCS) score. The systemic causes of the problems were then evaluated and corrected.

Statistical analysis

Statistical analysis was performed using Stata statistical software version 16.1 (Statacorp LLc, College Station, TX, USA). The distribution of data was assessed using the Kolmogorov-Smirnov and Shapiro-Wilk tests. The Mann-Whitney U-test and Student's t-test were used to analyze continuous variables depending on the distribution of the data. Normally distributed continuous variables are expressed as mean ± SD. Non-parametric variables are expressed as median (range). The Chi-square test and Fisher's exact test were used to compare categorical variables. Intention-to-treat analysis was used for the primary analysis. A p-value < 0.05 indicated statistical significance.

Ethic approval

The Research Ethics Committee No.2 of the Faculty of Medicine, Maharaj Nakorn Chiang Mai Hospital, Chiang Mai University (ANE-2563-07307) approved the study. Clinical trial registration: ClinicalTrials.gov Identifier: NCT04386642

RESULTS

In this preliminary study, twenty-five patients were enrolled. Twelve patients were randomized to the TXA group and thirteen patients were randomized to the placebo group. There were no dropouts or withdrawals. However, two patients in the placebo group received TXA during the operation due to life-threatening uncontrolled hemorrhage. The dosage of TXA administered to those two patients was 500 mg and 1,000 mg, respectively, which was significantly lower than that received by patients in the treatment group. We classified the two patients as belonging to the placebo group and included them in the intention-to-treat analysis. The consort diagram is shown in Figure 1.

The demographic characteristics and preoperative laboratory parameters of patients were comparable between the two groups (Table 1). The tumor volume was calculated by multiplication of three dimensions divided by 2.

$$(ABC)/2$$

A, B and C are the dimensions of the tumor measured by a radiologist using a recent CT / MRI brain (19).

The tumor volume of the two groups was similar: 100.58±35.63 cm^3 in the TXA group and 95.98±34.96 cm^3 in the placebo group, p = 0.747. Tumor location, duration of surgery, extension of

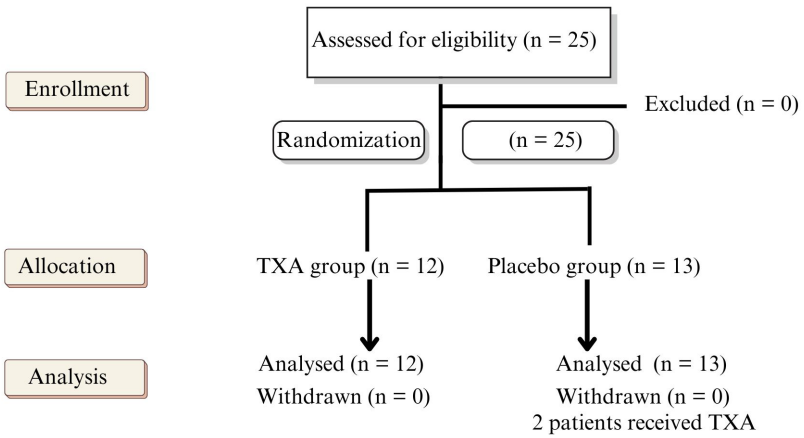

Figure 1. Consort diagram

Table 1. Demographic characteristics

Variables	TXA group (n=12)	Placebo group (n=13)	*p*-value
Age (years)	50.83±8.38	52.69±7.63	0.567
Male/female	1 [8.3%]/11 [91.6%]	5 [38.4%]/8 [61.5%]	0.160
BMI (kg/m^2)	24.79±5.37	24.44±4.89	0.867
Glasgow Coma Scale (GCS) score	15 (0.5)	15 (0.0)	0.659
Tumor volume (cm^3)	100.58±35.63	95.98±34.96	0.747
Pre-op hemoglobin (g/dL)	13.74±1.87	13.41±1.40	0.626
Pre-op platelet (cells/cu.mm.)	257,000±39,886	24,8384±54,386	0.658
Pre-op INR	0.98±0.04	1.01±0.06	0.197
Pre-op PTT ratio	0.85±0.12	0.82±0.12	0.553

Values are expressed as mean ± SD, median (IQR), number [%]
BMI, body mass index; INR, International Normalised Ratio; PTT partial thromboplastin time; TXA, tranexamic acid

Table 2. Demographic characteristics

Variables	TXA group (n=12)	Placebo group (n=13)	*p*-value
Duration of surgery (minutes)	541.2±146.4	493.4±113.7	0.369
Extent of resection (complete/partial)	4 [33.3%]/8 [66.6%]	5 [38.4]/8 [61.54]	1.000
Intraoperative crystalloid (mL)	2,525 (1,050)	2,150 (1,372)	0.2641
Intraoperative colloid (mL)	950 (750)	500 (1,000)	0.560
Intraoperative urine output (mL)	1,287±664	1,059±472	0.164
Intraoperative blood loss (mL) (median and IQR)	1,925 (1,575)	1,500 (1,700)	0.904
Intraoperative transfusion			
Packed red cells (mL)	801.5 (825.5)	493.0 (856.0)	0.883
Fresh frozen plasma (mL)	247 (548.5)	337 (1,017.0)	0.594
Platelets (mL)	0 (122.5)	0 (330.0)	0.302

Values are expressed as mean ± SD, median (IQR), number [%]
TXA, tranexamic acid

resection and anesthetic drug consumption were not different between groups. The amount of resuscitation fluid between groups was also alike (Tables 1 and 2).

The median intraoperative blood loss in TXA group was 1,925 (IQR=1,575) mL and in the placebo group was 1,500 (IQR=1,700) mL with no statistically significant difference between groups (p = 0.904) (Figure 2). The median intraoperative volume of packed RBCs was 801.5 (IQR=825.5) in the TXA group and 493 (IQR=856) in the placebo group (p = 0.883). There were no statistically significant differences in intraoperative blood transfusion volumes of packed RBCs, fresh frozen plasma or platelets (Table 2). The volume of blood transfused (mL) is a more precise measurement than the quantity of blood units as blood may occasionally be transfused in half-bag increments while patients are being transported to the ICU following the completion of surgery. The outcome remained unchanged when calculated in terms of blood units rather than blood volume in milliliters. Furthermore, there were no statistically significant differences in blood transfusion volumes in

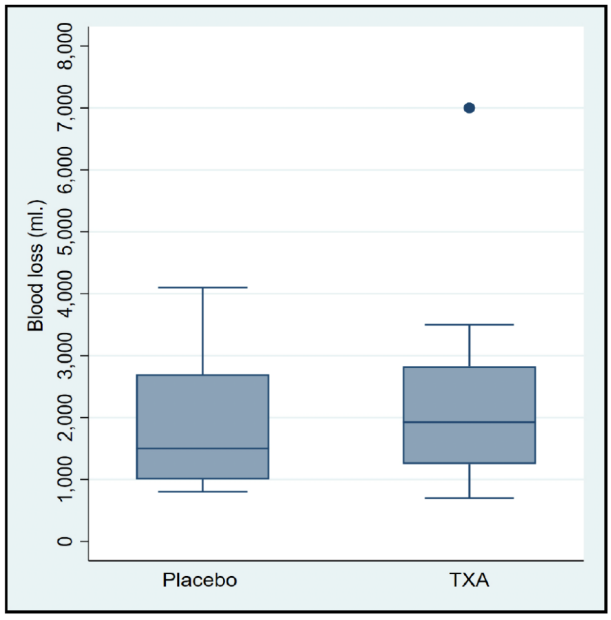

Figure 2. Volume of intraoperative blood loss (Primary outcome)

Table 3. Postoperative data

Variables	TXA group (n=12)	Placebo group (n=13)	*p*-value
Average volume of blood components received in the first 24 h of surgery			
Packed red cells (mL)	399	546	0.581
Fresh frozen plasma (mL)	0	0	0.797
Platelets (mL)	135	0	0.530
Number of patients who developed adverse events			
Thromboembolic events	1 (8.33%)	2 (15.38%)	1.000
Postoperative seizure	0.00	0.00	1.000

TXA, tranexamic acid

the first 24 hours after surgery in terms of packed RBCs, FFP or platelets (Table 3). There were no significant differences in the incidence of thromboembolic events and postoperative seizures between the two groups (Table 3).

DISCUSSION

Inarguably, surgical removal of intracranial meningioma is usually associated with massive hemorrhage and often requires a large volume of allogeneic blood transfusion. Factors correlated with significant blood loss in meningioma resection include large tumor size, tumors invading the sphenoid wing, a rich vascular supply, adjacent to the vessels, and accidental tearing of vessels (17). The larger the amount of meningioma resected the more tPA is released into the blood circulation. The tPA causes hyperfibrinolysis and interferes with clot formation. Massive blood transfusion further amplifies consumptive coagulopathy. Additionally, even a judicious volume of crystalloid solution causes dilutional coagulopathy. Some colloid solutions affect the coagulation pathway. TXA has been shown to reduce perioperative blood loss and transfusion in various surgical procedures, but there is only limited evidence for brain tumor removal, particularly meningioma surgery.

In our preliminary report of 25 patients, there was no significant difference in intraoperative blood loss between the two groups. The median intraoperative blood loss was 1,925 mL (IQR=1,575) in the TXA group and 1,500 mL (IQR=1,700) in the placebo group. There have been few studies of using TXA in patients undergoing excision intracranial meningioma. Those studies, which administered the same dose of TXA as in our study, reported that TXA could significantly reduce intraoperative blood loss during elective craniotomy for excision of intracranial meningioma by 27.00% (17), 46.43% (20) and 24.60% (21). Total intraoperative blood loss in our study was much higher in the placebo group (median 1,500 mL) than in studies by Hooda et al. (mean 1,124), Ravi et al. (mean 1,150 mL), Rebai et al. (mean 495 mL) (17, 20, 21). The reason for the differences might be due to differences in the size of the meningiomas. In our study, we enrolled patients with a tumor diameter > 5 cm in at least 2 dimensions, which is larger than in the previous studies. Ravi et al. recruited patient with tumor diameter > 5 cm in at least 1 dimension, while Hooda et al. and Rebai et al. recruited patients with meningioma regardless of the size of the tumor (17, 20-21). The tumor volume in our study is greater than those reported in previous studies. In the present study, the mean tumor volume was 100.58 cm^3 in the TXA group and 95.98 cm^3 in the placebo group. The Ravi et al. study reported a mean tumor volume of 63.79 cm^3 in the TXA group and 43.36 cm^3 in the placebo group (20). As mention earlier, a larger tumor can initiate a greater hemostatic disturbance by releasing greater amounts of tPA.

In the secondary outcomes, there was no significant difference in the transfusion requirement during the intraoperative period and the first 24 hours after surgery between the groups which is consistent with previous studies (17, 21-23). As is well known, TXA induces fibrinolytic suppression and promotes clot stabilization. Thus, the main theoretical risk of TXA is thromboembolic events. In our study, the incidence of thromboembolic events was similar between the groups which is consistent with previous studies. The other potential side effect of concern from TXA is seizure. In the setting of intracranial surgery, postoperative convulsion may result from the meningioma itself, from the surgical lesion, and may

possibly be TXA-induced. A previous systematic review showed that a newly-developed seizure after resection of meningioma occurred in 1.4% of patients and that it can significantly increase mortality (21). The incidence of TXA-associated seizures has been reported to be directly correlated with high doses of TXA (22). To reduce the risk of seizures, we chose to use an intermediate dose of TXA in the amount of 20 mg/kg loading 20 minutes before the skin incision and followed by a maintenance infusion of 1 mg/kg/h until the end of the operation. No postoperative seizures were observed in the present study. Our findings support what was reported in a CRASH-3 study which included 12,737 TBI patients. That study reported the incidence of thromboembolic events and seizures associated with the use of TXA were not higher in TBI patients (12).

This study had several limitations. This preliminary report, which involves a limited number of subjects, may lack sufficient statistical power to demonstrate a potential benefit of TXA, if such a benefit exists. Therefore, obtaining data from a larger sample as originally calculated may be required. Second, estimating blood loss by the visual method is subjective and can vary among the attending anesthesiologists. Based on the observed non-significant differences in outcomes between the two groups, the results of the present study indicate a reversal of prior evidence suggesting that TXA reduces blood loss during meningioma surgery. The authors chose to present the results of the study as preliminary findings.

CONCLUSIONS

As shown in this preliminary report, administration of TXA did not attenuate intraoperative blood loss during surgical removal of meningioma nor did it decrease transfusion requirements either intraoperatively or during the first 24 hours after surgery. The incidence of thromboembolic events in this study was similar between the two groups. No postoperative seizures occurred in our study. In future studies, obtaining the calculated desired sample size may be needed.

ACKNOWLEDGEMENTS

None

FUNDING

This research received a grant from the Faculty of Medicine, Chiang Mai University for tranexamic acid.

CONFLICTS OF INTEREST

The authors have no conflicts of interest to report.

REFERENCES

1. Ostrom Q, Cioffi G, Gittleman H, Patil N, Waite K, Kruchko C, et al. CBTRUS statistical report: primary brain and other central nervous system tumors diagnosed in the United States in 2012-2016. Neuro Oncol. 2019;21(Supplement_5):v1-v100. PubMed PMID: 31675094
2. Islim AI, Mohan M, Moon R, Srikandarajah N, Mills S, Brodbelt A, et al. Incidental intracranial meningiomas: a systematic review and meta-analysis of prognostic factors and outcomes. J Neurooncol. 2019;142:211-21.
3. Lemée J, Corniola M, Da Broi M, Joswig H, Scheie D, Schaller K, et al. Extent of Resection in Meningioma: Predictive Factors and Clinical Implications. Sci Rep. 2019;9:5944. PubMed PMID: 30976047
4. Choy W, Kim W, Nagasawa D, Stramotas S, Yew A, Gopen Q, Parsa AT, Yang I. The molecular genetics and tumor pathogenesis of meningiomas and the future directions of meningioma treatments. Neurosurg Focus. 2011;30:E6. PubMed PMID: 21529177
5. Goh K, Poon W, Chan D, Ip C. Tissue plasminogen activator expression in meningiomas and glioblastomas. Clin Neurol Neurosurg. 2005;107:296-300.
6. Sawaya R, Rämö O, Shi M, Mandybur G. Biological significance of tissue plasminogen activator content in brain tumors. J Neurosurg. 1991;74:480-6.
7. Goh K, Tsoi W, Feng C, Wickham N, Poon W. Haemostatic changes during surgery for primary brain tumours. J Neurol Neurosurg Psychiatry. 1997;63:334-8.
8. Hsu S, Huang Y. Characterization and prognostic implications of significant blood loss during intracranial meningioma surgery. Transl Cancer Res. 2016;5:797-804.
9. Wu W, Trivedi A, Friedmann P, Henderson W, Smith T, Poses R, et al. Association between hospital intraoperative blood transfusion practices for surgical blood loss and hospital surgical mortality rates. Ann Surg. 2012;255:708-14.
10. Budohoski K, Clerkin J, Millward C, O'Halloran P, Waqar M, Looby S, et al. Predictors of early progression of surgically treated atypical meningiomas. Acta Neurochir (Wien). 2018;160:1813-22.
11. Yates J, Perelman I, Khair S, Taylor J, Lampron J, Tinmouth A, et al. Exclusion criteria and adverse events in perioperative trials of tranexamic acid: a systematic review and meta-analysis. Transfusion. 2019;59:806-24.

12. CRASH-3 trial collaborators. Effects of tranexamic acid on death, disability, vascular occlusive events and other morbidities in patients with acute traumatic brain injury (CRASH-3): a randomised, placebo-controlled trial. Lancet. 2019;394:1713-23.
13. Sprigg N, Flaherty K, Appleton J, Al-Shahi Salman R, Bereczki D, Beridze M, et al. Tranexamic acid to improve functional status in adults with spontaneous intracerebral haemorrhage: the TICH-2 RCT. Health Technol Assess. 2019;23:1-48.
14. da Silva C, de Freitas P. Large and giant skull base meningiomas: The role of radical surgical removal. Surg Neurol Int. 2015;6:113. PubMed PMID: 26167365
15. Behari S, Das KK, Kumar A, Mehrotra A, Srivastava AK, Sahu RN, et al. Large/giant meningiomas of posterior third ventricular region: falcotentorial or velum interpositum? Neurol India. 2014;62:290-5.
16. Yasar S, Kirik A. Surgical Management of Giant Intracranial Meningiomas. Eurasian J Med. 2021;53:73-8.
17. Hooda B, Chouhan R, Rath G, Bithal P, Suri A, Lamsal R. Effect of tranexamic acid on intraoperative blood loss and transfusion requirements in patients undergoing excision of intracranial meningioma. J Clin Neurosci. 2017;41:132-8.
18. de Carvalho Barros L, Avancini C, Goncalves P, Paiva W, Gurgel R, Oliveira A. Efficacy, safety and dose patterns of tranexamic acid in meningioma surgery: a systematic review and updated meta-analysis of randomized controlled trials. Neurosurg Rev. 2025;48:23. PubMed PMID: 39760793
19. Opalak C, Parry M, Rock A, Sima A, Carr M, Chandra V, et al. Comparison of ABC/2 estimation and a volumetric computerized method for measurement of meningiomas using magnetic resonance imaging. J Neurooncol. 2019;144:275-82.
20. Ravi G, Panda N, Ahluwalia J, Chauhan R, Singla N, Mahajan S. Effect of tranexamic acid on blood loss, coagulation profile, and quality of surgical field in intracranial meningioma resection: A prospective randomized, double-blind, placebo-controlled study. Surg Neurol Int. 2021;12:272. PubMed PMID: 34221603
21. Rebai L, Mahfoudhi N, Fitouhi N, Daghmouri M, Bahri K. Intraoperative tranexamic acid use in patients undergoing excision of intracranial meningioma: Randomized, placebo-controlled trial. Surg Neurol Int. 2021;12:289. PubMed PMID: 34221620
22. Lin Z, Xiaoyi Z. Tranexamic acid-associated seizures: A meta-analysis. Seizure. 2016;36:70-3.
23. Komotar R, Raper D, Starke R, Iorgulescu J, Gutin P. Prophylactic antiepileptic drug therapy in patients undergoing supratentorial meningioma resection: a systematic analysis of efficacy. J Neurosurg. 2011;115:483-90.

Biomedical Sciences and Clinical Medicine 2025;64(2):158-166.
doi: 10.12982/BSCM.2025.18
https://he01.tci-thaijo.org/index.php/CMMJ-MedCMJ/index

Original Article

Open Access

Risk Assessment of Noise-induced Hearing Loss Among Workers with Occupational Noise Exposure in University Hospitals

Tanachot Thanomwong[1], Wichai Aekplakorn[1], Piyatad Bumrungwech[2], Nattida Phaipayom[2], Asadavudh Buachum[3], Wiyachatr Monklang[6], Nattacha Chumsunthorn[5], Narongpon Dumavibhat[4,6] and Chathaya Wongrathanandha[1]

[1]Department of Community Medicine, [2]Department of Occupational Health, Safety, and Environment, Faculty of Medicine Ramathibodi Hospital, [3]Occupational Health Division, Faculty of Medicine Siriraj Hospital, Mahidol University, [4]Siriraj Tuberculosis Comprehensive Center, Siriraj Hospital, [5]Chakri Naruebodindra Medical Institute, Faculty of Medicine Ramathibodi Hospital, Mahidol University, Samut Prakan, [6]Department of Preventive and Social Medicine, Faculty of Medicine Siriraj Hospital, Mahidol University, Bangkok, Thailand

Correspondence:
Chathaya Wongrathanandha, MD, Faculty of Medicine Ramathibodi Hospital, 270 Rama VI Road, Ratchathewi, Bangkok, 10400, Thailand.
E-mail: chathaya.won@mahidol.ac.th

Received: December 6, 2024;
Revised: February 11, 2025;
Accepted: March 11, 2025

ABSTRACT

OBJECTIVE Occupational noise-induced hearing loss (ONIHL) is prevalent among supporting healthcare workers in a hospital setting. The risk assessment of ONIHL using a risk matrix could be beneficial, particularly in settings with limited resources; however, it has rarely been applied, and no previous studies have evaluated its accuracy compared to audiogram results. This study aimed to develop a system to evaluate the accuracy of a risk matrix score as a screening tool for the risk of ONIHL.

METHODS This retrospective cohort study included hospital workers exposed to high workplace noise levels in Ramathibodi Hospital and Siriraj Hospital between 2016 and 2023. The noise levels were monitored in the workplaces, and workers' annual audiograms were obtained and interpreted. The risk matrix score was developed by multiplying the numerical value of each domain in the risk matrix (probability - P, consequences - C, and exposure time - E), resulting in a score range of 1 to 125. The accuracy of the risk scores for predicting ONIHL was evaluated using the ROC curve. The optimal cut-off value for the risk scores was determined based on sensitivity and specificity, and the scores were classified into five risk levels (R).

RESULTS A total of 239 workers were included in the study (45.6% male and 54.4% female), 38.5% of whom were diagnosed with ONIHL. For noise exposure level (P), most workers (70.7%) were exposed to occupational noise levels less than 80 dBA as an 8-hour time-weighted average (level 1). Regarding Consequences (C), the majority (38.5%) experienced moderate health effects from noise exposure (level 3). For exposure time (E), most workers (32.2%) had a job duration of 20 years or more (level 5). In terms of risk categories (R), most workers (40.2%) were in the moderate risk category (level 3), followed by 26.8% in the acceptable risk category (level 1), 20.5% in the low-risk category (level 2) and 12.6% in the high-risk category (level 4). The area under the curve (AUC) of the risk score for predicting ONIHL was 0.667. At a score of 8, the sensitivity and specificity for ONIHL were 65.2% and 55.1%, respectively.

CONCLUSIONS The risk matrix can moderately predict ONIHL. It should be employed to screen and prioritize high-risk workers for audiometry in settings with limited resources to promote early detection of ONIHL and further noise control.

KEYWORDS occupational noise-induced hearing loss, risk matrix, risk assessment, screening test, healthcare worker

INTRODUCTION

Occupational noise-induced hearing loss (ONIHL) is one of the most common occupational diseases globally. The global prevalence of ONIHL in 2019 ranged from 11.2 to 58.0% and was generally higher in developing countries (1). The cause is prolonged exposure to loud noise, typically over a period of 10 years, resulting in permanent injury to hair cells within the cochlea of the inner ear. ONIHL is sensorineural hearing loss (1). The gold standard for diagnosis of ONIHL is pure tone audiometry (PTA) (2). ONIHL has characteristic audiogram signatures: a notch presentation of hearing threshold at high frequencies, 3,000, 4,000, or 6,000 Hz, with a recovery observed at 8,000 Hz. ONIHL differs from presbycusis in that it shows a recovery pattern at 8,000 Hz, whereas presbycusis does not (3).

Presently, there are no ways to cure ONIHL (4). The catastrophic consequences of hearing loss are associated with poor health status, high unemployment rates, depression, dementia, and high mortality rates (5). ONIHL in workers also significantly increases the risk of work-related injuries (6, 7). The impact of ONIHL results in both a financial and disease burden at individual and country levels (8). In hospitals, workers in certain departments, such as laundry, nutrition, and engineering service units, may be exposed to loud noise. However, hearing conservation programs in many hospitals in Thailand are often overlooked and inadequately implemented.

The study by Pinosova et al. (9) used a three-dimensional risk matrix to assess the risk of ONIHL by using risk scores. The dimensions were Probability, Consequence, and Exposure time. The noise level in the workplaces increases the risk of ONIHL; therefore, it is defined as Probability. The Consequences include auditory effects, non-auditory effects, and injuries from noise exposure. The Exposure time is measured in years worked in high noise level units. The risk matrix can prioritize hazard management according to the risk scores. However, a study by Pinosova et al. (9) did not test the accuracy of the risk matrix scores by comparing them with the audiograms of the workers. To our knowledge, no previous studies have compared risk matrix scores with diagnosed ONIHL from audiograms, and there is no published evidence of a risk matrix of occupational noise exposure in Thailand. Such a matrix could help prioritize workers who should receive PTA testing to detect hearing damage and to suggest further preventive measures early. Moreover, such a risk assessment could serve as an educational tool to motivate employers and workers to comply with hearing conservation programs.

Ramathibodi and Siriraj Hospital, Mahidol University are among the largest tertiary care hospitals in Thailand. Both facilities have various working areas where hospital workers are exposed to high noise levels. At those institutions, hearing and noise monitoring data have been collected regularly. This study aimed to develop a risk matrix score and to assess its accuracy as a screening tool of ONIHL which could identify high-risk workers. Early detection of ONIHL would help protect the workers against more severe hearing damage and encourage organizations to manage the risk of noise hazards through a hierarchy of controls.

METHODS

This retrospective cohort study aimed to construct a three-dimensional risk matrix for use as a screening tool for ONIHL. The data sources were questionnaire interviews, annual audiometry records, and measurements of noise levels in the work environment.

Study population

The study population was all workers exposed to loud noise who were included in the hearing monitoring program. There were a total of 308 workers: 168 and 140 from Ramathibodi and Siriraj Hospitals, respectively. The departments included Laundry, Nutrition, Prosthetics and Orthotics, Engineering Service, Central Sterile Supply, OR OB-GYN, Printing, and Medical Gas System.

Sample characteristics

The inclusion criteria were: 1) workers who underwent PTA due to workplace noise exposure between 1 January 2016 and 30 September 2023, and 2) workers' departments which had annual noise monitoring data. Individuals were excluded who: 1) had retired or resigned, or 2) had permanent hearing loss from other causes, e.g., ototoxic drugs/chemicals, trauma, uncurable or congenital or genetic ear diseases, history of non-occupational acoustic trauma, etc.

After data collection, a total of 239 participants were identified from a group of 308 workers, or 77.6%, which was considered an acceptable response rate (10).

Power of the study

This study used all available data. The power of the retrospective cohort study was calculated using OpenEpi (11). The exposed group was defined as individuals who had a regular noise exposure level of 80 dBA and above, a level at which long-term exposure would increase the risk of ONIHL (2). The non-exposed group was defined as individuals having a noise exposure level of less than 80 dBA. The power of the study was 0.7 (70.0%), an acceptable statistical power.

Data collection

Questionnaire: The authors collected data through face-to-face interviews using an electronic questionnaire. The questionnaire content included demographics, auditory symptoms (e.g., tinnitus, communication problems), non-auditory symptoms (e.g., dizziness, headache), and injuries related to noise exposure in the workplace (e.g., slipping, falling, and amputation). Three occupational medicine physicians verified the validity of the questionnaire using the content validity index (CVI). Then a pilot study was done after which the questionnaire was adapted and used for data collection. The participants provided written permission to use their PTA results.

Noise exposure: Data on annual noise monitoring of the workers' departments were obtained. Industrial hygienists in each hospital measured noise levels using a sound level meter, then calculated the noise level as an 8-hour time weight average (TWA).

Hearing status: The annual hearing monitoring of hospital staff using PTA tested hearing at 500, 1,000, 2,000, 3,000, 4,000, 6,000, and 8,000 Hertz in both ears followed the ACOEM guidance statement 2018 (3). Audiograms made between 2016 and 2023 were obtained from both occupational health units. The latest audiogram was used to diagnose ONIHL.

Diagnosis of ONIHL from pure tone audiograms

ONIHL was diagnosed from annual audiograms according to the ACOEM ONIHL guidance statement 2018 (3) and Cole et al. (12), then verified by three occupational physicians. The diagnostic criteria were: 1) a notch at frequencies 3,000, 4,000, or 6,000 Hz of 10 dB or more compared with that at 1,000 or 2,000 Hz, and 2) a notch at frequencies 3,000, 4,000, or 6,000 Hz of 10 dB or more compared with that at 6,000 or 8,000 Hz.

Risk matrix

The individual risk matrix consisted of the following three parameters. The probability of risk occurrence (P) was the central value (median) of all annual workplace noise levels as an 8-hour TWA. The probability was divided into five levels according to the noise level (1 = 'less than 80 dBA', 2 = '80-84 dBA', 3 = '85-89 dBA', 4 = '90-94 dBA', and 5 = 'more than 94 dBA') (details in Supplement Table S1).

The risk of developing ONIHL increases with prolonged exposure to noise levels above 80 dBA as an eight-hour TWA, and the risk significantly increases when exposure exceeds 85 dBA (3). According to National Institute for Occupational Safety and Health (NIOSH) Occupational Noise Exposure Revised Criteria 1998, the estimated risk of significant hearing impairment after 40 years of work is 1.0% at 80 dBA with eight-hour TWA, 8.0% at 85 dBA, and 25.0% at 90 dBA (13).

The consequences or the severity of the risk (C) were the most severe health effects or injuries as obtained from the questionnaire. The consequences were divided into five levels according to the severity (1 = 'insignificant effects', 2 = 'minor effects', 3 = 'moderate effects', 4 = 'major effects', and 5 = 'catastrophic effects') (details in Supplement Table S2)

The exposure time (E) was the job-years of exposure to loud noise in the workplace. The exposure time was divided into five levels according to the duration (1 = less than 5 years, 2 = 5-9 years, 3 = 10-14 years, 4 = 15-19 years, and 5 = 20 years and above). (details in Supplement Table S3.)

The risk of ONIHL from prolonged noise exposure starts at 5 years (14). ONIHL progresses most rapidly during the first 10 to 15 years, after which the rate of hearing loss slows. This differs from age-related hearing loss, which speeds up as time progresses (3).

Finally, the risk scores were calculated: Risk score = P x C x E.

Statistical analyses

Receiver operating characteristic (ROC) analysis of the risk matrix scores. The accuracy of the risk matrix scores as a screening tool for ONIHL was tested using ROC analysis. The area under the curve (AUC), sensitivity, and specificity were calculated. The optimal cut-off for the risk matrix tool was determined based on sensitivity, specificity, and clinical significance.

New risk categories (R) in risk matrix development. After determining the cut-off point of ONIHL from risk scores, simple logistic regression was used to find the association between risk scores and the diagnosis of ONIHL. The odd ratios, 95% confidence interval, probability (odds/(1+odds)), and *p*-values were used to classify risk scores into five risk categories (R). A *p*-value less than 0.05 was considered statistically significant. The hazard management for each risk category was developed based on the studies of Piňosová et al. (9), Chaiklieng et al. (15), and Kadir et al. (16).

All data were analyzed using STATA software version 17.

Ethical approval

The research was approved by the human ethics committee of the Faculty of Medicine, Ramathibodi Hospital and the Faculty of Medicine Siriraj Hospital, Mahidol University, Bangkok, Thailand (COA No. MURA2023/783).

RESULTS

Demographic data, Proportion of ONIHL, and noise level

The participants were 239 workers: 130 (54.4%) from Ramathibodi and 109 (45.6%) from Siriraj Hospital. There were 109 male workers (45.6%) and 130 female (54.4%). The age ranged from 22 to 59 years old, with a mean (SD) of 41.4 (10.2). The average noise levels in work areas varied from 55.6 to 87.2 dBA, with a median (Q1, Q3) of 78 (72.4, 80.8). Years on the job ranged from 0 to 40, with a median (Q1, Q3) of 11 (6, 22). The participants by department are shown in Table 1. The proportion of workers with ONIHL was 38.5% (29.2% in Ramathibodi and 49.5% in Siriraj Hospital).

The annual noise monitoring levels from the different departments had medians of 65.6 to 86.7 dBA. The loudest areas were in the Engineering Service Department. Comparisons between the hospitals showed most departments had similar median noise levels, e.g., the Nutrition and the Central Sterile Supply Department. However, in the Prosthetics and Orthotics Unit, the noise levels were much higher in Siriraj Hospital (Table 2).

Characteristics of the risk matrix and risk scores

Regarding the probability (P), most participants were exposed to occupational noise levels less than 80 dBA (70.7%), followed by 80-84 dBA (24.3%) and 85-89 dBA (5.0%). Concerning consequences (C) or self-reported health effects and injuries from noise exposure, most workers (38.5%)

Table 1. Participants by departments of Ramathibodi and Siriraj Hospitals (N = 239)

Department	Participant number (%)		Total (n = 239)
	Ramathibodi Hospital (n = 130)	Siriraj Hospital (n = 109)	
Engineering Service	12 (9.2)	-	12
Nutrition	20 (15.4)	8 (7.3)	28
Central Sterile Supply	23 (17.7)	63 (57.8)	86
OR OB-GYN*	23 (17.7)	-	23
Prosthetics and Orthotics Unit	2 (1.5)	22 (20.2)	24
Laundry	50 (38.5)	2 (1.8)	52
Publishing	-	8 (7.3)	8
Medical Gas System Division	-	6 (5.5)	6
Total	130 (100.0)	109 (100.0)	

*Obstetrics and Gynecology operating room

Table 2. Medians of annual noise level (dBA) in work areas (8-hours TWA) of Ramathibodi and Siriraj Hospital between 2016 and 2023

Work areas	Noise level (dBA)	
	Ramathibodi Hospital	Siriraj Hospital
1. Engineering Service Department		
Grinding room	70.2	-
Vacuum generator room	86.7	-
Chiller room	85.6	-
Boiler room	79.6	-
2. Nutrition Department		
Steam rice area	77.1	-
Dish washing area	80.4	78.6
Blenderized diet room	76.6	-
3. Central Sterile Supply Department		
Washing room	81.7	84.5
Oven room	78.6	-
After washing process area	75.1	75.5
4. OR OB-GYN*		
Instrument cleaning room	74.9	-
5. Prosthetics and Orthotics Unit	65.6	81.5
6. Laundry Department		
Washing area	78.8	81.3
Drying machine area	-	80.0
Cloth sewing unit	78.8	-
7. Publishing Unit		
Printing room	-	83.0
8. Medical Gas System Division	-	77.0

*Obstetrics and Gynecology operating room

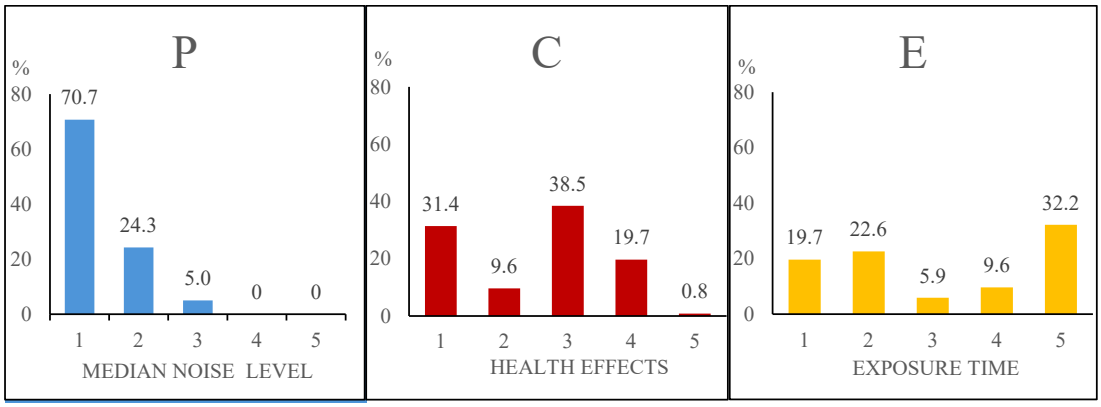

Figure 1. Percentages of workers by dimension and level in the Risk Matrix Model
Probability of risk occurrence (P): 1, 'less than 80 dBA'; 2, '80-84 dBA'; 3, '85-89 dBA'; 4, '90-94 dBA'; and 5, 'more than 94 dBA'. The consequence (C) or health effects and injuries from noise exposure: 1, 'insignificant effects'; 2, 'minor effects'; 3, 'moderate effects'; 4, 'major effects'; and 5, 'catastrophic effects'. The exposure time (E) or job years: (1, '<5 years'; 2, '5-9 years'; 3, '10-14 years'; 4, '15-19 years'; and 5, '≥20 years')

were classified as moderate (level 3), followed by insignificant (level 1) (31.4%). Finally, regarding exposure time (E), most participants had 20 or more years of on the job exposure (32.2%), followed by 5-9 years (22.6%) (Figure 1).

The calculated individual risk scores ranged from 1 to 60. The median score (Q1, Q3) was 8 (4, 15). The median risk scores by department are shown in Figure 2. The highest departmental risk scores were in the Laundry (Siriraj), the Engineering

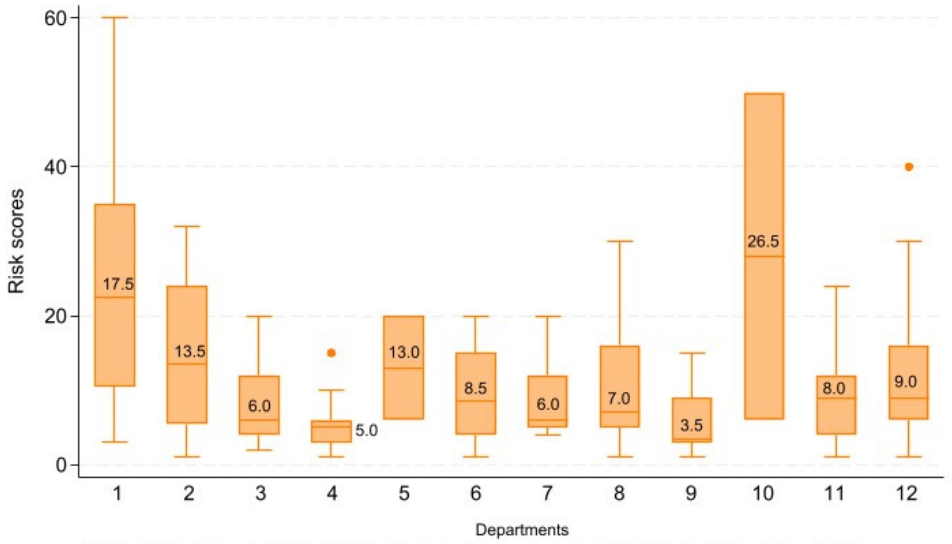

Figure 2. Median risk scores by department
Ramathibodi Hospital: 1, Engineering Service; 2, Nutrition; 3, Central Sterile Supply; 4, Obstetrics and Gynecology operating room; 5, Prosthetics and Orthotics; 6, Laundry
Siriraj Hospital : 7, Nutrition; 8, Publishing; 9, Medical Gas System; 10, Laundry; 11, Central Sterile Supply; 12, Prosthetics and Orthotics

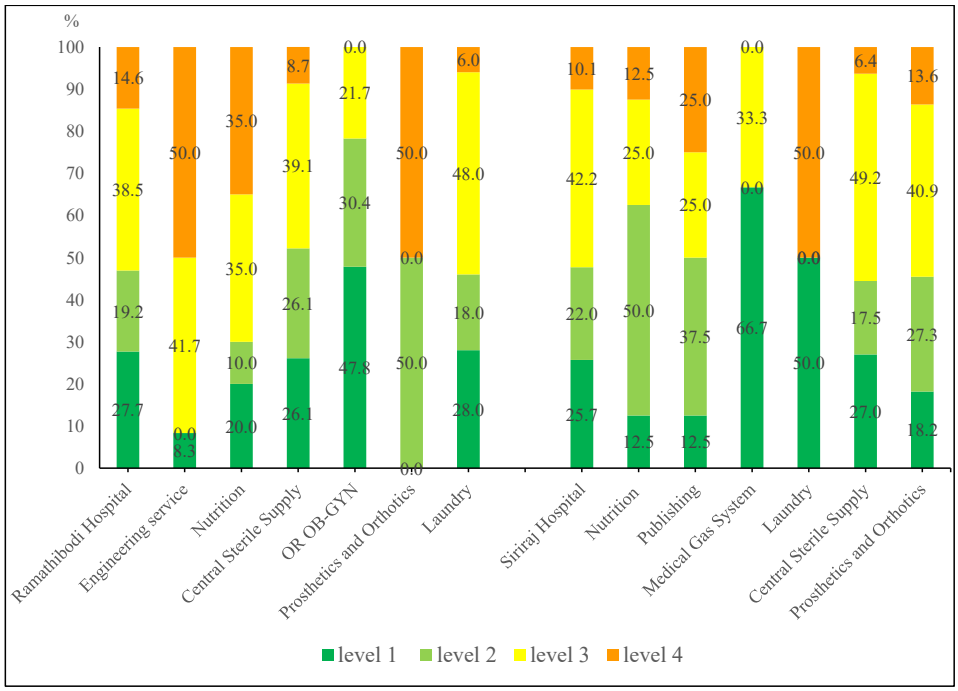

Figure 3. Proportion of individual risk level by department

Service (Ramathibodi), and the Nutrition Department (Ramathibodi). Regarding individual risk levels, most of the workers were at level 3 (moderate risk). The Engineering Service Department (Ramathibodi) had the highest proportion of workers at level 4 (high risk), followed by the Nutrition Department (Ramathibodi) (Figure 3).

Accuracy of the risk scores as a screening tool for ONIHL

The AUC of the ROC curve for predicting ONIHL was 0.667 (95%CI: 0.60-0.74). The optimal cut-off value of risk scores to discriminate between the ONIHL group and the non-ONIHL was selected at eight, with a sensitivity of 65.2% and a specificity of 55.1%. Another candidate cut-off value was a score of nine, with a sensitivity of 62.0% and a

Table 3. Association between risk categories and proportion of participants with ONIHL by simple logistic regression

Risk score	Risk level	Odds ratio (95%CI)	*p*-value	Probability	Frequency (%) (N = 239)
1-4	1	-	-	-	64 (26.8)
5-7	2	1.74 (0.76-3.96)	0.190	0.50	49 (20.5)
8-17	3	2.14 (1.05-4.35)	0.035*	0.67	96 (40.2)
18-64	4	8.98 (3.32-24.29)	< 0.001*	0.89	30 (12.6)

*Statistically significant ($p < 0.05$)

specificity of 63.9% (Supplement Table S4). However, the value of 8 is more suitable for practical use because a screening tool should have a sensitivity higher than its specificity to effectively identify high-risk workers for PTA. Early detection of ONIHL is important for the prevention of permanent hearing damage (1).

Risk score categorization (R) in the risk matrix model

The new Risk categorization (R) or Risk level was developed (Supplement Table S5) based on simple logistic regression analysis and on previous studies (9, 15, 16). Most participants were at risk level 3 (40.2%), followed by risk level 1 (26.8%). No participants were at risk level 5 (Table 3).

DISCUSSION

This study is the first to use a risk matrix and risk scores as the screening tool for the risk of ONIHL. The AUC was 0.667, which implies satisfactory performance (17, 18). At the cut-point score of eight, the sensitivity and specificity in predicting ONIHL were moderate and could be used to prioritize high-risk workers who should undergo PTA. The screening process is relatively low cost and requires no special skill set, making it suitable for limited resource settings. Another benefit is as a warning to workers who have refused to attend PTA. However, this risk matrix model should be used together with the laws or recommendations of each country regarding hearing conservation programs, e.g., NIOSH revised noise exposure criteria (13), and Occupational Safety and Health Administration (OSHA) Standard Number 1910.95 (Occupational noise exposure) (19).

The risk scores in this study were significantly lower than in another study at a metal cutting and welding center (9). In that study, risk scores ranged from 1 to 60, with a median (Q1, Q3) of 8 (4, 15). In contrast to the present study, most metal workers had unacceptable risk scores (risk scores more than 75), with median risk scores in the welding and the cutting center of 28 and 76, respectively. The difference could be a result of the lower noise level in the work environment and shorter exposure time due to shorter median job duration in the cutting and welding center (11 years compared to 18 years at the hospitals). Nevertheless, half the participants in this study (53.1% of Ramathibodi and 52.3% of Siriraj participants) were at risk levels 3 and 4, considered moderate and high risk, respectively. The hospital workplaces in those institutions need to implement further preventive measures following the hierarchy of controls as soon as possible, especially for workers at high risk. Their existing hearing conservation programs should be revised and improved. The recommendations for risk level 3 and above are similar to the study by Piňosová et al. (9), and are also applicable to other types of occupational hazards, e.g., chemical hazards in a study by Chaiklieng et al. (15).

It was noted that most workers with hearing loss (70 workers, or 76.2%) had been exposed to noise for 10 years or more and were classified as level 3 or higher for Exposure Time (E). This assigned risk category aligns with the fact that ONIHL development mostly occurred after 10 years of noise exposure (3, 14).

This study had some limitations. First, the retrospective nature of the study resulted in several issues. For example, recall biases could occur among participants with abnormal audiograms. Some workers could also have forgotten about the health effects of occupational noise exposure

in the past which could have led to underreporting of symptoms. Moreover, most participants lacked baseline audiograms; therefore, excluding hearing loss from non-occupational causes was problematical. Second, work arrangements could differ from regular eight-hour shifts during the study period. For example, some participants could have to work overtime or rotate to other worksites. Therefore, the occupational noise exposure level could deviate from the estimated value. For workers who worked more than eight hours per day, the risk assessment might underestimate the risk, while those who worked less than the average might overestimate the risk category. Additionally, this study used ambient noise monitoring in the workplace for exposure assessment which might not accurately represent individual exposure. Using personal noise dosimeter data in future studies could improve the exposure assessment. Third, some workers didn't have confirmation audiograms after abnormal results, which could have led to overdiagnosis. However, the like lihood of a temporary threshold shift, the main cause of ONIHL misdiagnosis, was quite low because most workers were not exposed to loud noise for at least 12 hours before undergoing PTA (20).

Finally, some departments in this study, such as the Laundry Department at Siriraj and the Prosthetics and Orthotics Units at Ramathibodi, had small sample sizes, which might not accurately represent their actual risk. To improve the accuracy of the risk matrix screening tool, further studies should include a larger sample size and validate other settings.

CONCLUSIONS

The risk matrix to assess the risk of ONIHL was developed from three dimensional factors: probability, exposure, and concentration. The risk matrix can predict the risk of hearing loss with moderate accuracy and could help warn workers exposed to loud noise in the workplace. It should be used to screen and prioritize high-risk workers who should undergo pure tone audiometry in settings with limited resources as a means of promoting early detection of ONIHL and further noise control.

ACKNOWLEDGMENTS

The authors would like to express their gratitude to the experts who helped with questionnaire validation and the academic support staff in the Department of Community Medicine, Faculty of Medicine at Ramathibodi Hospital.

FUNDING

This study did not receive any specific funding from public, commercial, or nonprofit organizations.

CONFLICTS OF INTEREST

The authors declare no conflicts of interest.

ADDITIONAL INFORMATION

Supplementary materials

The following supporting information can be downloaded at: Supplementary materials

REFERENCES

1. Chen KH, Su SB, Chen KT. An overview of occupational noise-induced hearing loss among workers: epidemiology, pathogenesis, and preventive measures. Environ Health Prev Med. 2020;25:65. PubMed PMID: 33129267
2. Musiek FE, Shinn J, Chermak GD, Bamiou DE. Perspectives on the Pure-Tone Audiogram. J Am Acad Audiol. 2017;28:655-71.
3. Mirza R, Kirchner DB, Dobie RA, Crawford J. Occupational Noise-Induced Hearing Loss. J Occup Environ Med. 2018;60:e498-e501.
4. Boisvert I, Reis M, Au A, Cowan R, Dowell RC. Cochlear implantation outcomes in adults: A scoping review. PLoS One. 2020;15:e0232421. PubMed PMID: 32369519
5. Stevens G, Flaxman S, Brunskill E, Mascarenhas M, Mathers CD, Finucane M. Global and regional hearing impairment prevalence: an analysis of 42 studies in 29 countries. Eur J Public Health. 2013;23:146-52.
6. Girard SA, Leroux T, Courteau M, Picard M, Turcotte F, Richer O. Occupational noise exposure and noise-induced hearing loss are associated with work-related injuries leading to admission to hospital. Inj Prev. 2015;21(e1):e88-92.
7. Yoon JH, Roh J, Kim CN, Won JU. The risk of occupational injury increased according to severity of noise exposure after controlling for occupational environment status in Korea. Noise Health. 2016;18(85):355-61.
8. Zhou H, Zhou Y, Zhang H, Yu A, Zhu B, Zhang L. Socio-economic disparity in the global burden of occupational noise-induced hearing loss: an analysis for 2017 and the trend since 1990. Occup Environ Med. 2021;78:125-8.

9. Piňosová M, Andrejiova M, Badida M, Moravec M. Analysis and evaluation of risks from exposure to noise in a working environment. Acta Mechanica Slovaca. 2018;22:44-52.
10. Baruch Y. Response rate in academic studies - a comparative analysis. Human Relations. 1999;52:421-38.
11. Sullivan KM, Dean A, Soe MM. OpenEpi: a web-based epidemiologic and statistical calculator for public health. Public Health Rep. 2009;124:471-4.
12. Coles RR, Lutman ME, Buffin JT. Guidelines on the diagnosis of noise-induced hearing loss for medicolegal purposes. Clin Otolaryngol Allied Sci. 2000;25:264-73.
13. Chan HS. Criteria for a recommended standard: occupational noise exposure: Revised Criteria 1998. 1998.
14. Sriopas A, Chapman RS, Sutammasa S, Siriwong W. Occupational noise-induced hearing loss in auto part factory workers in welding units in Thailand. J Occup Health. 2017;59:55-62.
15. Chaiklieng S, Suggaravetsiri P, Autrup H. Biomatrix of health risk assessment of benzene-exposed workers at Thai gasoline stations. J Occup Health. 2021;63:e12307. PubMed PMID: 34957641
16. A.Kadir Z, Mohammad R, Othman N. An advanced risk matrix analysis approach for safety evaluation at major ports in Malaysia. Journal of Advanced Research in Business and Management Studies. 2020;18:31-41.
17. Metz CE. Basic principles of ROC analysis. Semin Nucl Med. 1978;8:283-98.
18. Yang S, Berdine G. The receiver operating characteristic (ROC) curve. The Southwest Respiratory and Critical Care Chronicles. 2017;5:34.
19. OSHA. Standard Number 1910.95 - Occupational noise exposure [Internet]. [cited 2023 Aug 9]. Available from: https://www.osha.gov/laws-regs/regulations/standardnumber/1910/1910.95
20. Dudarewicz A, Pawlaczyk-Łuszczyńska M, Zaborowski K, Pontoppidan NH, Wolniakowska A, Bramsløw L, et al. The adaptation of noise-induced temporary hearing threshold shift predictive models for modelling the public health policy. Int J Occup Med Environ Health. 2023;36:125-38.

Supplementary materials

P (probability of risk occurrence): the central value (median) of all annual noise levels as 8-hour TWA in the workplaces (Table S1.)

Table S1. Probability of risk occurrence (P)

Probability	Value	Noise level (dBA)	Description of probability
Rare	1	< 80	The likelihood of risk occurrence is nearly eliminated.
Unlike	2	80-84	Risk occurrence is improbable but feasible.
Possible	3	85-89	Risk occurrence is likely (occurs intermittently).
Likely	4	90-94	Risk occurrence is highly likely.
Almost certain	5	> 94	The danger of risk occurrence is highly likely.

C (consequence or severity of the risk): the most severe health effects and injuries from occupational noise exposure, obtaining from the questionnaire (Table S2)

Table S2. Consequence or severity of the risk (C)

Level	Value	Description of health effects and injuries
Insignificant	1	No compliant the impact of loud noise
Minor	2	Mild concentration difficulties, palpitation, fatigue, mild to moderate distress during work
Moderate	3	Headache, dizziness, temporary hearing loss, severe distress during work, severe concentration difficulties, mild muscle pain/spasm, tinnitus, mild to moderate communication problems
Major	4	Serious communication problems, severe sleeping disturbances, moderate to severe muscle pain/ spasm, injury at noisy work with day off < 3 days
Catastrophic	5	Injury at noisy work with day off ≥3 days

E (exposure time): job years in the current work areas (Table S3)

Table S3. Exposure time (E)

Exposure Level	Value	Time [year]
Negligible exposure time	1	0-4
Significant exposure time	2	5-9
High exposure time	3	10-14
Very high exposure time	4	15-19
Excessive exposure time	5	≥ 20

Table S4. Performance of Risk matrix scores (screening tool) through the comparison of cut-off value in identifying workers at risk for ONIHL

Cut-off Value	Sensitivity	Specificity
≥ 1	100%	0%
≥ 2	97.8%	6.1%
≥ 3	95.7%	15.7%
≥ 4	85.9%	24.5%
≥ 5	83.7%	33.3%
≥ 6	73.9%	42.2%
≥ 8	65.2%	55.1%
≥ 9	62.0%	64.0%
≥ 10	58.7%	70.1%
≥ 12	52.2%	72.8%
≥ 15	39.1%	82.3%
≥ 16	28.3%	92.5%
≥ 18	23.9%	94.6%
≥ 20	23.9%	95.2%
≥ 24	16.3%	96.6%

Cut-off Value	Sensitivity	Specificity
≥ 30	10.9%	98.0%
≥ 32	5.4%	99.3%
≥ 40	5.4%	100%
≥ 50	3.3%	100%
≥ 60	2.2%	100%

Table S5. Newly developed Risk score categories (R) in the Risk Matrix model

Risk level	Risk Scores	Risk Category	Action
Acceptable	1-4	1	No action required.
Low	5-7	2	No supplementary controls required. Monitoring required to ensure the maintenance of controls including annual noise level monitoring
Moderate	8-17	3	Necessary to take preventive measures to reduce the risk including annual hearing monitoring
High	18-64	4	Necessary to take preventive measurements very soon to reduce the risk as well as risk level 3

Very high (Unacceptable)	65-125	**5**	The work must be stopped until the elimination of the risk.

Departments with workers with the risk level 2 and above should have annual noise level monitoring. Moreover, departments with workers with risk level 3 and above should have both the preventive measurements and the annual PTA. Nevertheless, the risk matrix should be used together with each country's occupational health and safety laws and regulations.

Biomedical Sciences and Clinical Medicine 2025;64(2):167-175.
doi: 10.12982/BSCM.2025.12
https://he01.tci-thaijo.org/index.php/CMMJ-MedCMJ/index

Review Article

Open Access

Impact of Microglia in Neurodevelopmental Disorders: A Review

Pushpalatha K[1], Devika Sanil kumar[2], Sushma Daripelli[3], Sovan Bagchi[4], Rajkumar Krishnan Vasanthi[5], Sumod Khedekar[6] and Danti Joseph[7]

[1]JSS Medical College, JSSAHER, Mysuru, [2]Research Officer, Panimalar Medical College Hospital and Research Institute, Chennai, Tamil Nadu, [3]Department of Anatomy, Government Medical College, Jangaon, Telangana, India, [4]Department of Biomedical Sciences, Gulf Medical University, United Arab Emirates, [5]Faculty of Health and Life Sciences, INTI International University, Nilai, Negeri Sembilan, Malaysia, [6]Department of Kaumarbhritya, Gomantak Ayurveda Mahavidyalaya & Research Centre, Shiroda, Goa, India, [7]Department of Physiology, Sree Balaji Medical College and Hospital, India

Correspondence:
Devika Sanil Kumar, PhD, Research Officer, Panimalar Medical College Hospital and Research Institute, Chennai, Tamil Nadu, India.
E-mail: devikasds2980@gmail.com

Received: September 13, 2024;
Revised: November 15, 2024;
Accepted: December 13, 2024

ABSTRACT

OBJECTIVE Microglia, immune cells that dwell in the brain, have essential functions in neurodevelopment and are responsible for synaptic pruning, neuronal circuit creation, and inflammatory responses. Disrupted microglial activity can contribute to conditions such as autism spectrum disorders, schizophrenia, and ADHD by impacting the health and connections of neurons through the production of pro-inflammatory cytokines. These cells, which arise during central nervous system (CNS) development and have the ability to regenerate themselves throughout an individual's lifespan, display considerable functional variation. Microglia, which have traditionally been known for their immunological functions, also play a role in regulating neurodevelopmental processes such as programmed synaptogenesis, synaptic pruning and cell death. Recent genetic and preclinical research indicates that abnormalities in microglial activity can result in a range of neurological health, varying in intensity from moderate to severe. The critical function of microglia in the development of the CNS is determined by their interactions with neurons and other glial cells, that have an impact on the structure of synapses and on the formation of new neurons. This review aims to fill gaps in earlier research by examining the diverse nature of microglial cells and their crucial functions in the development of the nervous system. It specifically focuses on current discoveries related to the rearrangement of synapses, the regeneration of neurons, and the impact of environmental stimuli. Comprehending these interactions is essential for creating precise treatments for neurodevelopmental diseases, emphasizing the necessity for ongoing investigation into microglial processes and measures to reduce their negative impact on brain development.

KEYWORDS microglia in synaptic; neural regeneration, neurodevelopmental disorders, environmental changes and brain development

INTRODUCTION

Microglia, which are highly motile and attentive macrophages located in the brain, constitute a substantial percentage of neuroglia in the central nervous system (CNS). These cells, which are created during the formation of the CNS, have the ability to renew themselves throughout an animal's lifespan, therefore sustaining their numbers in healthy tissues (1). Microglia are primarily recognized for their immunological tasks, including

the removal of pathogens and debris by phagocytosis, as well as their involvement in inflammatory responses during neurodegenerative illnesses. However, they also have essential roles in the formation, maintenance, and restoration of the CNS (2). Microglia, which are important regulators of the brain's microenvironment, display molecular and state-specific functional diversity across the CNS. Our comprehension of this variability is now in its nascent phase. The lack of healthy microglia can lead to a variety of repercussions, ranging from minor dysregulation of microglial status to severe pediatric-onset leukoencephalopathy, as shown by recent findings from human genetic studies and preclinical (3). During steady conditions, microglia serve as the main immune cells in the CNS. These myeloid cells, known as macrophages, have a role in several processes inside the CNS, such as regulating inflammation, combating infections, and eliminating cellular waste through phagocytosis (4). In addition to their conventional functions, current studies have emphasized the significance of microglia in intricate neurodevelopmental processes. Throughout these processes, their phagocytic and signalling functions play a crucial role in 1) controlling programmed cell death to determine the destiny of neurons, 2), stimulating the growth of neurites, the formation of synapses, and the bundling of axons, and 3) removing surplus synapses from developing neurons to facilitate the creation of functional neural circuits. Microglia originate uniquely, enabling them to occupy a specific niche as resident macrophages in an area that is usually considered immune-privileged. Research on the origins of microglia has demonstrated that they mostly come from yolk-sac erythromyeloid progenitors (5). These progenitors migrate to the developing neuroepithelium and settle in the CNS. Despite the prior assumption that macrophages may change their gene expression in response to their surroundings, bone marrow-derived macrophages (BMDMs) do not acquire the same gene expression profile as microglia when they enter the brain tissue (6). In mice, microglia have been eliminated by using diphtheria toxin under the CX3CR1 promoter and by blocking the CSF-1 receptor, which is necessary for microglial survival and is also found in other macrophages (7). Manipulating microglia makes them a great target for studying the etiology of neurodevelopmental diseases. Microglia, the macrophages that live in the CNS, are recognized for their functions in combating infection, eliminating cellular waste, and preserving tissue equilibrium. In addition to their conventional immune roles, microglia also participate in complex neurodevelopmental processes, including neurogenesis and synaptic pruning (8). During these activities, glial cells engage in interactions with neurons and other glial cells offer nourishing support, react to cytokine and metabolic signals from the nearby neural environment, and assist in refining functioning neuronal circuits. Microglia, the immune cells that live in the CNS, which includes the brain, spinal cord, and retina, were initially identified as innate immune cells responsible for protecting against bacterial and viral invasions inside the CNS (9). Microglias were initially believed to predominantly participate in pathological circumstances such as aging, chronic stress, and Alzheimer's disease by facilitating neuroinflammatory processes. Although several activities of microglia in the adult brain have been identified, there has been very limited study on their roles in the embryonic brain (10). These cells move around a lot in the developing brain wall and interact with nearby neural lineage cells (neural progenitors and mature neurons) and vascular endothelial cells. Microglia engage in extensive patrolling to carry out many activities during the processes of neurogenesis and vascular formation in development (11).

THE ROLE OF MICROGLIA IN SYNAPTIC RECONFIGURATION

Microglia have a crucial role in building functioning neuronal circuits by exerting influence on synaptogenesis, synapse development, and synaptic activity. Recent research has shown novel ways in which microglia influence the functioning of synapses in different cellular, geographical, and temporal situations. For instance, in prenatal animals lacking microglia, certain neocortical Lhx6+ inhibitory interneurons may not be appropriately situated in the lamina, which is essential for the functioning of the circuit (12). Microglia have the ability to directly contact the dendrites of pyramidal neurons in the somatosensory cortex. This interaction leads to the deposition of actin and an increase in calcium ion transients. As a

result, it promotes the production of filopodia and spines (13). The number of spines and the development of excitatory synapses are reduced by pharmacologically inhibiting microglia. In addition to this intricate nature, the reduction of microglia in adult mice results in a rise in the quantity of synapses and intensifies the functioning of both excitatory neurons and inhibitory parvalbumin interneurons in the visual cortex (14). The apparent inconsistencies in these findings highlight the significance of examining the variations in time and space of microglia during their maturation. The reciprocal interplay between microglia and neurons is an additional key element in regulating synaptic activity. Adolescent mice have hippocampal neurons that become active and release Il33 (15). This Il33 then causes microglial cells to change the structure of their spines and engulf the extracellular matrix. As a result, the frequency of excitatory postsynaptic currents increases. Further research, utilizing different genetically modified mouse models to disturb the balance of microglial cells throughout the development of the CNS, has shown that microglia have a crucial function in inhibiting neuronal activity in a way that is reliant on ATP to prevent excessive activation and seizures (16). These investigations indicate that the process of synaptic pruning by microglia has a function in protecting the neurons. Reactive microglia in adult mice physically damage inhibitory presynaptic terminals in the somata of cortical neurons. Microglia controls the formation and modification of synapses in both normal and diseased conditions through several processes, which are determined by their specific cellular, geographical, and temporal contexts. Glial biologists have shown that microglia have important functions in the development of the brain, especially at the key periods when synaptic pruning occurs in areas like the retinogeniculate system and the hippocampus (17). Studies on microglia in the retinogeniculate system have resulted in the formulation of a "punishment model." This model proposes that neuronal synapses that are weaker or less functioning do not provide a defensive chemical signal, rendering them vulnerable to being swallowed by microglia. Phagocytic cells eliminate less robust synapses in order to build efficient synaptic circuits. Through ongoing improvements, this model has become more precise. Recent research suggests that microglia, under the influence of interleukin-33 (IL-33) released by astrocytes, also play a role in synaptic pruning in the reticular thalamic nucleus and in the hippocampus (18). Microglia can be considered a heterogeneous population *in vivo* due to the impact of environmental signals on macrophage activity and the distinct molecular environments of various areas within the CNS. Hence, a comprehensive method for comprehending glial-glial and neuronal-glial communication is insufficient. Microglial traits, including their morphological complexity, motility, electrical properties, and transcriptional profiles, differ depending on their location. It is hypothesized that deficiencies in synaptic pruning have a role in illnesses such as autism spectrum disorder (ASD) and schizophrenia (19). These disorders are characterized by either excessive or insufficient connections in areas such as the amygdala, prefrontal cortex, and components of the default mode network. Neuronal dopaminergic signalling plays a crucial role in reward-seeking and social behavior. In adolescent male rats, a lack of microglial clearance of (Dopamine Receptor D1 has been associated with decreased social play and exploration. This suggests that microglia are involved in behavioral outcomes via refining synaptic connections.

MICROGLIA'S ROLE IN NEURAL REGENERATION PROCESSES

Microglia are thought to have a vital role in neurogenesis, which encompasses the process of precursor cells transforming and developing into neurons. These cells play a crucial role in removing waste material, which is important because of the programmed cell death that occurs during the formation of new neurons (20). Studies investigating the involvement of microglia in the process of neurogenesis commonly utilize laboratory techniques conducted outside of a living organism or focus on the development of new neurons in adult organisms. This is due to the challenges associated with researching embryonic systems. Published reports have shown that microglia play a crucial role in important elements of neurogenesis by engaging in phagocytosis and signalling activities, as well as by regulating inflammation within the central nervous system. It is postulated that disturbances to the microglial transcriptome,

particularly decreased phagocytic activity, may impede synaptic refinement or support for neurogenesis, perhaps resulting in aberrant synaptic connections or alterations in the survival of migratory neuroblasts (21). Recent research has emphasized important connections between microglia and (Neural precursor cells) NPCs, which have a considerable impact on neurogenesis and the general development of the brain in vertebrates. Microglia control the process of generating new neurons during brain growth in different parts of the brain by engulfing and digesting cellular debris. Microglia in the subgranular zone engulf apoptotic neuroblasts during the early postnatal period in order to regulate their incorporation into hippocampal circuits. While the specific processes behind microglial selection of NPC phagocytosis remain unclear, a growing amount of data suggests that microglial released substances have a role in controlling NPCs and neurogenesis to facilitate brain growth. When murine NPCs are cultivated in isolation, they lose the capacity to generate specialized neuroblasts (22). However, this ability is regained when they are cultured along with microglia or are exposed to a medium conditioned by microglia. These findings demonstrate how microglia regulate the formation of NPCs and neurogenesis through both phagocytic and secretory processes. Further investigation into the reciprocal communication mechanisms, whether by secretion or other means, that are involved in phagocytosis will provide a clearer understanding of the intricate connections between NPCs and microglia throughout the develop ment of the nervous system. Reactivating microglia in the retina has been shown to results in a limited recovery of neurogenesis. Recent research has demonstrated that microglial processes form distinct connections with the cell bodies of growing neurons during the embryonic, early postnatal, and adult phases of neurogenesis (23). The interaction between microglia and immature neurons in the growing brain and the impact of these interactions on the complexity of neural networks in the adult brain exists. Additional investigation is required to elucidate the exact cellular communication channels by which microglia influence neuronal growth and the establishment of neural networks. (Figure 1)

MICROGLIA AND THEIR CONTRIBUTION TO NEURODEVELOPMENTAL DISORDERS

Although there is evidence of sexual dimorphism in adult microglia and variations in microglial activity depending on sex, it is still unclear whether genetic sex differences or sex hormones have an impact on microglial specifications. Studying the impact of gender on microglia is essential for comprehending the gender-related prejudices that play a role in different neurodevelopmental and neurodegenerative illnesses (24). External variables can have a substantial impact on the maintenance of microglial homeostasis. Gut-brain interactions have an impact on the states and activities of microglia. Prenatal mice that are reared in germ-free surroundings exhibit changes in the growth and maturation of microglia which differ depending on the sex and brain area (25). The ingestion of omega-3 fatty acids by the mother is crucial for the development of the hippocampus in children. This growth is aided by the process of microglial phagocytosis. A new study has discovered a distinct subgroup of microglia in mice called capillary-associated microglia.

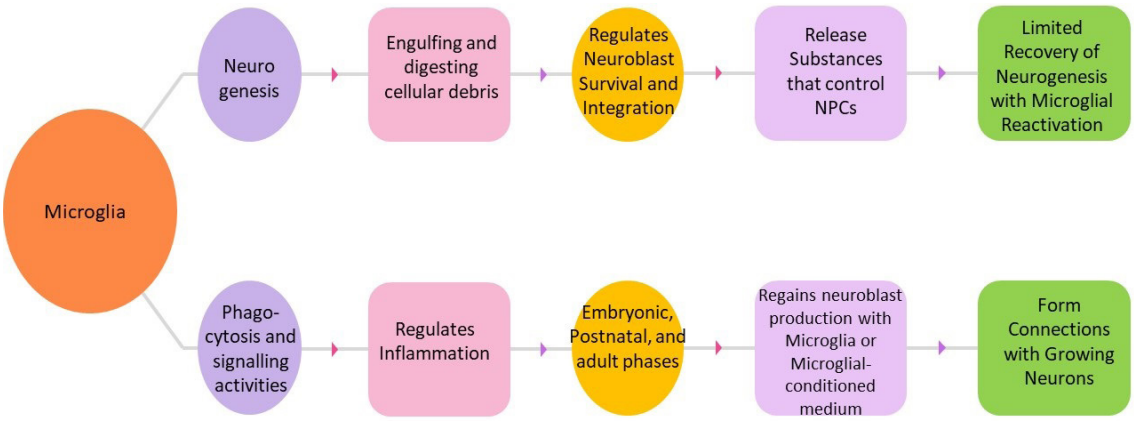

Figure 1. Role of microglia in the neural regeneration processes

These microglia are found along brain capillaries and have a role in controlling vasodilation and blood flow (26). Microglia can enhance vessel sprouting in murine aortic ring cultures by releasing secreted factors. The involvement of microglia in embryonic angiogenesis is intricate and encompasses several processes, presenting numerous opportunities for future exploration of the interactions between microglia and endothelial cells in neurodevelopment. Early-life infections and inflammation can disturb delicate neurodevelopmental processes, leading to developmental impairments seen in neurological illnesses such as autism spectrum disorders (ASD) and schizophrenia (27). Investigations investigating of the function of microglia in neurogenesis frequently depend on *in vitro* techniques or examinations of adult neurogenesis, mostly because of challenges associated with embryonic systems. Research has demonstrated that the pro-inflammatory cytokine IL-6 is significantly involved in causing neurodevelopmental impairments. When IL-6 is administered alone, it can lead to the development of pathological conditions. However, the negative effects of maternal immune activation (MIA) can be reduced by using IL-6 neutralizing antibodies (28). Although MIA has its difficulties and restrictions, it is a valuable tool for investigating the immune-related origins of neurodevelopmental diseases until more efficient developmental neuroimmunological models are established. Recent meta-analyses have demonstrated a male sex bias in both ASD and schizophrenia (29). These conditions can be replicated in rats. Behavioural assessments conducted in these animal models primarily evaluate characteristics associated with ASD or schizophrenia, including ultrasonic vocalizations, social interactions, repetitive behaviors, and anxiety. The diagnostic criteria for schizophrenia are hallucinations, delusions, disordered speech, and catatonia. Although MIA mice have some characteristics associated with autism, such as impairments in social interaction, communication, and repetitive activities, it is difficult to apply these results to more intricate neurological illnesses. However, MIA remains a helpful method for studying the immune-related causes of neurodevelopmental disorders.

EFFECTS OF ENVIRONMENTAL CHANGES ON MICROGLIAL ACTIVITY

A recent study suggests that elevated maternal inflammation during pregnancy is associated with diverse psychosocial consequences in children throughout their life. Research using direct measures of inflammatory activation has established a link between maternal infection exposure during pregnancy and an increased likelihood of children having mental disorders, including autism, schizophrenia, bipolar disorder, and major depressive disorder. Mouse models of maternal inflammation generated by LPS treatment was used to uncover alterations in gene expression in newborn microglia in comparison to control groups treated with saline. According to the study conducted on the impact of the presence of harmful substances in the environment and socioeconomic circumstances experienced during pregnancy found that they resulted in long-lasting behavioral problems and alterations in brain network activity associated with social interactions in male offspring (30). These effects were linked to the disrupted process of microglial synapse pruning. Nasu-Hakola disease (NHD), characterized by early-onset cognitive dementia, is associated with the absence of a functioning Trem2 signaling pathway, highlighting the significance of microglial activity in brain development (31). Moreover, new research has linked maternal environmental variables, such as viral or bacterial infections, atypical immunological responses, and dietary circumstances, to anomalous fetal brain development and neurological problems in children. For instance, when pregnant mice were administered poly(I) on day 12.5 of their pregnancy, microglia in the brains of the fetuses from day 16 showed a notably increased production of IL-6 compared to microglia from control mice that were not treated (32). In order to reduce the likelihood of neurological diseases in children that are linked to inflammation in the mother, further investigation is required to comprehend the effects of MIA and environmental elements on fetal microglia. The chromatin alterations and enhancer selections in tissue microenvironments have an impact on the transcriptional control of local microglial phenotypes. Although there is evidence of sexual differences in adult microglia and variations in their behavior depending on sex,

external variables may be important in preserving microglial homeostasis, e.g., the way stomach and brain communication affects the states and activities of microglia. In particular, prenatal mice that are germ-free have compromised growth and maturation of microglia, with variations seen based on sex and brain location. Furthermore, it is crucial for human mothers to consume omega-3 fatty acids in order to promote the growth of the hippocampus in their children. This development is assisted by the process of microglial phagocytosis, as stated. Various studies have examined other environmental elements that may impact microglial homeostasis (33).

MICROGLIAL CONTRIBUTIONS TO BRAIN DEVELOPMENT

Microglia, driven by their geographical and temporal diversity, have a crucial impact on the formation of the developing brain. They promote brain growth and regulate homeostasis by engaging in complex interactions with many types of brain cells, both neuronal and non-neuronal (34). Microglia have a role in several elements of blood vessel generation throughout the development of the CNS. Microglia have been observed in close proximity to recently developed blood vessels in both animal models and people, as shown by initial imaging investigations (35). NPCs play a crucial role in the production of both neurons and several types of glial cells (36). The initial examination of microglia during typical development and their subsequent participation in cell death in mice and birds emphasized their function in molding the developing CNS. Additional investigation employing inducible genetic targeting methods would be beneficial in validating these findings, considering the current limited comprehension of the efficacy and permeation of inhibitory antibodies in brain tissue during embryonic and postnatal periods. While the precise processes behind microglial phagocytosis of NPCs remain incompletely understood, mounting evidence suggests that substances produced by microglia play a vital role in regulating NPCs and neurogenesis, hence promoting brain growth. Murine NPCs undergo a loss of neuroblast production when grown alone. However, this capacity may be regained by co-culturing the NPCs with microglia or microglial-conditioned medium. Microglial colonization and mobility rely heavily on blood vessels, whereas microglia, in turn, aid in the creation of blood vessels. The proper growth of retinal blood vessels relies on the presence of a substantial number of resident microglia. In mouse models of ischemic retinopathy, a drop in microglia is found along with the typical decline in vasculature throughout the postnatal period (37). Furthermore, research has demonstrated that at the 15th week of gestation, when the development of retinal blood vessels is just commencing from the optic disc, in the human embryonic retina microglia may be found throughout the whole retinal surface (38). Studies of the brain during the neonatal and adult stages have shown that microglia are involved in several aspects of vascular development, such as extending blood vessels, creating branches and regulating their width, promoting blood flow circulation, and maintaining the integrity of the blood-brain barrier. But, there is a scarcity of studies about the role of microglia in the developing brain during the embryonic stage (39). Studying microglial activity during this early period might offer valuable information on the effects of abnormally active microglia on the development and function of blood vessels in the fetal brain (Figure 2). Research on microglia in neurodevelopmental disorders, including ASD and schizophrenia, has increasingly highlighted the therapeutic potential of targeting microglial dysfunction. Studies have revealed that aberrant microglial activity can disrupt synaptic pruning, brain connectivity, and neuroinflammation, all contributing to disease pathology. Clinical trials are currently exploring microglia-modulating drugs, such as minocycline and other anti-inflammatory agents, to address these disruptions. For example, a 2022 pilot study on minocycline in ASD patients showed reduced inflammatory markers and improved behavioral symptoms in 30% of participants (40). Long-term clinical data are needed, but initial results support the viability of precision-targeted therapies in managing symptoms, promoting neuroprotection, and minimizing side effects in neurodevelopmental disorders.

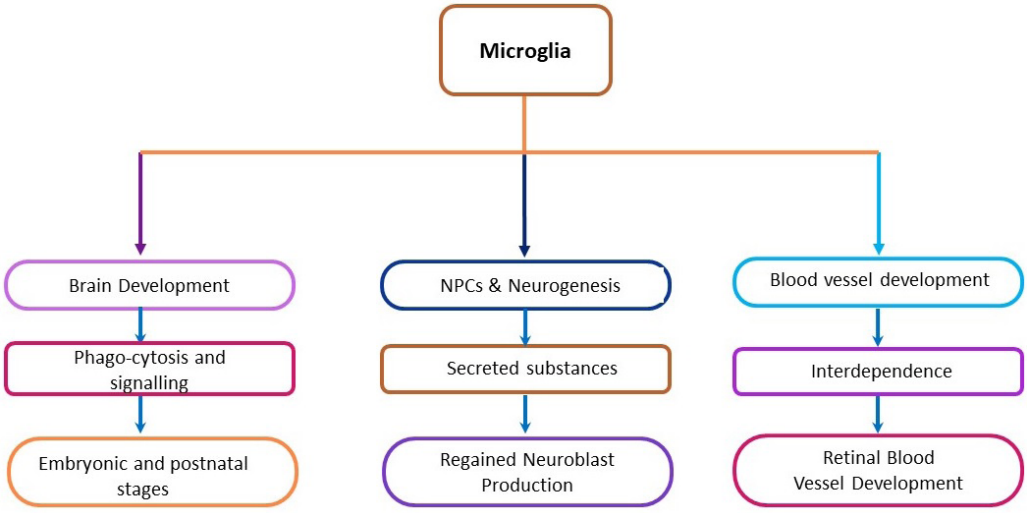

Figure 2. Microglial contributions

CONCLUSIONS

Microglia play a crucial role in the growth, upkeep, and restoration of the CNS. They perform a diverse range of tasks, including immunological responses and the regulation of neurodevelopmental processes. The diverse functionality of microglia, influenced by molecular and environmental variables, highlights the intricate nature of their significance in the CNS. The current review highlights the significant influence of microglial dysregulation on neurological well-being, establishing a connection between it and illnesses such as ASD, schizophrenia, and other neurodevelopmental disorders. Moreover, the interplay between microglia and external stimuli, such as maternal inflammation and nutritional variables, elucidates the wider framework within which these cells function. Future research should prioritize the investigation of the precise processes by which microglial cells function and interact with other cells in the CNS.

ACKNOWLEDGMENTS

None.

FUNDING

This research received no specific grant from any funding agency in the public, commercial, or not-for-profit sectors.

CONFLICTS OF INTEREST

The authors have no conflicts of interest to report.

ADDITIONAL INFORMATION

Author contributions

P.L.: conceptualization; D.S.K., P.V.: data curation; S.B.: writing—draft preparation; S.D.: original draft preparation, review and editing; D.S.K.: supervision.

REFERENCES

1. Lannes N, Eppler E, Etemad S, Yotovski P, Filgueira L. Microglia at center stage: a comprehensive review about the versatile and unique residential macrophages of the central nervous system. Oncotarget. 2017;8:114393. PubMed PMID: 29371994
2. Yanuck S. Microglial phagocytosis of neurons: diminishing neuronal loss in traumatic, infectious, inflammatory, and autoimmune CNS disorders. Front Psychiatry. 2019;10:712. PubMed PMID: 31632307
3. Oosterhof N, Chang I, Karimiani E, Kuil L, Jensen D, Daza R, et al. Homozygous mutations in CSF1R cause a pediatric-onset leukoencephalopathy and can result in congenital absence of microglia. Am J Hum Genet. 2019;104:936-47.
4. Yu F, Wang Y, Stetler A, Leak R, Hu X, Chen J. Phagocytic microglia and macrophages in brain injury and repair. CNS Neurosci Ther. 2022;28:1279-93.
5. Gomez Perdiguero E, Klapproth K, Schulz C, Busch K, Azzoni E, Crozet L, et al. Tissue-resident macrophages originate from yolk-sac-derived erythro-myeloid progenitors. Nature. 2015;518:547-51.
6. Kawanishi S, Takata K, Itezono S, Nagayama H, Konoya S, Chisaki Y, et al. Bone-marrow-derived microglia-like cells ameliorate brain amyloid pathology and cognitive impairment in a mouse model of Alzheimer's disease. J Alzheimers Dis. 2018;64:563-85.
7. Kitic M, See P, Bruttger J, Ginhoux F, Waisman A. Novel microglia depletion systems: a genetic approach utilizing conditional diphtheria toxin receptor expression and a pharmacological model based on the blocking of macrophage colony-stimulating factor 1

receptor. In: Ginhoux F, editor. Microglia: Methods and Protocols. New York: Springer; 2019. p. 217-30.
8. Mordelt A, de Witte L. Microglia-mediated synaptic pruning as a key deficit in neurodevelopmental disorders: Hype or hope?. Curr Opin Neurobiol. 2023;79:102674. PubMed PMID: 36657237
9. Lisak R, Benjamins J, Bealmear B, Nedelkoska L, Yao B, Land S, et al. Differential effects of Th1, monocyte/macrophage and Th2 cytokine mixtures on early gene expression for glial and neural-related molecules in central nervous system mixed glial cell cultures: neurotrophins, growth factors and structural proteins. J Neuroinflammation. 2007;4:30. PubMed PMID: 18088439
10. Gray S, Kinghorn K, Woodling N. Shifting equilibriums in Alzheimer's disease: The complex roles of microglia in neuroinflammation, neuronal survival and neurogenesis. Neural Regen Res. 2020;15:1208-19.
11. Elmore M, Najafi A, Koike M, Dagher N, Spangenberg E, Rice RA, et al. Colony-stimulating factor 1 receptor signaling is necessary for microglia viability, unmasking a microglia progenitor cell in the adult brain. Neuron. 2014;82:380-97.
12. Squarzoni P, Oller G, Hoeffel G, Pont-Lezica L, Rostaing P, Low D, et al. Microglia modulate wiring of the embryonic forebrain. Cell Rep. 2014;8:1271-9.
13. Delatour L, Yeh P, Yeh H. Prenatal exposure to ethanol alters synaptic activity in layer V/VI pyramidal neurons of the somatosensory cortex. Cereb Cortex. 2020;30:1735-51.
14. Liu YJ, Spangenberg EE, Tang B, Holmes TC, Green KN, Xu X. Microglia elimination increases neural circuit connectivity and activity in adult mouse cortex. J Neurosci. 2021;41:1274-87.
15. Wang Y, Fu W, Cheung K, Hung KW, Chen C, Geng H, et al. Astrocyte-secreted IL-33 mediates homeostatic synaptic plasticity in the adult hippocampus. Proc Natl Acad Sci U S A. 2021;118(1):e2020810118. PubMed PMID: 33443211
16. Badimon A, Strasburger H, Ayata P, Chen X, Nair A, Ikegami A, et al. Negative feedback control of neuronal activity by microglia. Nature. 2020;586:417-23.
17. Paolicelli R, Bolasco G, Pagani F, Maggi L, Scianni M, Panzanelli P, et al. Synaptic pruning by microglia is necessary for normal brain development. Science. 2011;333:1456-8.
18. Vainchtein I, Chin G, Cho FS, Kelley KW, Miller JG, Chien EC, et al. Astrocyte-derived interleukin-33 promotes microglial synapse engulfment and neural circuit development. Science. 2018;359:1269-73.
19. Eltokhi A, Santuy A, Merchan-Perez A, Sprengel R. Glutamatergic dysfunction and synaptic ultrastructural alterations in schizophrenia and autism spectrum disorder: Evidence from human and rodent studies. Int J Mol Sci. 2020;22:59. PubMed PMID: 33374598
20. Aarum J, Sandberg K, Haeberlein S, Persson M. Migration and differentiation of neural precursor cells can be directed by microglia. Proc Natl Acad Sci U S A. 2003;100:15983-8.
21. Fu R, Shen Q, Xu P, Luo J, Tang Y. Phagocytosis of microglia in the central nervous system diseases. Mol Neurobiol. 2014;49:1422-34.
22. Baudry M, Yao Y, Simmons D, Liu J, Bi X. Postnatal development of inflammation in a murine model of Niemann-Pick type C disease: Immunohistochemical observations of microglia and astroglia. Exp Neurol. 2003;184:887-903.
23. Cserep C, Schwarcz AD, Posfai B, Laszlo Z, Kellermayer A, Kornyei Z, et al. Microglial control of neuronal development via somatic purinergic junctions. Cell Rep. 2022;40:111369. PubMed PMID: 36130488
24. Villa A, Della Torre S, Maggi A. Sexual differentiation of microglia. Front Neuroendocrinol. 2019;52:156-64.
25. Hui C, St-Pierre A, El Hajj H, Remy Y, Hébert S, Luheshi G, et al. Prenatal immune challenge in mice leads to partly sex-dependent behavioral, microglial, and molecular abnormalities associated with schizophrenia. Front Mol Neurosci. 2018;11:13. PubMed PMID: 29472840
26. Madore C, Leyrolle Q, Morel L, Rossitto M, Greenhalgh A, Delpech J, et al. Essential omega-3 fatty acids tune microglial phagocytosis of synaptic elements in the mouse developing brain. Nat Commun. 2020;11:6133. PubMed PMID: 33257673
27. Nakagawa Y, Chiba K. Involvement of neuroinflammation during brain development in social cognitive deficits in autism spectrum disorder and schizophrenia. J Pharmacol Exp Ther. 2016;358:504-15.
28. Han V, Patel S, Jones H, Dale R. Maternal immune activation and neuroinflammation in human neurodevelopmental disorders. Nat Rev Neurol. 2021;17:564-79.
29. Santos S, Ferreira H, Martins J, Gonçalves J, Castelo-Branco M. Male sex bias in early and late onset neurodevelopmental disorders: Shared aspects and differences in autism spectrum disorder, attention deficit/hyperactivity disorder, and schizophrenia. Neurosci Biobehav Rev. 2022;135:104577. PubMed PMID: 35167846
30. Block C, Eroglu O, Mague S, Smith CJ, Ceasrine A, Sriworarat C, et al. Prenatal environmental stressors impair postnatal microglia function and adult behavior in males. Cell Rep. 2022;40 :111161. PubMed PMID: 35926455
31. Ohgidani M, Kato T, Setoyama D, Sagata N, Hashimoto R, Shigenobu K, et al. Direct induction of ramified microglia-like cells from human monocytes: dynamic microglial dysfunction in Nasu-Hakola disease. Sci Rep. 2014;4:4957. PubMed PMID: 24825127
32. Katoh Y, Iriyama T, Yano E, Sayama S, Seyama T, Kotajima-Murakami H, et al. Increased production of inflammatory cytokines and activation of microglia in the fetal brain of preeclamptic mice induced by angiotensin II. J Reprod Immunol. 2022;154:103752. PubMed PMID: 36202022
33. Laye S, Nadjar A, Joffre C, Bazinet R. Anti-inflammatory effects of omega-3 fatty acids in the brain: physiological mechanisms and relevance to pharmacology. Pharmacol Rev. 2018;70:12-38.
34. Greter M, Merad M. Regulation of microglia develop-

ment and homeostasis. Glia. 2013;61:121-7.
35. Matcovitch-Natan O, Winter D, Giladi A, Vargas Aguilar S, Spinrad A, Sarrazin S, et al. Microglia development follows a stepwise program to regulate brain homeostasis. Science. 2016;353:aad8670. PubMed PMID: 27338705
36. Martínez-Cerdeño V, Noctor S. Neural progenitor cell terminology. Front Neuroanat. 2018;12:104. PubMed PMID: 30574073
37. Ritter MR, Banin E, Moreno S, Aguilar E, Dorrell M, Friedlander M. Myeloid progenitors differentiate into microglia and promote vascular repair in a model of ischemic retinopathy. J Clin Invest. 2006;116:3266-76.
38. Checchin D, Sennlaub F, Levavasseur E, Leduc M, Chemtob S. Potential role of microglia in retinal blood vessel formation. Invest Ophthalmol Vis Sci. 2006;47:3595-602.
39. Hattori Y, Naito Y, Tsugawa Y, Nonaka S, Wake H, Nagasawa T, et al. Transient microglial absence assists postmigratory cortical neurons in proper differentiation. Nat Commun. 2020;11:1631. PubMed PMID: 32242005
40. Pardo C, Buckley A, Thurm A, Lee L, Azhagiri A, Neville D, Swedo S. A pilot open-label trial of minocycline in patients with autism and regressive features. J. Neurodev. Disord. 2013;5:9. PubMed PMID: 23566357

Biomedical Sciences and Clinical Medicine 2025;64(2):176-181.
doi: 10.12982/BSCM.2025.17
https://he01.tci-thaijo.org/index.php/CMMJ-MedCMJ/index

Case Report | Open Access

Diagnostic Challenges and Clinical Implications of Seromucinous Ovarian Neoplasm in Anatomical Dissection: A Case Report

Subhadra Devi Velichety[1], Sirajunnisa Begum Chittoor Rahim[1], Savitha Selvam[1] and Jyothi Ashok Kumar[2]

[1]Apollo Institute of Medical Sciences and Research, Chittoor, Andhra Pradesh, [2]Government Medical College, Khammam, Telangana, India

Correspondence:
Jyothi Ashok Kumar, PhD.,
Government Medical College,
Khammam, Telangana, India
E-mail: jyothiashok.anatomist@gmail.com

Received: August 19, 2024;
Revised: March 21, 2025;
Accepted: April 1, 2025

ABSTRACT

Ovarian cysts are a common finding, yet their discovery in cadavers during anatomical dissection is relatively rare. Seromucinous ovarian neoplasms represent a distinct subtype of ovarian epithelial tumors, often exhibiting benign behavior. While these tumors typically present with clinical symptoms, their incidental discovery in asymptomatic individuals underscores the diagnostic challenges. The cadaver in this study belonged to a 67-year-old woman with no known medical history of ovarian pathology or related symptoms. Medical records revealed no previous surgeries or interventions related to the reproductive system. The decedent did not report pelvic pain, abnormal uterine bleeding, or palpable abdominal masses during her lifetime. Gross examination revealed an incidental ovarian mass measuring 12x10x5.5 cm, characterized by an enlarged, congested, and cystic external surface. Further examination of the cut surface revealed multiloculated and mucoid material filling the cyst cavity, estimated to be approximately 250 cc in volume. Histopathological examination using hematoxylin and eosin (H&E) stained slides confirmed the diagnosis of a seromucinous ovarian neoplasm. Microscopic analysis depicted a lamellated cyst wall with a single layer of bland mucinous and serous epithelium, accompanied by mucoid secretions. The incidental discovery of a seromucinous ovarian neoplasm in this cadaver underscores the diagnostic challenges associated with ovarian pathology, even in the absence of clinical symptoms. This case highlights the importance of thorough anatomical dissections and understanding of the histopathological features of seromucinous tumors essential for accurate diagnosis and appropriate management strategies.

KEYWORDS ovarian cyst, seromucinous ovarian neoplasm, cadaver, anatomical dissection, histopathological examination

INTRODUCTION

Seromucinous ovarian neoplasms present significant diagnostic challenges due to their heterogeneous nature and evolving classification systems (1). These tumors, often associated with endometriosis, exhibit a spectrum from benign to malignant and are characterized by papillary architecture with stratified seromucinous epithelium (2). There are several primary classifications for epithelial ovarian carcinomas (EOCs), including serous, mucinous, clear cell, endometrioid, transitional, and squamous cell carcinomas (3). Previously classified as the Müllerian or endocervical subtype of mucinous tumors, seromucinous ovarian tumors are unusual neoplasms. Fox and Langley first used the term “seromucinous tumor”

in 1976 to characterize a tumor consisting of serous-type cells and endocervical-type mucinous epithelium (4).

The 2014 World Health Organization (WHO) categorization of neoplasms of the female reproductive organs included the first description of seromucinous tumors, a subtype of ovarian epithelial tumors. Seromucinous tumors are epithelial tumors that primarily consist of mucinous epithelium of the serous and endocervical types. These tumors frequently have foci that exhibit distinct differentiation of cells, endometrioid, or squamous tissue (5). Seromucinous tumors are classified as ovarian neoplasms connected to endometriosis, which is frequently linked to it (5). The distinctive microscopic observations include a combination of several types of epithelial cells and papillary formations with branching patterns (5). Seromucinous borderline tumors make up a small percentage (5-7%) of all borderline tumors. (4). Relatively speaking, seromucinous cystadenomas are uncommon; according to prior research, they make up about 4% of all ovarian neoplasms (6). Seromucinous tumors are divided into three categories by the WHO (2014): seromucinous carcinomas, seromucinous borderline tumors, and seromucinous cystadenomas/adenofibromas (5).

CASE REPORT

We present the case of a thinly built female cadaver, incidentally discovered to have a substantial ovarian cyst during routine anatomical dissection at our institution. The cadaver of the 67-year-old woman who had no known medical history of ovarian pathology or related symptoms was obtained for educational purposes and underwent routine dissection.

Clinical presentation

The decedent had no documented history of gynecological complaints or symptoms suggestive of ovarian pathology. Medical records indicated no previous surgeries or interventions related to the reproductive system. There were no reported instances of pelvic pain, abnormal uterine bleeding, or palpable abdominal masses during the decedent's lifetime.

Pathological findings

Upon gross examination, an incidental ovarian mass measuring 12x10x5.5 cm was identified. The external surface appeared congested and cystic, with no evidence of papillary projections or areas. Further examination of the cut surface revealed multiloculated and mucoid material filling the cyst cavity, estimated to be 250 cc in volume (Figures 1, 2). The cyst walls were markedly thickened, indicative of a significant fibrotic component.

Histopathological examination

Microscopic examination of hematoxylin and eosin (H&E) stained slides confirmed the diagnosis of a seromucinous cystadenoma. The slides depicted a lamellated cyst wall with a single layer of bland mucinous and serous epithelium, accompanied by mucoid secretions. These findings were consistent with the characteristic histological features of seromucinous cystadenoma (Figures 3, 4).

Ethical consideration

We obtained written informed consent from blood relatives of the deceased for the donation of the body to the medical college, explicitly for the purposes of advancing medical education and

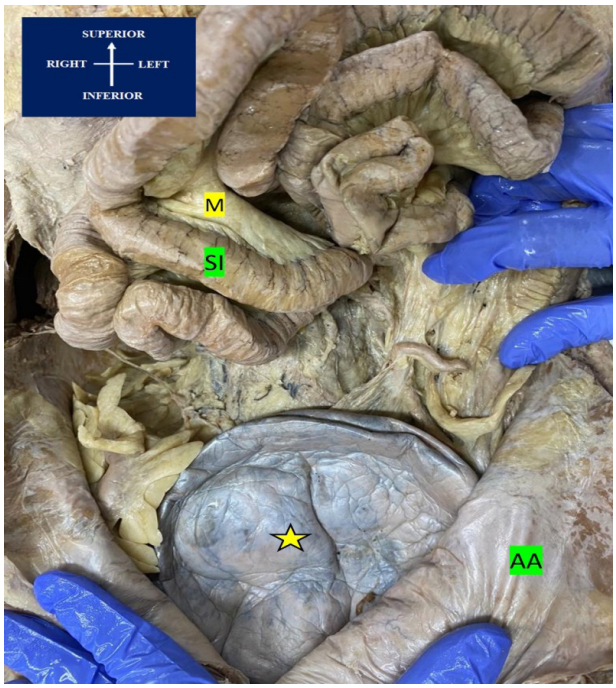

Figure 1. Photograph showing seromucinous ovarian neoplasm; *, seromucinous ovarian neoplasm; SI, Small intestine; M, mesentry, AA, anterior abdomen wall

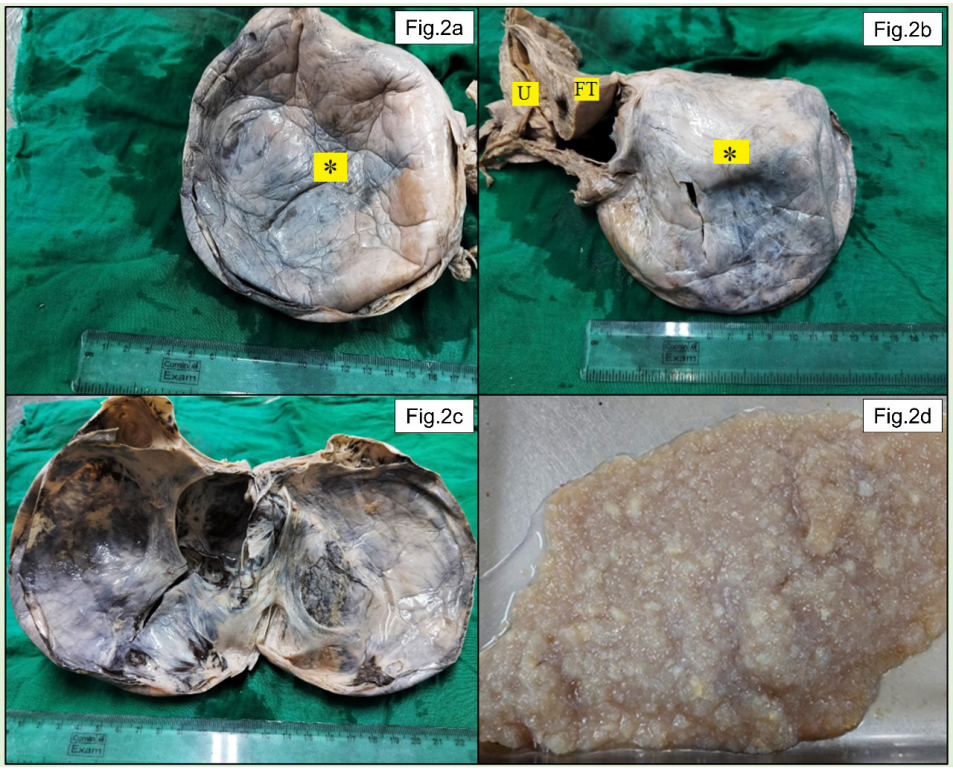

Figure 2. Photograph showing a) Isolated seromucinous cystadenoma, b) Isolated seromucinous ovarian cystadenoma with uterus (UT) and fallopian tube (FT), c) Opened seromucinous ovarian cyst, d) Mucoid material

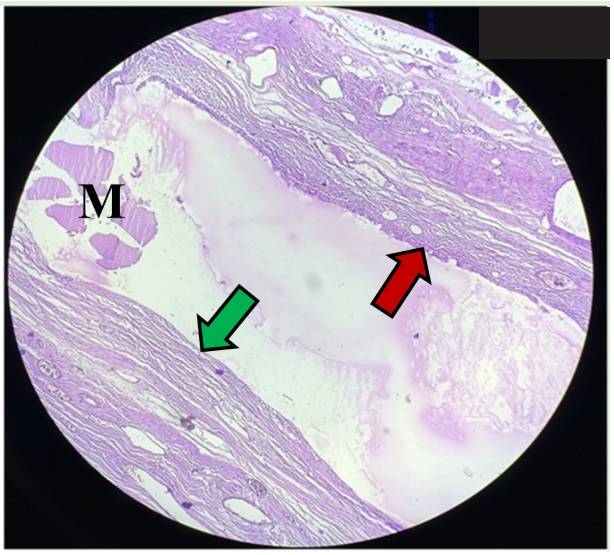

Figure 3. Photomicrograph showing Isolated seromucinous cystadenoma

research. In accordance with the guidelines set forth by the Institutional Review Board (IRB) and Research Ethics Committee, separate consent and approval for this case study were deemed unnecessary, as it arose from an anatomical dissection conducted in the context of educational and research activities. We hereby affirm that all relevant ethical standards have been rigorously adhered to and necessary approvals have been secured for the publication of this case report.

DISCUSSION

The incidental discovery of a huge congested ovarian seromucinous cystadenoma in a thinly built female cadaver, first observed during routine dissection in the department of anatomy, highlights the importance of thorough anatomical examinations in uncovering unsuspected pathologies. This case presents intriguing pathological findings that warrant further investigation and clinical correlation. The gross examination of the ovarian lesion revealed its substantial size, measuring 12x10x5.5 cm, with an enlarged, congested, and cystic external surface. The cut surface displayed multiloculation and mucoid material, indicative of a significant cystic component. Importantly, the absence of papillary projections or areas suggests a benign nature of the lesion, ruling out malignant features on gross examination.

Microscopically, the histological analysis confirmed the diagnosis of a seromucinous cystadenoma. The H&E-stained microscopic slides revealed a lamellated cyst wall with a single layer of bland mucinous and serous epithelium, accompanied by mucoid secretions. These findings

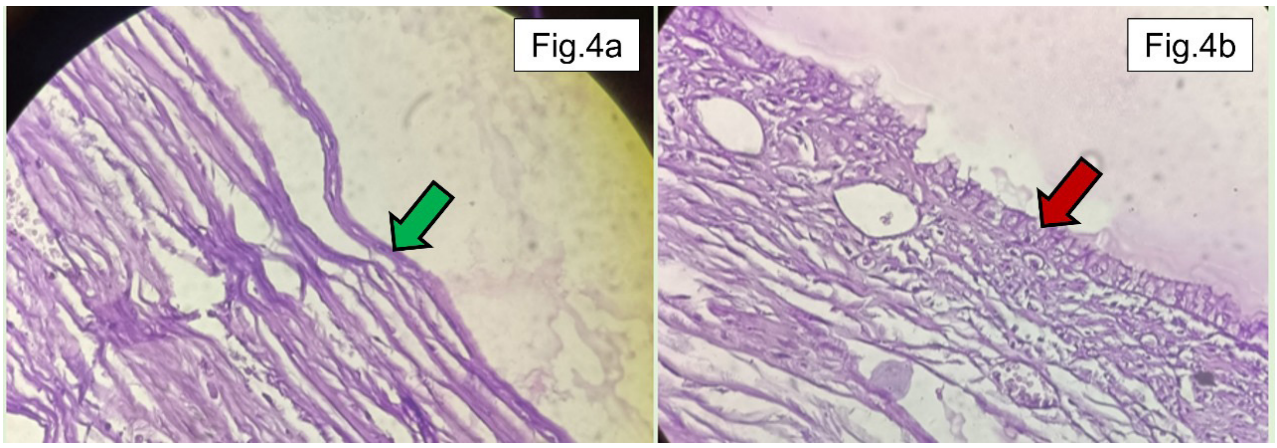

Figure 4. Photomicrograph showing Isolated seromucinous cystadenoma

align with the characteristic histological features of seromucinous tumors, which typically exhibit a mixed pattern of mucinous and serous differentiation. Seromucinous ovarian neoplasms represent a distinct subtype of ovarian epithelial tumors, characterized by their dual mucinous and serous differentiation. While most seromucinous tumors are benign, exhibiting indolent behavior, rare cases of malignancy have been reported (4, 7). Therefore, accurate pathological diagnosis and clinical correlation are essential for appropriate management and prognosis. Epithelial tumors originating in the ovary manifest in three forms, i.e., benign, borderline, and malignant (8). Typically occurring in adults, particularly those in the later reproductive age group, seromucinous cysts are believed to stem from endometriosis (9).

Ovarian cysts are a common occurrence in women across their lifespan, often resolving on their own, with documented sizes reaching up to 148.6 kg as reported by Spolin in 1922 (9). Giant ovarian cysts are ovarian tumors characterized by diameters exceeding 10.0 cm (10) A novel classification of ovarian neoplasms known as seromucinous tumors was added to the WHO Classification of Tumors of the Female Reproductive Organs in 2014 (11). A significant improvement in the categorization of epithelial ovarian tumors is the identification of this particular category. As far as we know, the term "seromucinous tumor" was first used by Fox and Langley in 1976 to characterize a tumor consisting of serous-type cells and mucinous epithelium of the endocervical type (4). Subsequently, in 1988, Rutgers and Scully separated borderline tumors that seemed identical into two groups. Pure endocervical-type epithelium made up one, while a combination of endocervical-type mucinous, serous, and endometrioid cells in various cells with an abundance of eosinophilic cytoplasm made up the other (12, 13).

Benign and borderline seromucinous tumors are still considered separate entities in the 2020 WHO classification. Previous studies have indicated that seromucinous borderline tumors typically occur in young females aged between 33–44 and have a mean size of 8–10 cm (14–16). Consequently, because this situation is similarly unilateral, it is consistent with other research. The pathological results demonstrate that seromucinous tumors are usually thick-walled and cystic. Sporobolus, oedematous, and occasionally sclerotic stroma are common microscopic characteristics of seromucinous borderline tumors, characterized by papillary structures (17, 18). Prior research mostly identified ovarian seromucinous cystadenoma from a pathologic perspective in living subjects; however, this particular instance was discovered in a cadaver.

The incidental nature of the present case finding underscores the importance of comprehensive anatomical examinations in identifying clinically significant lesions, even in asymptomatic individuals. In the context of medical education, the inclusion of such cases in anatomical teaching can enhance students' understanding of pathological conditions and their anatomical manifestations. Furthermore, from a research perspective, the documentation of incidental findings contributes to our understanding of disease prevalence and pathological variability within the population. Such data are valuable for epidemiological studies and may inform clinical practice guidelines regarding

the management of incidental ovarian lesions. This case underscores the diagnostic challenges and clinical implications associated with anatomical pathology, emphasizing the importance of comprehensive postmortem examinations in uncovering clinically significant lesions. Additionally, continued documentation and analysis of incidental findings contribute to our understanding of disease prevalence and pathological variability within the population.

CONCLUSION

In conclusion, this case emphasizes the diagnostic complexities surrounding the incidental discovery of seromucinous cystadenoma during anatomical dissections of cadavers. Despite the absence of clinical symptoms in the decedent, the identification of a substantial ovarian cyst highlights the need for meticulous pathological examinations. Understanding the histopathological features of such tumors is crucial for accurate diagnosis and management, particularly in asymptomatic individuals. This underscores the importance of comprehensive anatomical dissections in uncovering unsuspected pathologies and contributes to our knowledge of ovarian pathology in postmortem settings. The diagnostic challenges encountered in the present case highlight the need for further research to explore optimal management policies for seromucinous ovarian neoplasms that are discovered incidentally.

ACKNOWLEDGMENT

We would like to extend our deepest gratitude to the cadaver donors and their families, whose selfless contributions have made this study on ovarian neoplasm in cadavers possible. Their generosity in donating their bodies to science provides invaluable insights and advances our understanding of medical conditions, ultimately contributing to the betterment of healthcare and medical education. We are profoundly grateful for their willingness to contribute to this important work.

FUNDING

This research received no specific grant from any funding agency in the public, commercial, or not-for-profit sectors.

CONFLICTS OF INTEREST

There are no conflicts of interest.

ADDITIONAL INFORMATION

Data access

The data supporting the findings of this study are available from the corresponding author upon reasonable request.

Authors contribution

S.V.: conceptualisation, methodology, software, validation, formal analysis, investigation, resources, data curation, writing - original draft, writing - review & editing, visualisation, supervision, project administration

J.K.: conceptualisation, methodology, software, validation, formal analysis, investigation, resources, data curation, writing - original draft, writing - review & editing, visualisation

S.R.: methodology, writing - original draft, writing-review & editing, supervision, project administration

S.S.: methodology, writing - original draft, writing - review & editing

REFERENCES

1. Talia K, Parra-Herran C, McCluggage W. Ovarian mucinous and seromucinous neoplasms: problematic aspects and modern diagnostic approach. Histopathology. 2022;80:255-78.
2. Storms A, Sukumvanich P, Monaco S, Beriwal S, Krivak T, Olawaiye A, et al. Mucinous tumors of the ovary: diagnostic challenges at frozen section and clinical implications. Gynecol Oncol. 2012;125:75-9.
3. Choi J, Sohn G, Chay D, Cho H, Kim J. Preoperative serum levels of cancer antigen 125 and carcinoembryonic antigen ratio can improve differentiation between mucinous ovarian carcinoma and other epithelial ovarian carcinomas. Obstet Gynecol Sci. 2018; 61:344-51.
4. Kurman R, Shih I. Seromucinous tumors of the ovary. What's in a name? Int J Gynecol Pathol. 2016;35:78-81.
5. Nagamine M, Mikami Y. Ovarian seromucinous tumors: pathogenesis, morphologic spectrum, and clinical issues. Diagnostics (Basel). 2020;10:1-9.
6. Karpathiou G, Chauleur C, Corsini T, Venet M, Habougit C, Honeyman F, et al. Seromucinous ovarian tumor A comparison with the rest of ovarian epithelial tumors. Ann Diagn Pathol. 2017;27:28-33.
7. Abu Sulb A, Abu El Haija M, Muthukumar A. Incidental finding of a huge ovarian serous cystadenoma in an adolescent female with menorrhagia. SAGE Open

Med Case Rep. 2016;4:2050313X16645755. PubMed PMID: 27489715
8. Limaiem F, Lekkala MR, Mlika M. Ovarian cystadenoma. StatPearls [Internet]. 2019. Available from: https://pubmed.ncbi.nlm.nih.gov/30725635/
9. Seidman J, Krishnan J. Ovarian epithelial inclusions with mucinous differentiation: a clinicopathologic study of 42 cases. Int J Gynecol Pathol. 2017;36:372-6.
10. Yeika E, Efie D, Tolefac P, Fomengia J. Giant ovarian cyst masquerading as a massive ascites: a case report. BMC Res Notes. 2017;10:1-4.
11. Jo V, Fletcher C. WHO classification of soft tissue tumours: an update based on the 2013 (4th) edition. Pathology. 2014;46:95-104.
12. Rutgers J, Scully R. Ovarian mullerian mucinous papillary cystadenomas of borderline malignancy. A clinicopathologic analysis. Cancer. 1988;61:340-8.
13. Rutgers J, Scully R. Ovarian mixed-epithelial papillary cystadenomas of borderline malignancy of mullerian type: A clinicopathologic analysis. Cancer. 1988;61: 546-54.
14. Hauptmann S, Friedrich K, Redline R, Avril S. Ovarian borderline tumors in the 2014 WHO classification: evolving concepts and diagnostic criteria. Virchows Arch. 2017;470:125-42.
15. Shappell H, Riopel M, Sehdev A, Ronnett B, Kurman R. Diagnostic criteria and behavior of ovarian seromucinous (endocervical-type mucinous and mixed cell-type) tumors: atypical proliferative (borderline) tumors, intraepithelial, microinvasive, and invasive carcinomas. Am J Surg Pathol. 2002;26:1529-41.
16. Rodriguez I, Irving J, Prat J. Endocervical-like mucinous borderline tumors of the ovary: a clinicopathologic analysis of 31 cases. Am J Surg Pathol. 2004;28: 1311-8.
17. Dubé V, Roy M, Plante M, Renaud M, Têtu B. Mucinous ovarian tumors of Mullerian-type: an analysis of 17 cases including borderline tumors and intraepithelial, microinvasive, and invasive carcinomas. Int J Gynecol Pathol. 2005;24:138-46.
18. Hada T, Miyamoto M, Ishibashi H, Kawauchi H, Soyama H, Matsuura H, et al. Ovarian seromucinous borderline tumors are histologically different from mucinous borderline tumors. In Vivo. 2020;34:1341-6.